

GLOBAL STABILITY AND SENSITIVITY ANALYSIS OF NUMERICAL AND EXPERIMENTAL FLOW FIELDS WITH FOCUS ON FLOW CONTROL

Simone Camarri

University of Pisa

Contributing authors

- Dr. Andrea Fani, University of Pisa, now at EPFL Lausanne
- Dr. B. Fallenius, KTH Stockholm
- Prof. Jens Fransson, KTH Stockholm
- Dr. Flavio Giannetti, University of Salerno
- Prof. Angelo Iollo, University of Bordeaux
- Prof. Paolo Luchini, University of Salerno
- Prof. Maria Vittoria Salvetti, University of Pisa



Introduction

- Global stability analysis provides important information for several classes of unstable flows
- Adjoint methods are often used to study the sensitivity of a global instability to a wide range of perturbations
 - provide information on the nature and hidden characteristics of the instability
 - provide hints on how to control the investigated instabilities
- Rigorous application of these methods is limited to low Reynolds numbers
- For given classes of flows (bluff-bodies), application of these methods to mean flow fields, even neglecting Reynolds stresses, provide accurate estimation of some properties of the saturated instability

Overview

- Global stability and sensitivity analysis: a concise introduction
- Applications with focus on:
 - Flow control
 - Application to a case at high Reynolds number

Global stability and sensitivity analysis: a concise introduction



Global stability analysis

- Starting point: a steady solution of the NS equations (Baseflow \mathbf{U}_b):

$$\mathbf{U}_b \cdot \nabla \mathbf{U}_b + \nabla P_b - \frac{1}{Re} \nabla^2 \mathbf{U}_b = \mathbf{0}$$
$$\nabla \cdot \mathbf{U}_b = 0$$

- Perturbation of \mathbf{U}_b in modal form:

$$\mathbf{U}(\mathbf{x}, t) = \mathbf{U}_b(\mathbf{x}, t) + \epsilon \mathbf{u}(\mathbf{x}) e^{\sigma t}$$
$$P(\mathbf{x}, t) = P_b(\mathbf{x}, t) + \epsilon p(\mathbf{x}) e^{\sigma t}$$

- Linearized ($\epsilon \ll 1$) dynamics of the perturbation: resulting eigenvalue problem:

$$\sigma \mathbf{u} + \mathbf{u} \cdot \nabla \mathbf{U}_b + \mathbf{U}_b \cdot \nabla \mathbf{u} + \nabla p - \frac{1}{Re} \nabla^2 \mathbf{u} = \mathbf{0}$$
$$\nabla \cdot \mathbf{u} = 0$$

- Given the mode (σ, \mathbf{u}, p)

Real(σ) amplification factor (>0 unstable)

Imag(σ)/(2 π) frequency of the mode



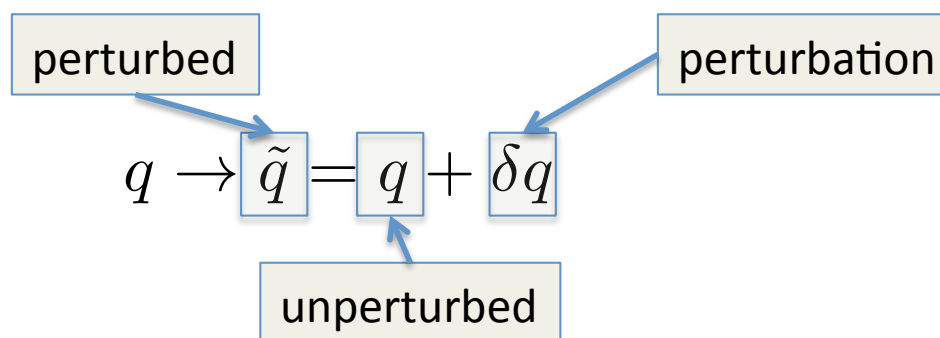
Sensitivity analysis

- Stability properties can be affected by modifications of the flow
- Sensitivity of the instability to particular modifications add information on its physical origin/properties
- Information on sensitivity can be used also to control the instability by proper modifications on the flow

Adjoint methods have been used in the last years to systematically characterize the sensitivity of unstable modes to various parameters in the linear framework

Sensitivity analysis

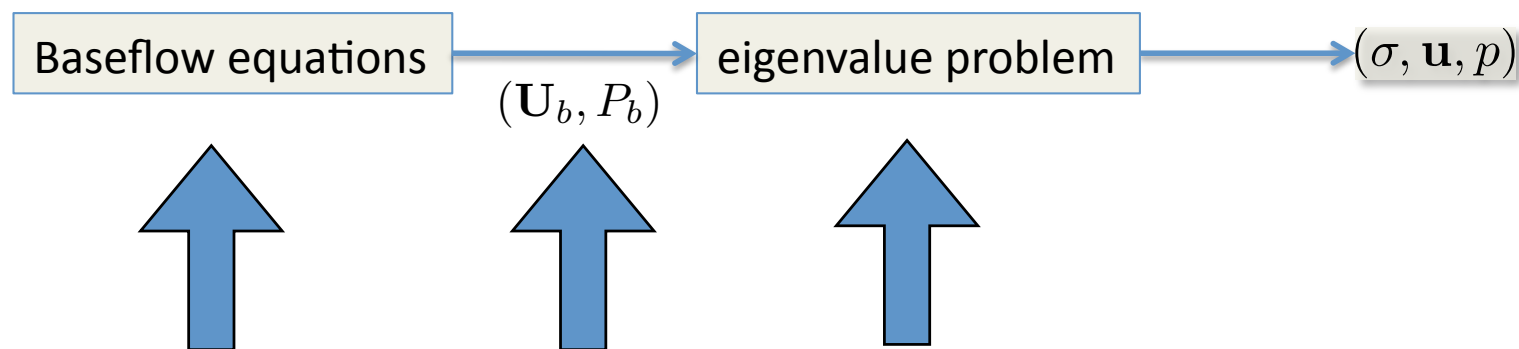
- When the eigenvalue problem is perturbed each eigenfunction/ eigenvalue changes consequently:



- Objective: study the variation of a considered eigenvalue σ
- Linear framework: the analysis is linearized

Sensitivity analysis

- Different perturbations can be applied. For instance:
 - 1) perturbations acting only on the stability equations
 - 2) Generic perturbations of the base flow field
 - 3) Perturbations acting on the baseflow equations





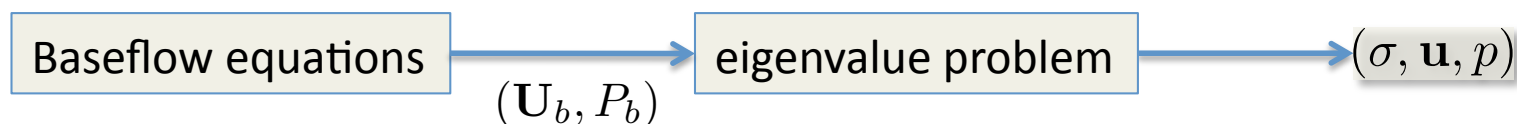
Sensitivity analysis

perturbation of the linearized perturbation equations

- Unperturbed problem:

$$\sigma \mathbf{u} + \mathbf{u} \cdot \nabla \mathbf{U}_b + \mathbf{U}_b \cdot \nabla \mathbf{u} + \nabla p - \frac{1}{Re} \nabla^2 \mathbf{u} = \mathbf{0}$$

$$\nabla \cdot \mathbf{u} = 0$$



Sensitivity analysis

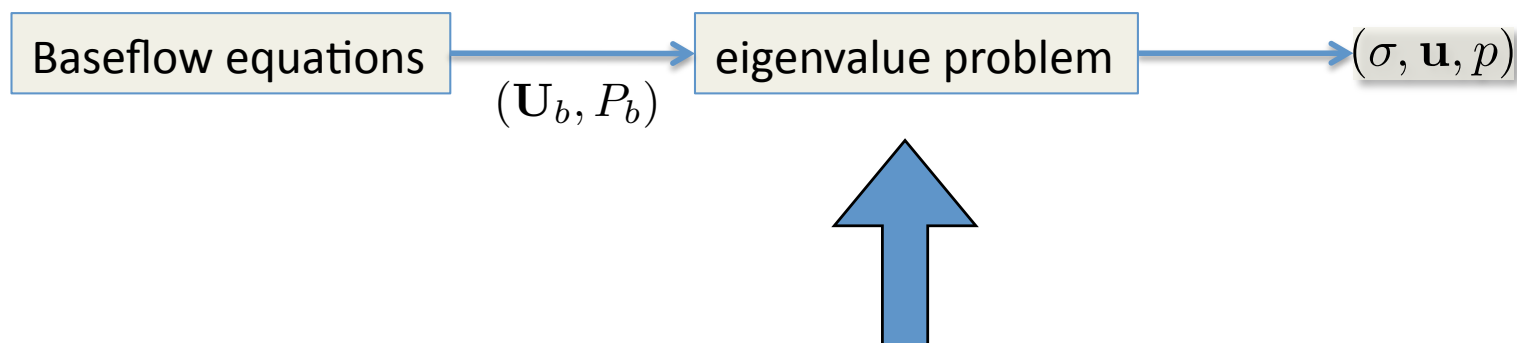
perturbation of the linearized perturbation equations

- Perturbed problem ($\delta\mathbf{H}$ linear):

$$\tilde{\sigma}\mathbf{u} + \tilde{\mathbf{u}} \cdot \nabla \mathbf{U}_b + \mathbf{U}_b \cdot \nabla \tilde{\mathbf{u}} + \tilde{\nabla} p - \frac{1}{Re} \nabla^2 \tilde{\mathbf{u}} = \delta\mathbf{H}(\mathbf{u}, p)$$

$$\nabla \cdot \tilde{\mathbf{u}} = 0$$

Perturbation
(linear functional)



Sensitivity analysis

perturbation of the linearized perturbation equations

- Perturbed problem ($\delta\mathbf{H}$ linear):

$$\tilde{\sigma}\mathbf{u} + \tilde{\mathbf{u}} \cdot \nabla \mathbf{U}_b + \mathbf{U}_b \cdot \nabla \tilde{\mathbf{u}} + \nabla \tilde{p} - \frac{1}{Re} \nabla^2 \tilde{\mathbf{u}} = \delta\mathbf{H}(\mathbf{u}, p)$$

$$\nabla \cdot \tilde{\mathbf{u}} = 0$$

Perturbation
(linear functional)

- Result of the sensitivity analysis for a mode (σ, \mathbf{u}, p)

$$\delta\sigma = \frac{\langle \mathbf{u}^+, \delta\mathbf{H}(\mathbf{u}, p) \rangle}{\langle \mathbf{u}^+, \mathbf{u} \rangle}$$

Adjoint eigenvalue problem associated to the linearized equations

$$\sigma^* \mathbf{u}^+ + \nabla \mathbf{U}_b \cdot \mathbf{u}^+ - \mathbf{U}_b \cdot \nabla \mathbf{u}^+ + \nabla p^+ - \frac{1}{Re} \nabla^2 \mathbf{u}^+ = \mathbf{0}$$

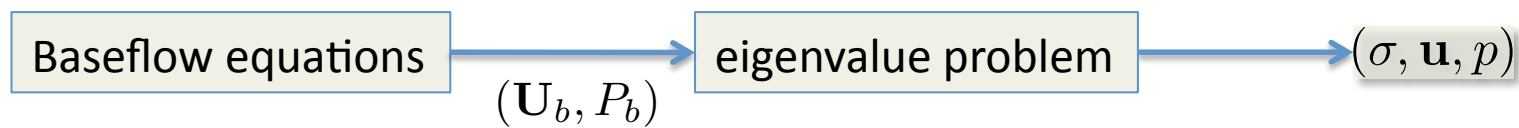
$$\nabla \cdot \mathbf{u}^+ = 0$$

Sensitivity analysis

perturbation of the baseflow field

- Unperturbed problem:

$$\sigma \mathbf{u} + \mathbf{u} \cdot \nabla \mathbf{U}_b + \mathbf{U}_b \cdot \nabla \mathbf{u} + \nabla p - \frac{1}{Re} \nabla^2 \mathbf{u} = \mathbf{0}$$
$$\nabla \cdot \mathbf{u} = 0$$

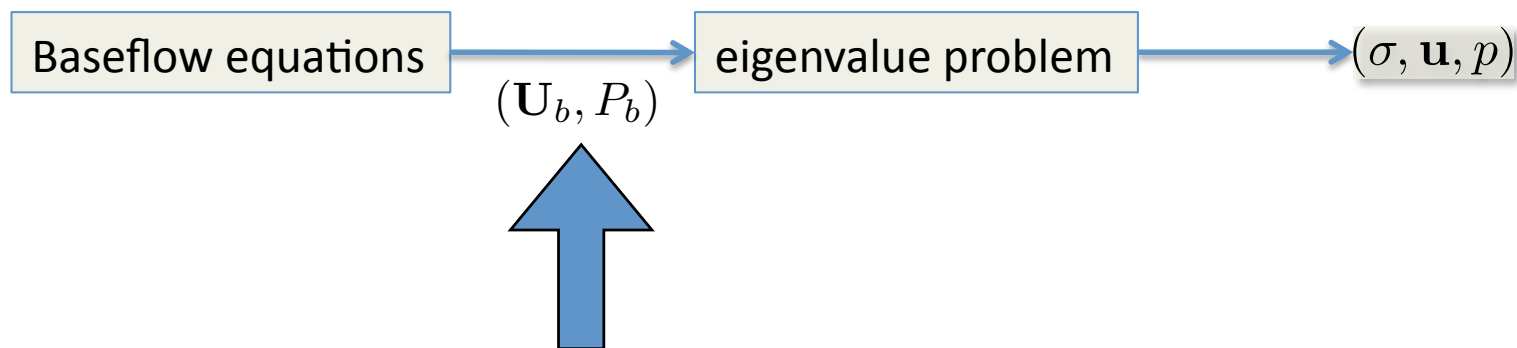


Sensitivity analysis

perturbation of the baseflow field

- Perturbed problem:

$$\tilde{\sigma} \mathbf{u} + \tilde{\mathbf{u}} \cdot \nabla \tilde{\mathbf{U}}_b + \tilde{\mathbf{U}}_b \cdot \nabla \tilde{\mathbf{u}} + \tilde{\nabla} p - \frac{1}{Re} \nabla^2 \tilde{\mathbf{u}} = \mathbf{0}$$
$$\nabla \cdot \tilde{\mathbf{u}} = 0$$





Sensitivity analysis

perturbation of the baseflow field

- Perturbed problem:

$$\tilde{\sigma} \mathbf{u} + \tilde{\mathbf{u}} \cdot \nabla \tilde{\mathbf{U}}_b + \tilde{\mathbf{U}}_b \cdot \nabla \tilde{\mathbf{u}} + \tilde{\nabla} p - \frac{1}{Re} \nabla^2 \tilde{\mathbf{u}} = \mathbf{0}$$

$$\nabla \cdot \tilde{\mathbf{u}} = 0$$

- Result of the sensitivity analysis (adjoint stab. equations involved) for mode (σ, \mathbf{u}, p)

$$\delta\sigma = \frac{(M^+, \delta\mathbf{U}_b)}{(\hat{\mathbf{u}}^+, \hat{\mathbf{u}})}$$
$$M^+ = \hat{\mathbf{u}}^* \cdot \nabla \hat{\mathbf{u}}^+ - \nabla \hat{\mathbf{u}}^* \cdot \hat{\mathbf{u}}^+$$

Sensitivity analysis

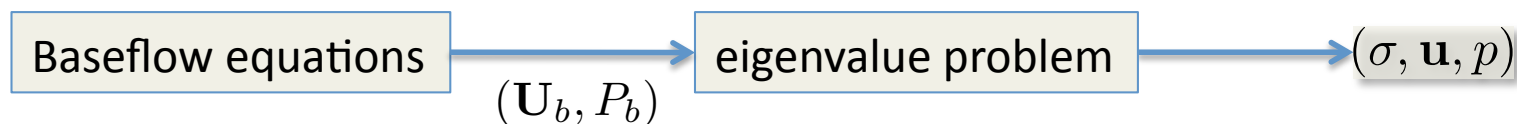
perturbation of the base-flow equations

- Unperturbed problem:

$$\mathbf{U}_b \cdot \nabla \mathbf{U}_b + \nabla P_b - \frac{1}{Re} \nabla^2 \mathbf{U}_b = \mathbf{0}$$

$$\nabla \cdot \mathbf{U}_b = 0$$

$$\sigma \mathbf{u} + \mathcal{L}(\mathbf{U}_b, P_b) \mathbf{u} = 0$$



Sensitivity analysis

perturbation of the base-flow equations

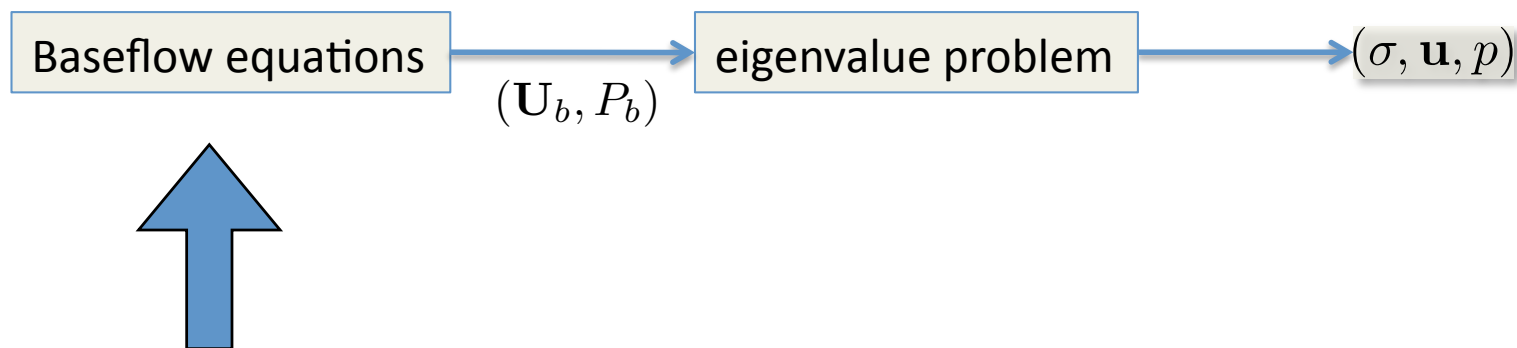
- Perturbed problem:

$$\tilde{\mathbf{U}}_b \cdot \nabla \tilde{\mathbf{U}}_b + \nabla \tilde{P}_b - \frac{1}{Re} \nabla^2 \tilde{\mathbf{U}}_b = \delta \mathbf{F}(\tilde{\mathbf{U}}_b, \tilde{P}_b)$$

$$\nabla \cdot \tilde{\mathbf{U}}_b = 0$$

$$\tilde{\sigma} \tilde{\mathbf{u}} + \mathcal{L}(\tilde{\mathbf{U}}_b, \tilde{P}_b) = 0$$

Perturbation
(linear functional)



Sensitivity analysis

perturbation of the base-flow equations

- Perturbed problem:

$$\tilde{\mathbf{U}}_b \cdot \nabla \tilde{\mathbf{U}}_b + \nabla \tilde{P}_b - \frac{1}{Re} \nabla^2 \tilde{\mathbf{U}}_b = \delta \mathbf{F}(\tilde{\mathbf{U}}_b, \tilde{P}_b)$$

$$\nabla \cdot \tilde{\mathbf{U}}_b = 0$$

$$\sigma \tilde{\mathbf{u}} + \mathcal{L}(\tilde{\mathbf{U}}_b, \tilde{P}_b) = 0$$

Perturbation
(linear functional)

- Result of the sensitivity analysis for mode (σ, \mathbf{u}, p)

$$\delta \sigma = \frac{\langle \mathbf{U}_b^+, \delta \mathbf{F} \rangle}{\langle \hat{\mathbf{u}}^+, \hat{\mathbf{u}} \rangle}$$

Forced adjoint problem associated to the baseflow equations

$$\nabla \mathbf{U}_b \cdot \mathbf{U}_b^+ - \mathbf{U}_b \cdot \nabla \mathbf{U}_b^+ + \nabla P_b^+ - \frac{1}{Re} \nabla^2 \mathbf{U}_b^+ = \hat{\mathbf{u}}^* \cdot \nabla \hat{\mathbf{u}}^+ - \nabla \hat{\mathbf{u}}^* \cdot \hat{\mathbf{u}}^+$$

$$\nabla \cdot \mathbf{U}_b^+ = 0$$



Sensitivity analysis

discrete vs continuous approaches

Continuous approach: starting from PDEs governing the eigenvalue, equivalent PDEs governing adjoint problems are derived. In order to obtain numerical results, all the so-obtained PDEs are discretized separately.

Discrete approach: starting point is the semi-discretized (in space) Navier-Stokes equations (quadratic ODE): the stability problem and related adjoint problems are derived directly for the discrete ODE system.

The two approaches are in sense parallel.....

Sensitivity analysis at discrete level

- Semi-discretized (in space) NS equations; resulting ODE:

$$B_{ij} \frac{d u_j^c}{dt} + N_{ijk} u_j^c u_k^c + L_{ij} u_j^c = 0$$

- Discrete eigenvalue problem:

$$N_{ijk} U_j U_k + L_{ij} U_j = 0$$

Baseflow eqs.

$$\underbrace{(N_{i,j,k} U_k + N_{i,k,j} U_k + L_{ij})}_{L_{ij}^C(\mathbf{U})} u_j + \sigma B_{ij} u_j = 0$$

Eigenvalue probl.

- Perturbed discrete eigenvalue problem:

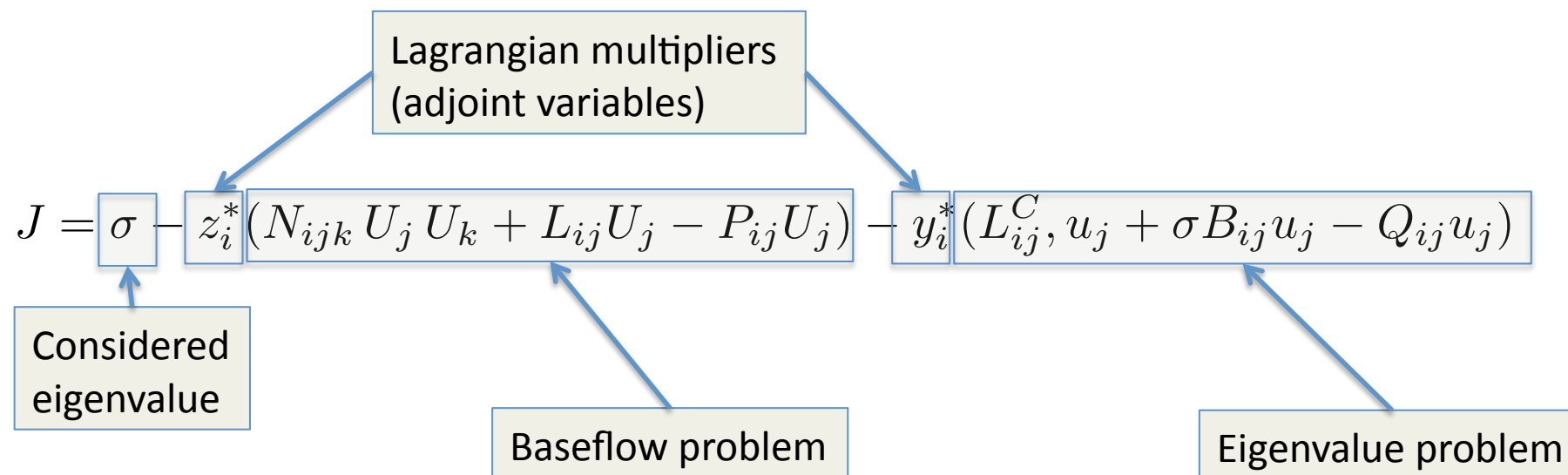
$$N_{ijk} \tilde{U}_j \tilde{U}_k + L_{ij} \tilde{U}_j = P_{ij} \tilde{U}_j$$

Perturbation

$$\tilde{L}_{ij}^C(\mathbf{U}) \tilde{u}_j + \tilde{\sigma} B_{ij} \tilde{u}_j = Q_{ij} \tilde{u}_j$$

Sensitivity analysis at discrete level

- Objective of the analysis: find the perturbation of the eigenvalue as a function of generic perturbations δP , δQ around the unperturbed system ($P=Q=0$)
- Straightforward method: lagrangian formulation
(index repetition implies summation)



Sensitivity analysis at discrete level

Variations of J with respect to the single variables is set to 0:

$$\frac{\delta J}{\delta z_i} \delta z_i = 0 \rightarrow N_{ijk} U_j U_k + L_{ij} U_j - P_{ij} U_j = 0$$

Original baseflow equations

$$\frac{\delta J}{\delta y_i} \delta y_i = 0 \rightarrow L_{ij}^C u_j + \sigma B_{ij} u_j - Q_{ij} u_j = 0$$

Original eigenvalue problem

$$\frac{\delta J}{\delta u_j} \delta u_j = 0 \rightarrow y_i^* L_{ij}^C + y_i^* \sigma B_{ij} = 0$$

Adjoint linear eigenvalue problem

$$\frac{\delta J}{\delta U_j} \delta U_j = 0 \rightarrow z_i^* (N_{ijk} U_k + N_{ikj} U_k + L_{ij} - P_{ij}) + y_i^* (N_{ikj} + N_{ijk} + L_{ij}) u_j = 0$$

Adjoint forced baseflow problem

$$\frac{\delta J}{\delta \sigma} \delta \sigma = 0 \rightarrow y_i^* B_{ij} u_j = 1$$

Normalization cond.

$$\frac{\delta J}{\delta P} \delta P = \frac{\delta \sigma}{\delta P} \delta P = z_i^* \delta P_{ij} U_j$$

Eigenvalue variation with respect to a generic matrix **P**

$$\frac{\delta J}{\delta Q} \delta Q = \frac{\delta \sigma}{\delta Q} \delta Q = y_i^* \delta Q_{ij} u_j$$

Eigenvalue variation with respect to a generic matrix **Q**



Sensitivity analysis at discrete level

Discrete formulation

Continuous formulation

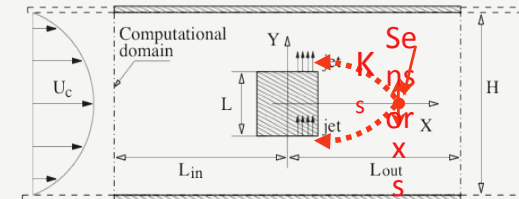
$N_{ijk} U_j U_k + L_{ij} U_j = 0$	$\mathbf{U}_b \cdot \nabla \mathbf{U}_b + \nabla P_b - \frac{1}{Re} \nabla^2 \mathbf{U}_b = \mathbf{0}$ $\nabla \cdot \mathbf{U}_b = 0$
$L_{ij}^C u_j + \sigma B_{ij} u_j - Q_{ij} u_j = 0$	$\sigma \mathbf{u} + \mathbf{u} \cdot \nabla \mathbf{U}_b + \mathbf{U}_b \cdot \nabla \mathbf{u} + \nabla p - \frac{1}{Re} \nabla^2 \mathbf{u} = \mathbf{0}$ $\nabla \cdot \mathbf{u} = 0$
$y_i^* L_{ij}^C + y_i^* \sigma B_{ij} = 0$	$\sigma^* \mathbf{u}^+ + \nabla \mathbf{U}_b \cdot \mathbf{u}^+ - \mathbf{U}_b \cdot \nabla \mathbf{u}^+ + \nabla p^+ - \frac{1}{Re} \nabla^2 \mathbf{u}^+ = \mathbf{0}$ $\nabla \cdot \mathbf{u}^+ = 0$
$z_i^* (N_{ijk} U_k + N_{ikj} U_k + L_{ij} - P_{ij}) =$ $= -y_i^* (N_{ikj} + N_{ijk} + L_{ij}) u_j = 0$	$\nabla \mathbf{U}_b \cdot \mathbf{U}_b^+ - \mathbf{U}_b \cdot \nabla \mathbf{U}_b^+ + \nabla P_b^+ - \frac{1}{Re} \nabla^2 \mathbf{U}_b^+ = \hat{\mathbf{u}}^* \cdot \nabla \hat{\mathbf{u}}^+ - \nabla \hat{\mathbf{u}}^* \cdot \hat{\mathbf{u}}^+$ $\nabla \cdot \mathbf{U}_b^+ = 0$
$\frac{\delta \sigma}{\delta P} \delta P = z_i^* \delta P_{ij} U_j$	$\delta \sigma = \frac{(\mathbf{U}_b^+, \delta \mathbf{F})}{(\hat{\mathbf{u}}^+, \hat{\mathbf{u}})}$
$\frac{\delta \sigma}{\delta Q} \delta Q = y_i^* \delta Q_{ij} u_j$	$\delta \sigma = \frac{\langle \mathbf{u}^+, \delta \mathbf{H}(\mathbf{u}, \mathbf{p}) \rangle}{\langle \mathbf{u}^+, \mathbf{u} \rangle}$

Applications to flow analysis and control

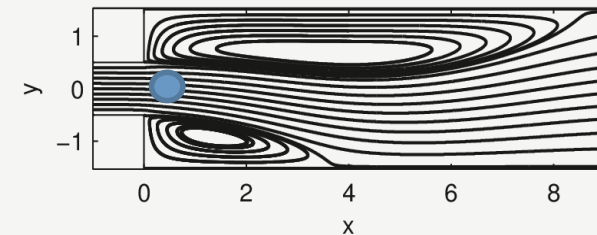


UNIVERSITÀ DI PISA

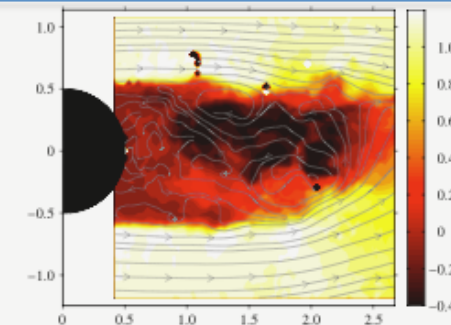
Perturbation of linearized equation:
Prop. Feedback control of vortex shedding
S. Camarri and A. Iollo, PoF 22(094102), 2010



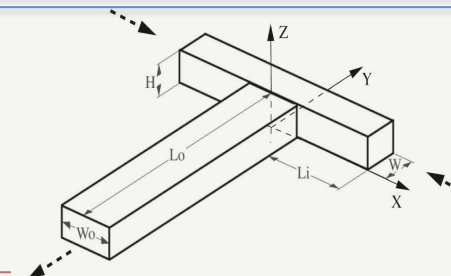
Perturbation of the base-flow equations
Passive control of a pitchfork bifurcation by a control
cylinder in the flow
A. Fani, S. Camarri, and M. V. Salvetti, PoF 24(084102), 2012.



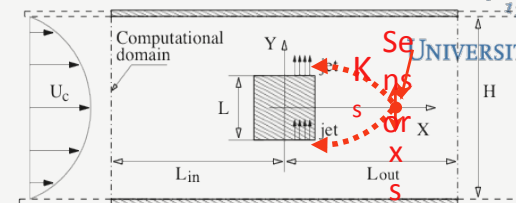
Sensitivity analysis at high Reynolds number:
Application to PIV data past a porous cylinder
S. Camarri, B. E. G. Fallenius, and J. H. M. Fransson, JFM 715, 2013.



Sensitivity analysis and control maps for fully 3D configs:
Application to a fully 3D T-Mixer
A. Fani, S. Camarri, and M. V. Salvetti, accepted, PoF 2013



Perturbation of linearized equation:
 Prop. Feedback control of vortex shedding
S. Camarri and A. Iollo, PoF 22(094102), 2010



Applications to flow analysis and control

Perturbation of linearized equation for the
 design of a proportional feedback control
 of vortex shedding past a bluff body

Flow control by means of a perturbation of the linearized disturbance equations

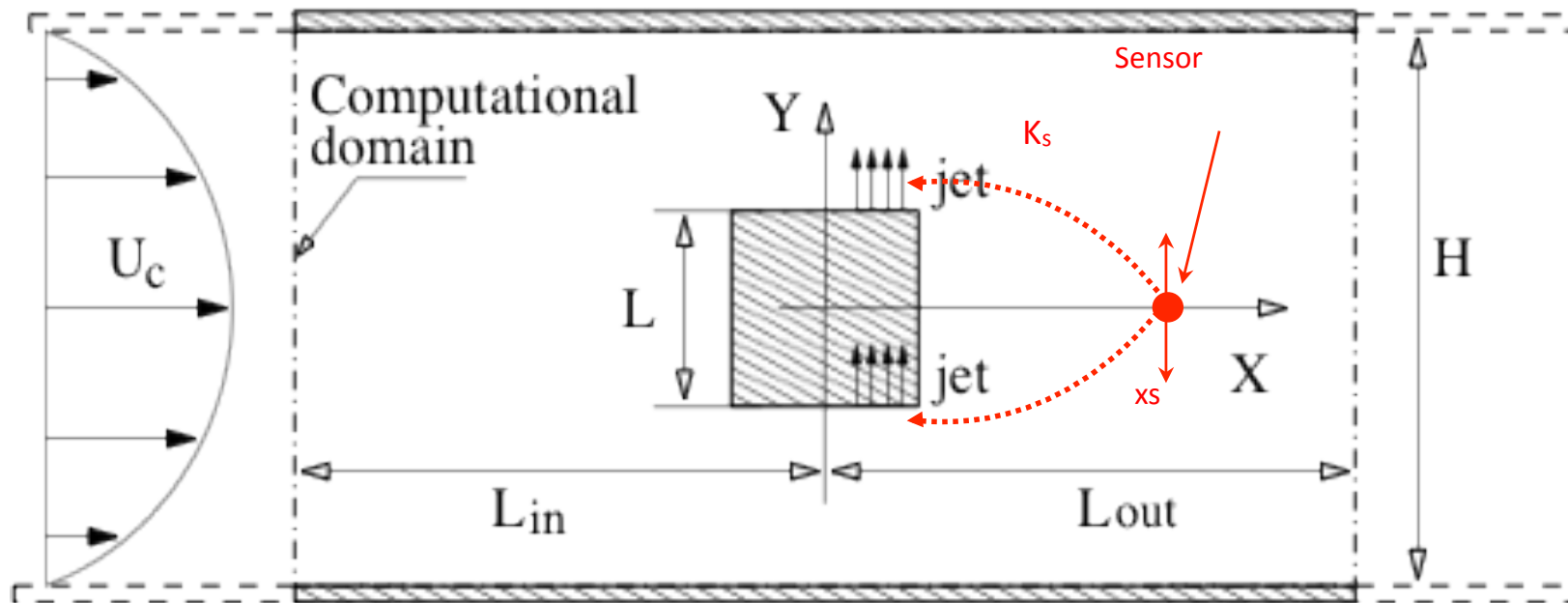
- Typical case when the applied control leaves the mean flow unaltered and the control acts only on the linearized equations
- Example: a feedback control based only on the perturbation field to control the vortex shedding instability past a cylinder:
 - Proof of concept for the use of sensitivity analysis for flow control
 - Realizable control: a few velocity probes, surface jets as actuators, simple proportional feedback control
 - Objective of control: to make the steady flow linearly stable
 - Proposal of an iterative strategy because the control based solely on the sensitivity analysis of uncontrolled flow can be misleading (action of control out of the linear range).

Flow control by means of a perturbation of the linearized disturbance equations



UNIVERSITÀ DI PISA

- Flow configuration (incompressible 2D flow):

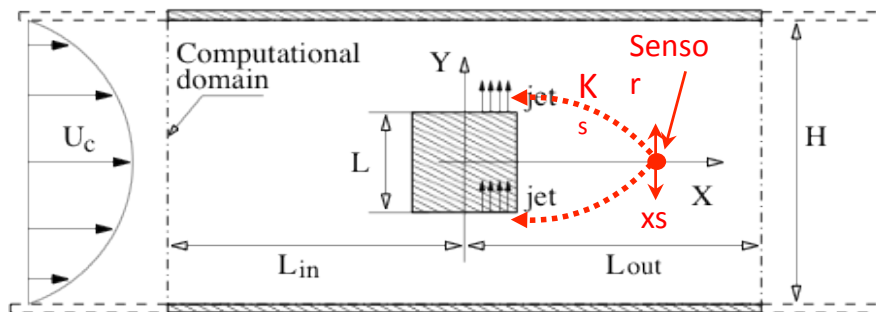


Flow control by means of a perturbation of the linearized disturbance equations



UNIVERSITÀ DI PISA

- Flow configuration (incompressible 2D flow):



Jet width: $0.16 L$

Comp. domain dims:

$-12.5L \leq x \leq 20.5L$

$-4L \leq x \leq 4L$

GR1 540X330 ($\sim 5 \cdot 10^5$ dof)

GR2 810X494 ($\sim 10^6$ dof)

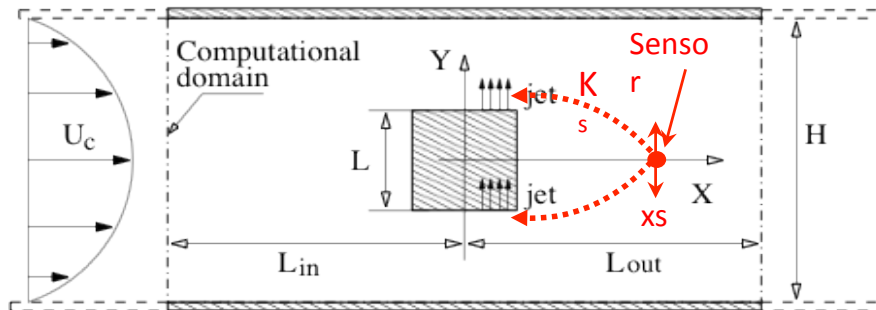
- Reference quantities: U_c, L
- Critical Reynolds number for primary instability: $Re_{cr} \simeq 59$
- Objective of control: **linearly stabilize the steady unstable solution for $Re > 59$**

Flow control by means of a perturbation of the linearized disturbance equations



UNIVERSITÀ DI PISA

- Flow configuration (incompressible 2D flow):



- **Boundary conditions on the jet surface S_j** : proportional feedback from a set of ideal velocity probes.
- Only the difference between the measured flow and the steady unstable field is fed back to the actuators: **the steady unstable flow remains a solution of the controlled flow**



Sensitivity analysis at discrete level

- This control perturbs only the linearized stability equations:

$$L_{ij}^C u_j + \sigma B_{ij} u_j - Q_{ij} u_j = 0$$

- The control matrix Q at discrete level can be represented as follows:

$$Q = - \sum_{s=1}^{N_s} K_s C(x_s, y_s, \theta_s)$$

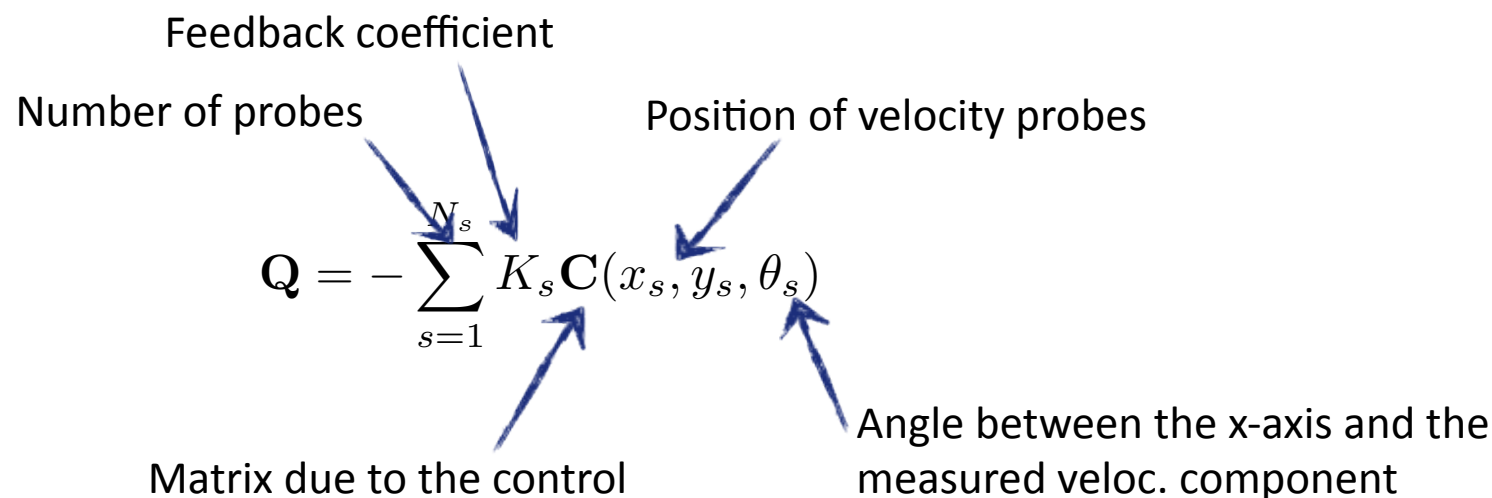


Sensitivity analysis at discrete level

- This control perturbs only the linearized stability equations:

$$L_{ij}^C u_j + \sigma B_{ij} u_j - Q_{ij} u_j = 0$$

- The control matrix Q at discrete level can be represented as follows:



Sensitivity analysis at discrete level

- This control perturbs only the linearized stability equations:

$$L_{ij}^C u_j + \sigma B_{ij} u_j - Q_{ij} u_j = 0$$

- The control matrix Q at discrete level can be represented as follows:

$$Q = - \sum_{s=1}^{N_s} K_s C(x_s, y_s, \theta_s)$$

- The effect of perturbation is computed by the adjoint stab. problem:

$$y_i^* L_{ij}^C + y_i^* \sigma B_{ij} = 0$$

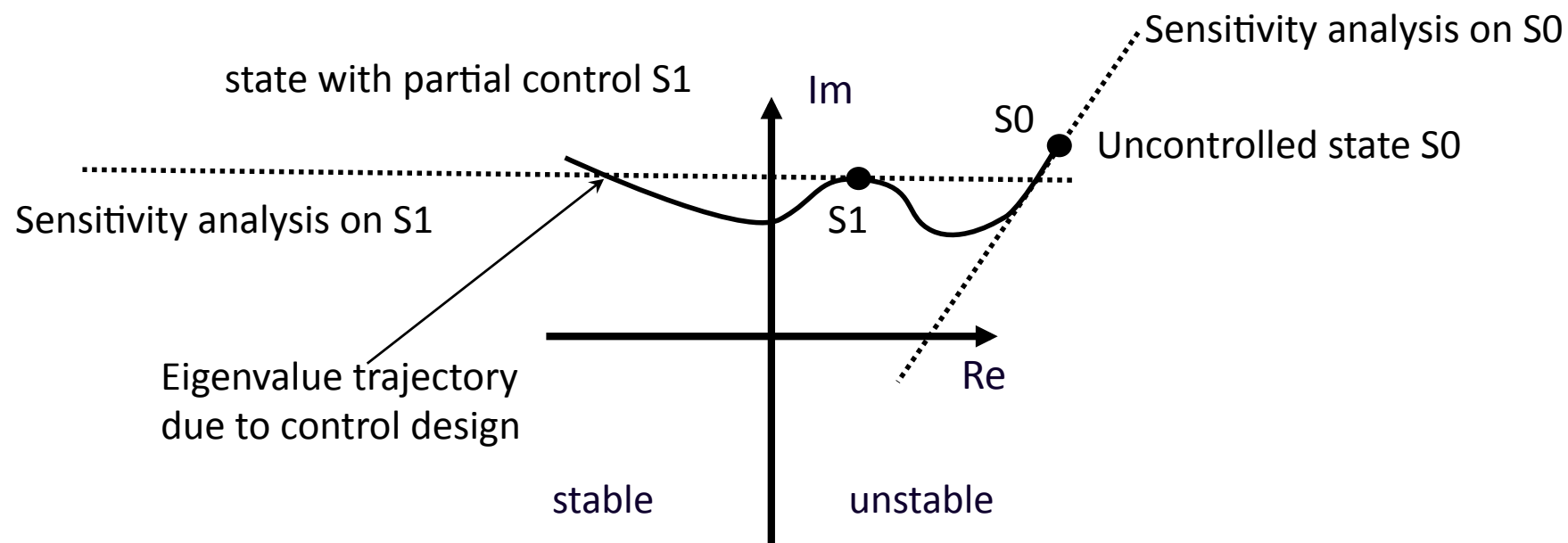
$$\delta\sigma = y_i^* \delta Q_{ij} u_j$$

- To design the control we need to know the perturbation matrix Q as a function of the control parameters (feedback coeff and position of probes)

$$\delta Q = \sum_{s=1}^{N_s} \left\{ [C(x_s, y_s, \theta_s)] \delta K_s + \left[K_s \frac{\partial C}{\partial x_s}(x_s, y_s, \theta_s) \right] \delta x_s + \left[K_s \frac{\partial C}{\partial y_s}(x_s, y_s, \theta_s) \right] \delta y_s + \left[K_s \frac{\partial C}{\partial \theta_s}(x_s, y_s, \theta_s) \right] \delta \theta_s \right\}$$

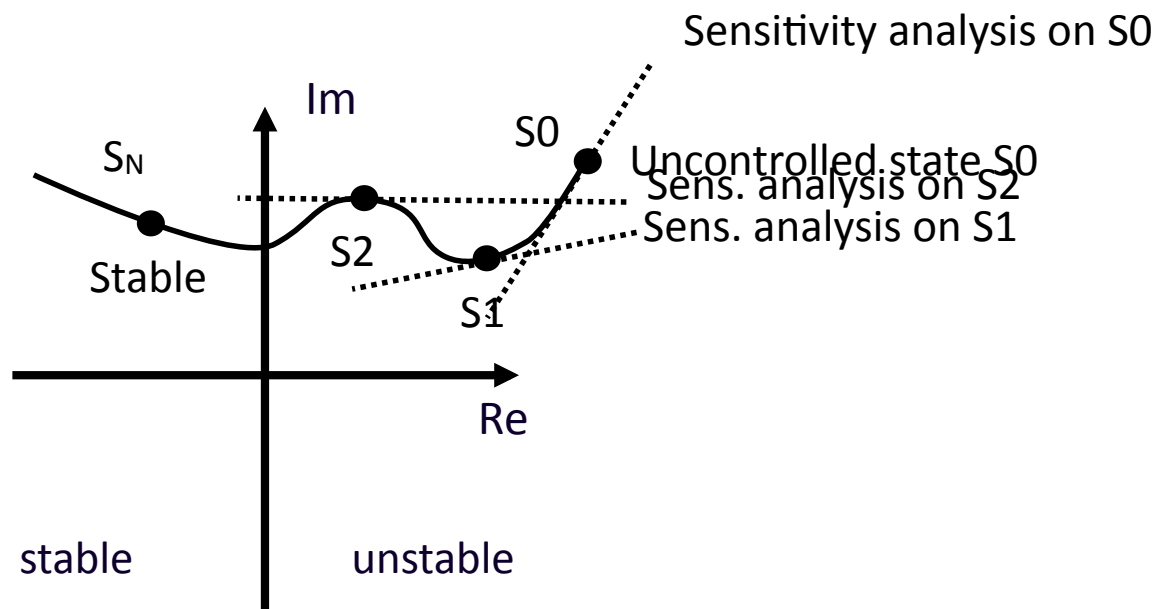
Design of the control

The adjoint analysis allows to predict the shift of the eigenvalue of the discrete system as the control parameters (feedback coefficients, sensor positions, measured veloc. component) are perturbed.



Design of the control

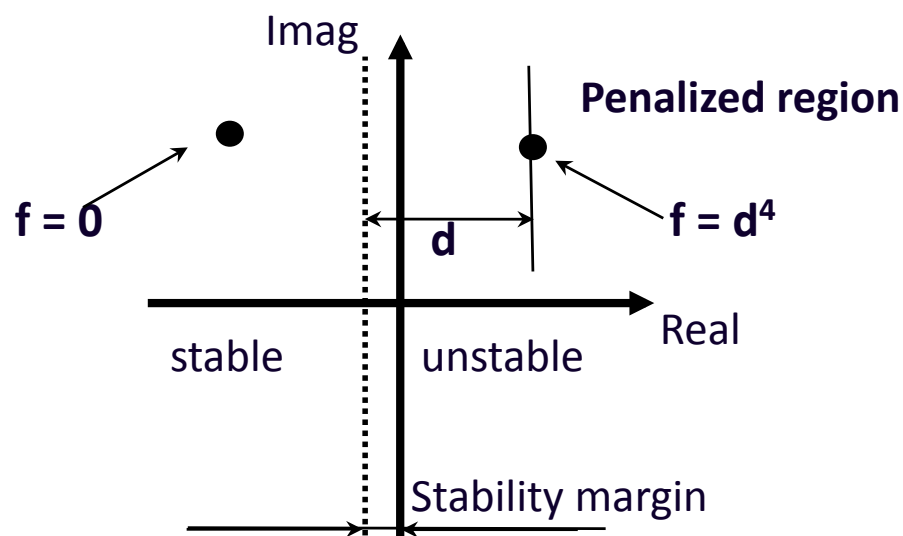
We can design the control strategy iteratively, by driving the unstable eigenvalues in the stable region of the complex plane



Design of the control

- Stable eigenvalues are perturbed also by the control and may eventually become unstable
- Adopted strategy to control the spectrum: define a function of the spectrum of the controlled system such that the minimum is reached when the system is stabilized. The previous analysis allows the computation of the gradient of the function.
- The control is designed by minimizing this function f , which depends on the control parameters

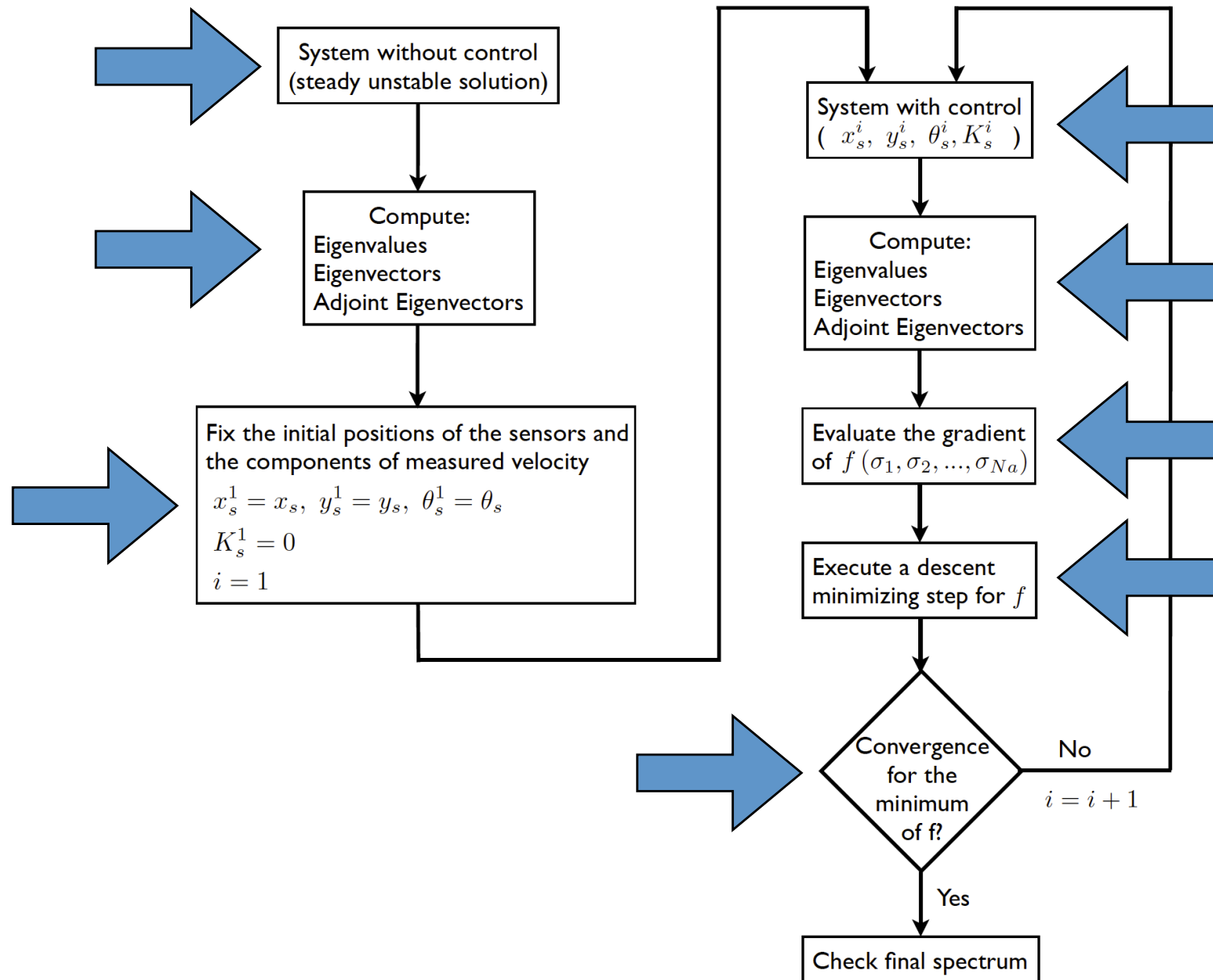
The minimum of f ($=0$) is obtained when all the eigenvalues are stable



Design of the control



UNIVERSITÀ DI PISA

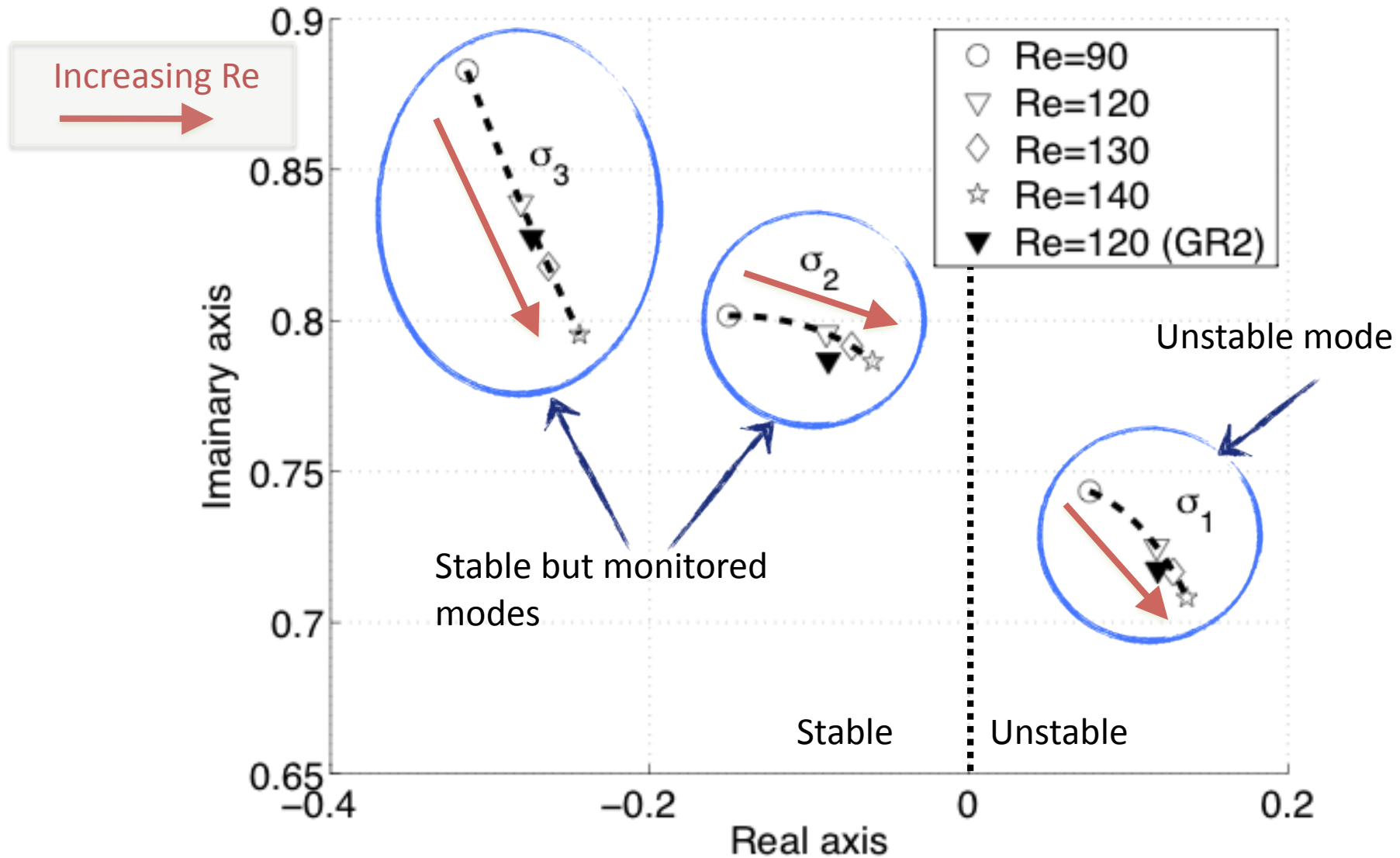


Iterative process:
to bypass the fact
that the sensitivity
analysis gives results
that are accurate
only for a small
perturbation of the
control parameters
(linearized analysis).

Results: spectrum of the uncontrolled system



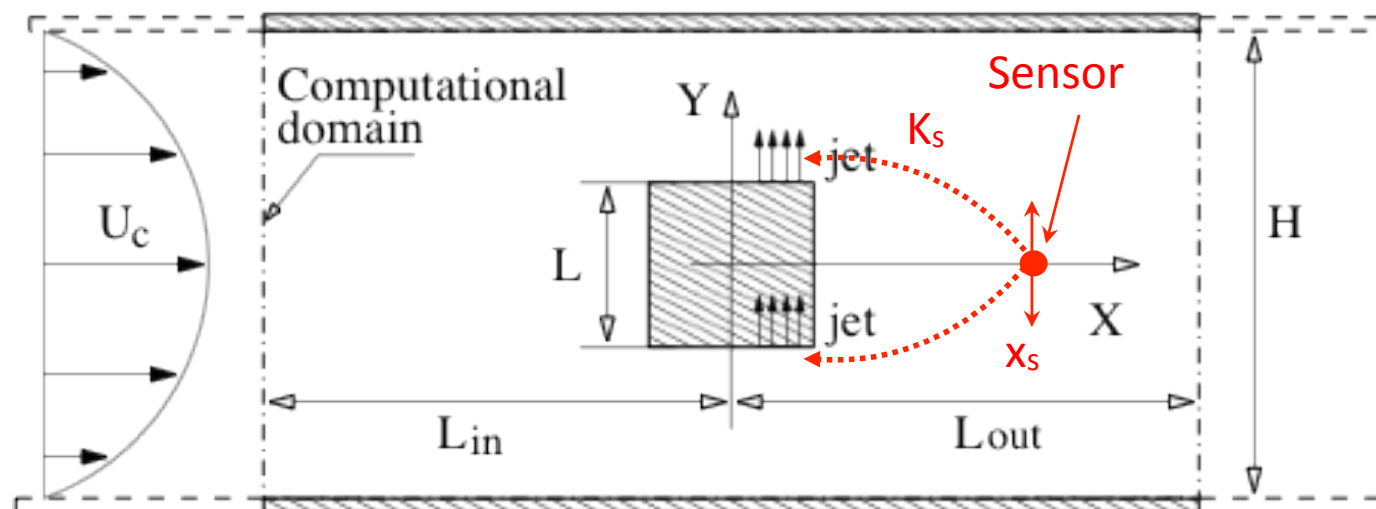
UNIVERSITÀ DI PISA



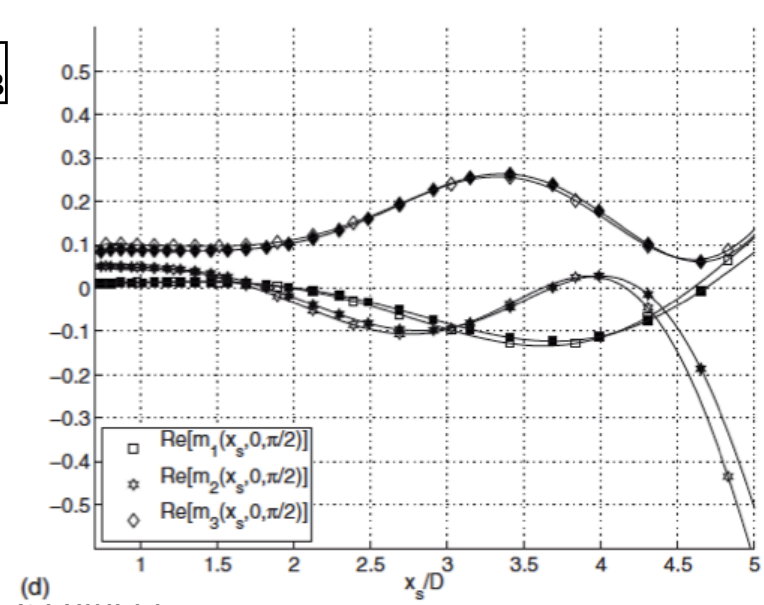
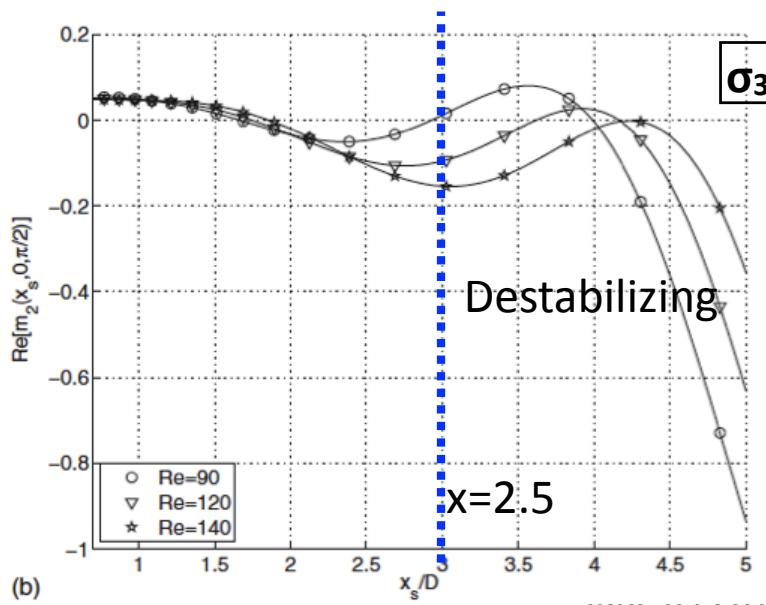
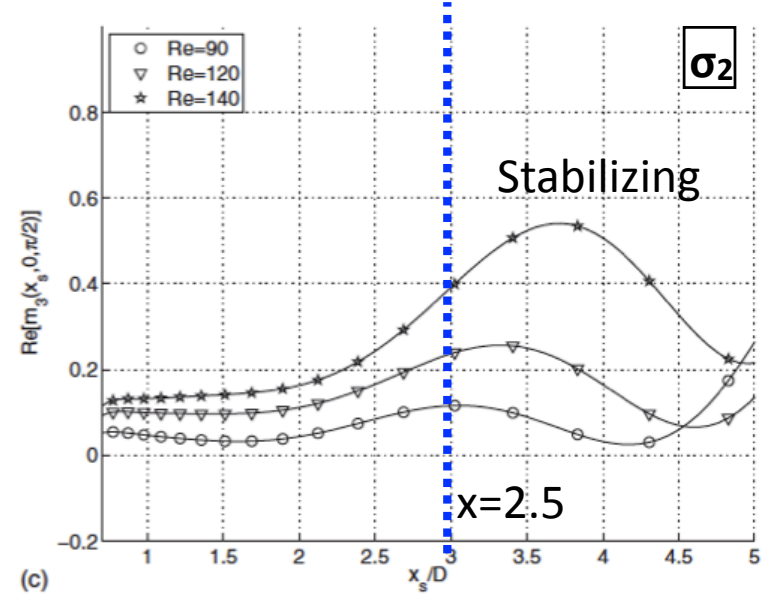
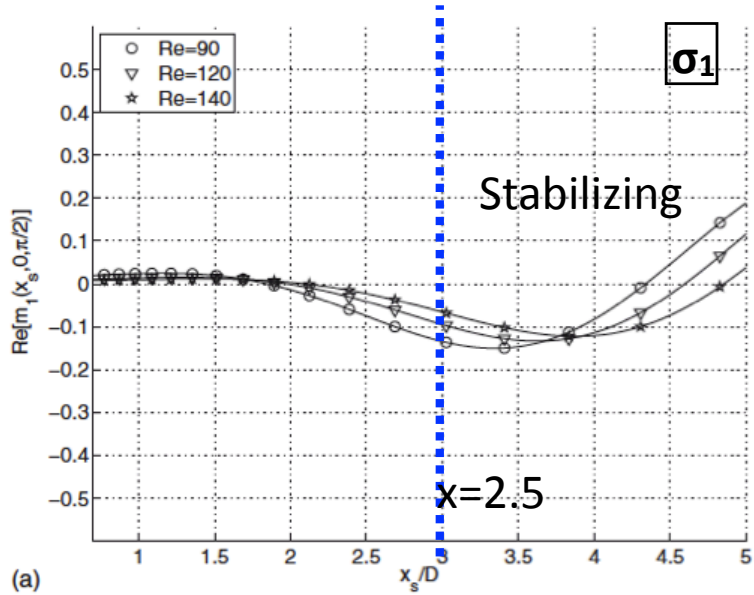
Results

Examples of controls using one velocity sensor placed in the wake on the symmetry line, measuring the vertical component of velocity.

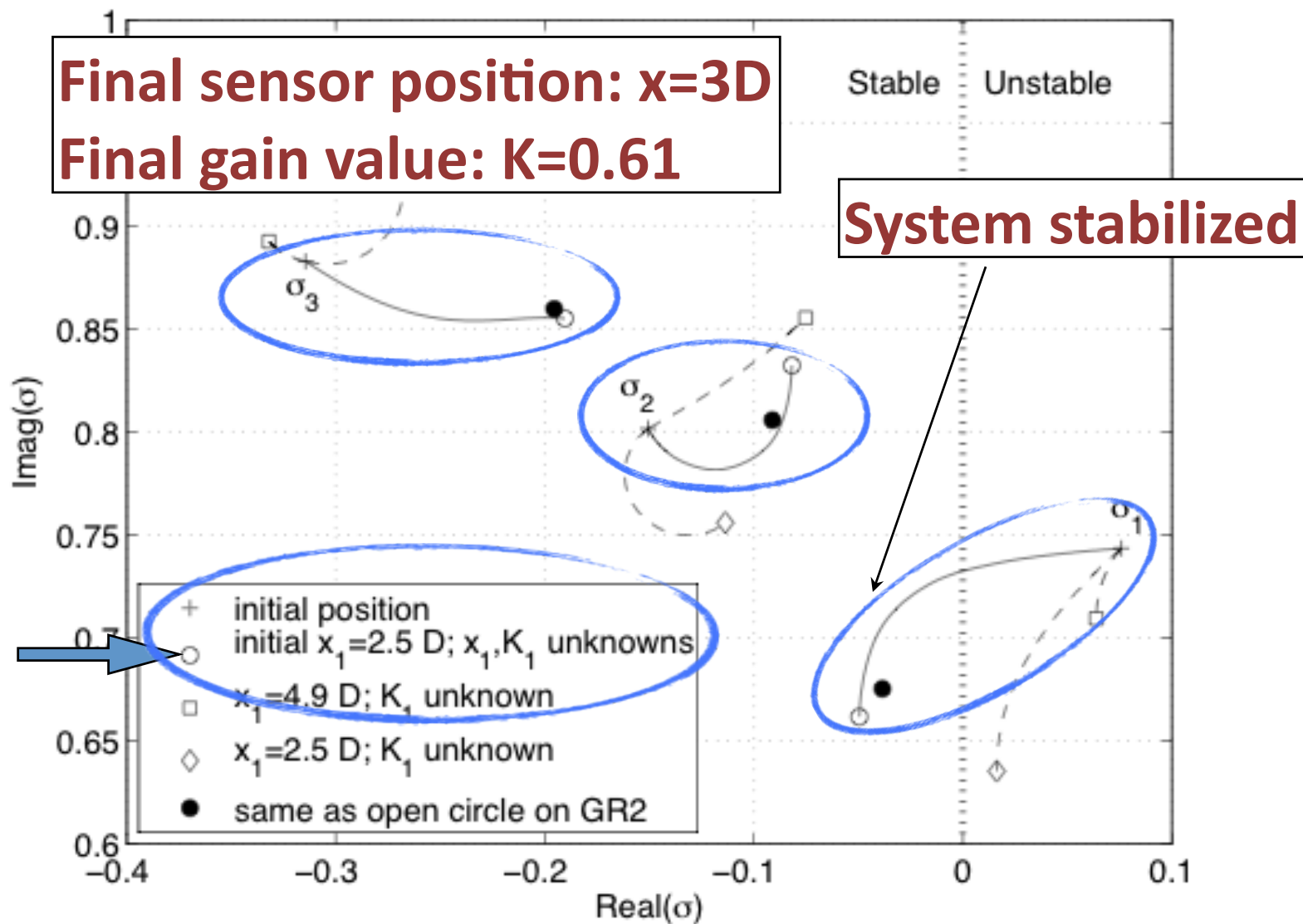
Control parameters: x_s , k_s



Results: sensitivity maps with respect to the uncontrolled state (constraint: $y_s=0$, vert. veloc)

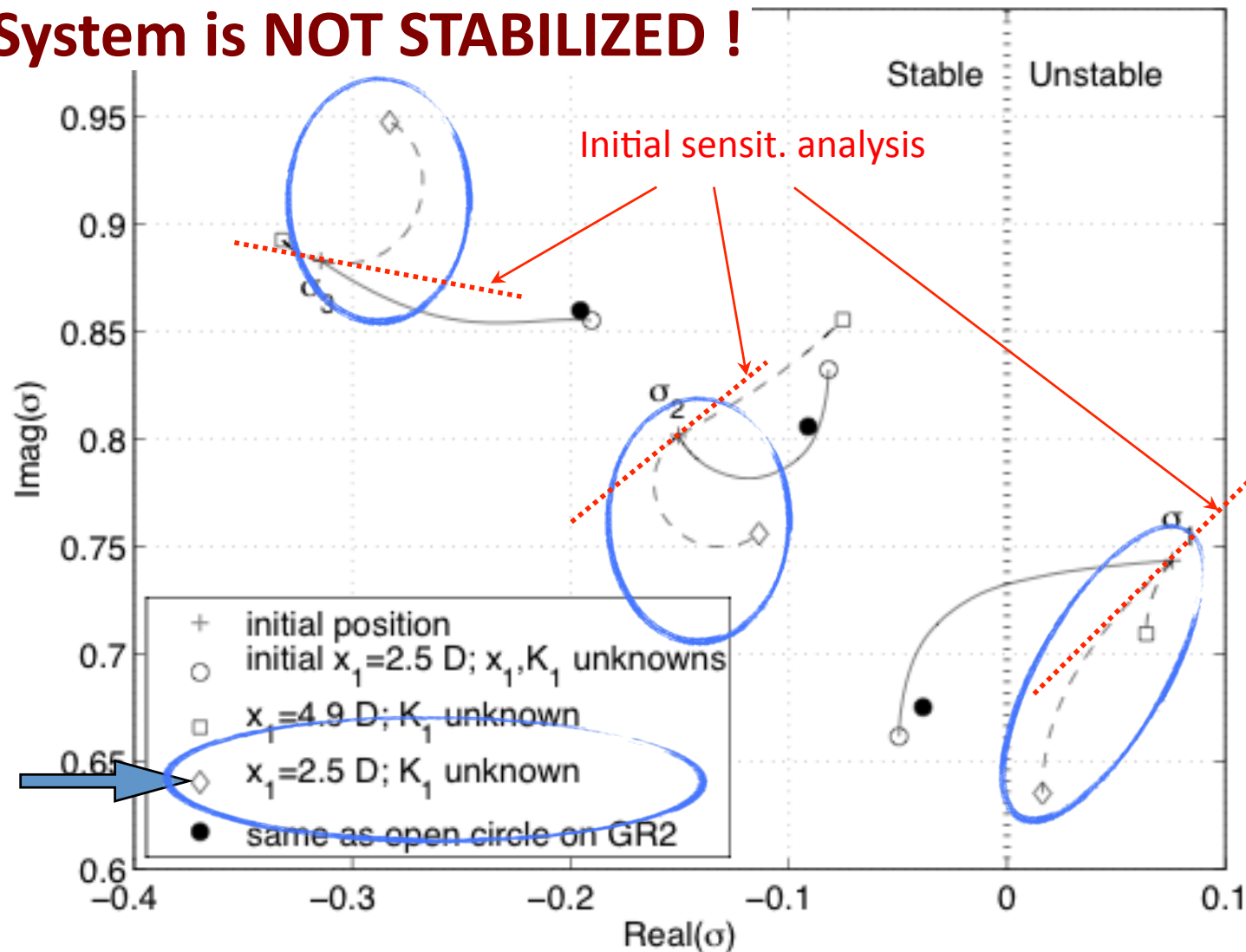


Results: examples of control at $\text{Re}=90$ (constraint: one vert.veloc. sensor with $y_s=0$)



Results: examples of control at $\text{Re}=90$ (constraint: sensor position fixed)

System is NOT STABILIZED !

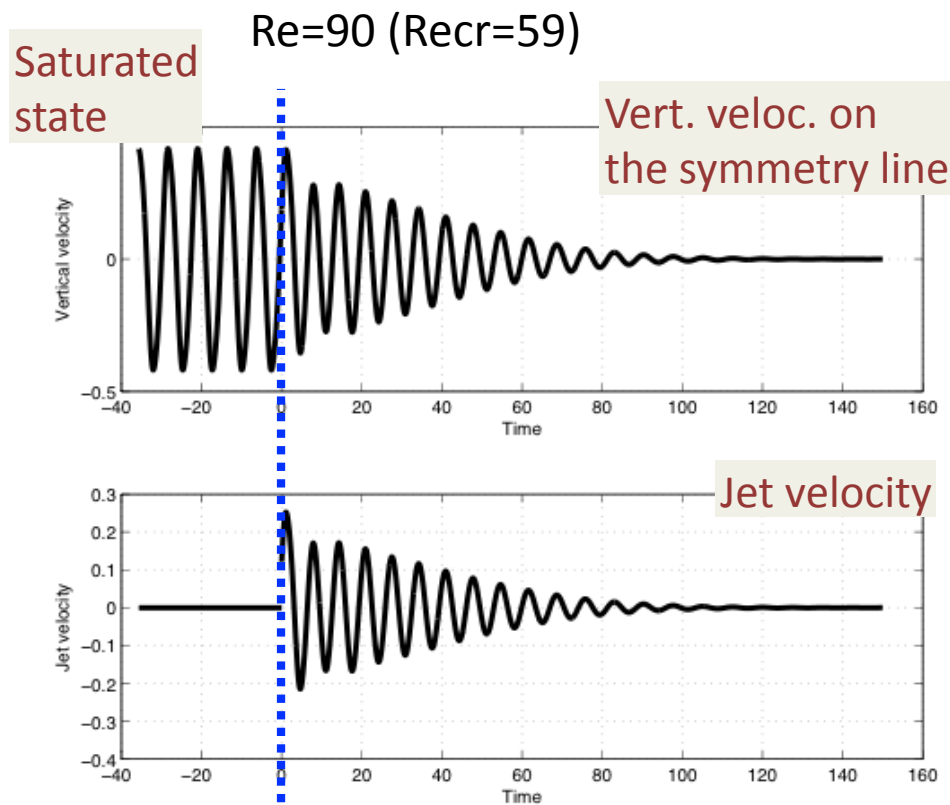


Attraction basin of the stabilized system (a-posteriori tests)

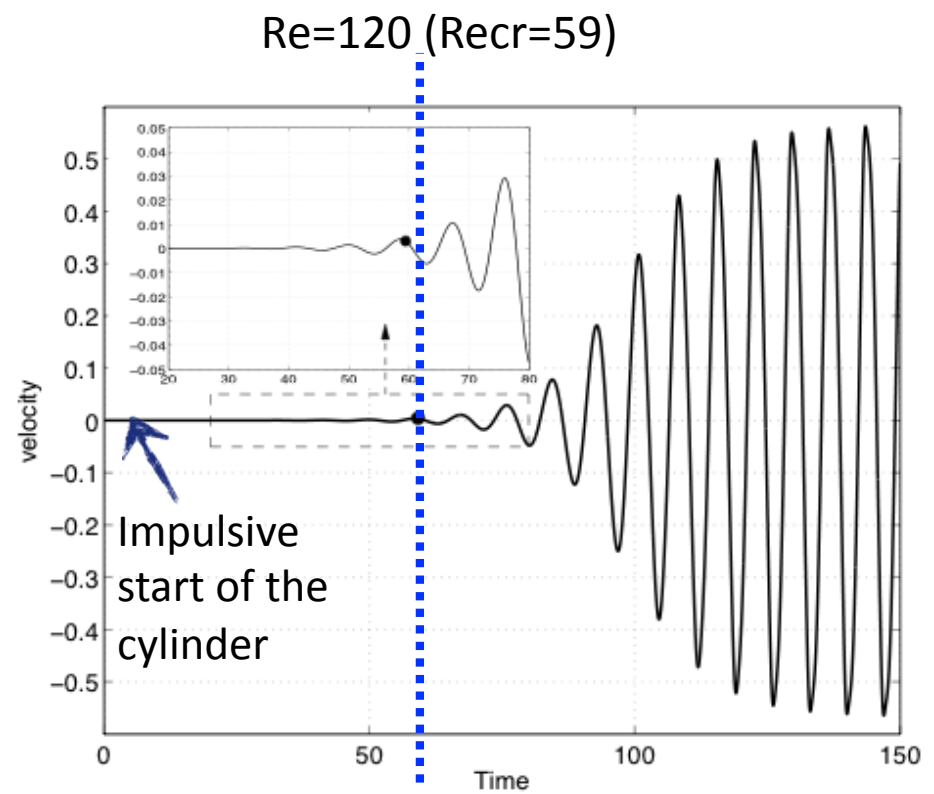


UNIVERSITÀ DI PISA

The design guarantees that, when finished with success, the steady solution is linearly stable. The basin of attraction of this stable point for the system needs to be explored a-posteriori.

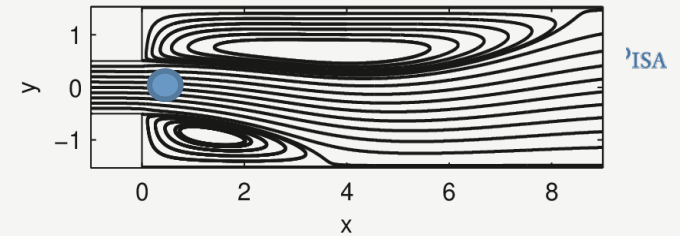


Impulsive application of the control



Maximum amplitude of the unstable mode counter-acted by the control

Perturbation of the base-flow equations
 Passive control of a pitchfork bifurcation by a control
 cylinder in the flow
A. Fani, S. Camarri, and M. V. Salvetti, PoF 24(084102), 2012.



Applications to flow analysis and control

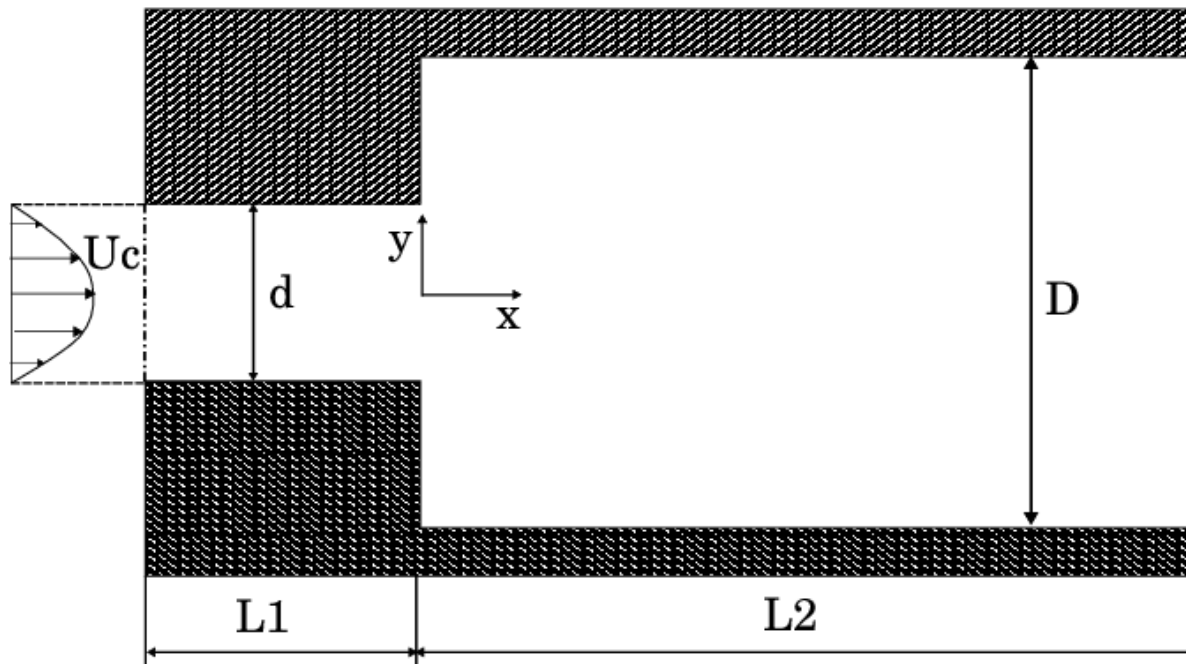
Passive control of the pitchfork instability
 in a symmetric plane channel with a
 sudden expansion

Symmetric plane channel with a sudden expansion



UNIVERSITÀ DI PISA

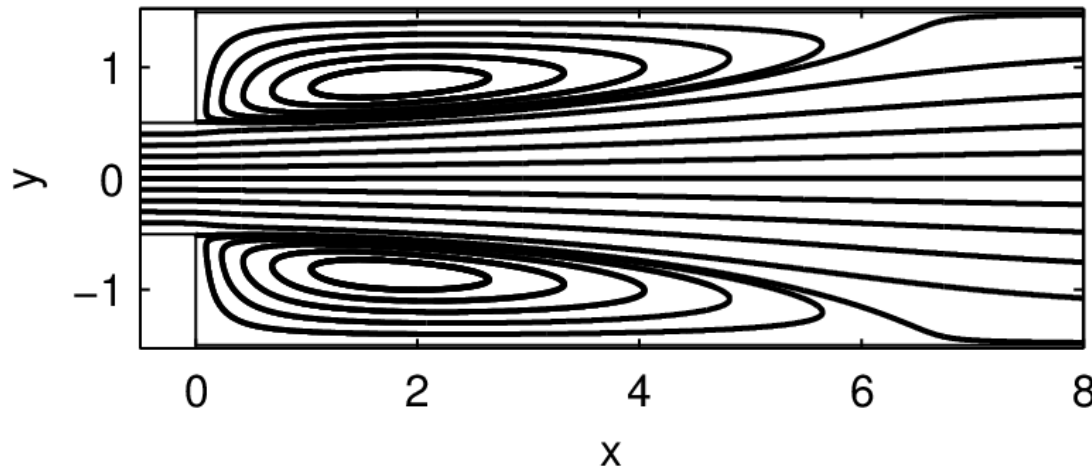
Incompressible flow in a 2-D plane channel with $ER=D/d=3$



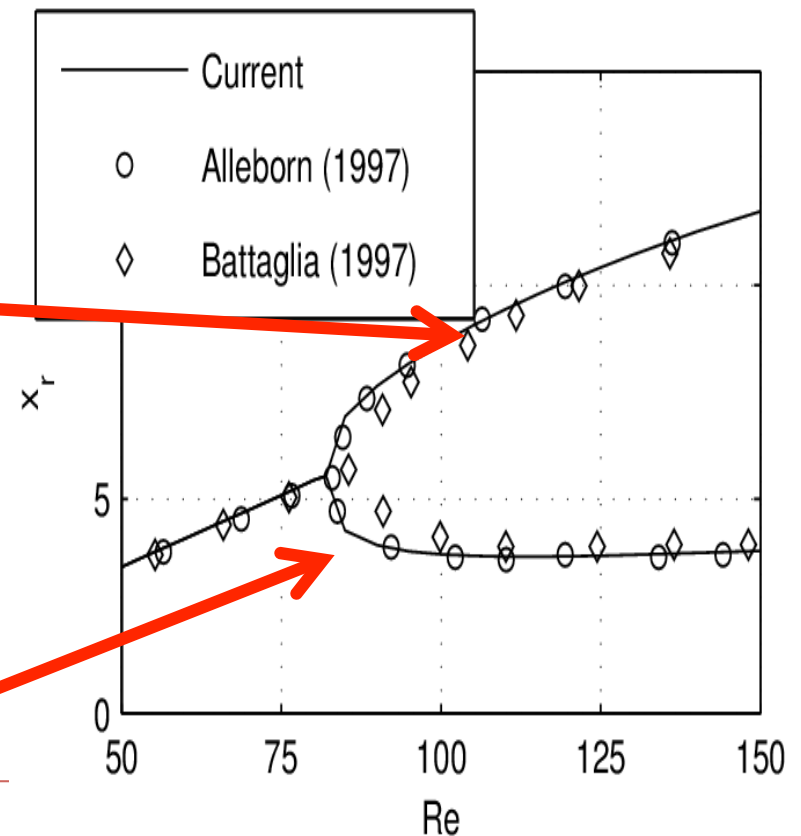
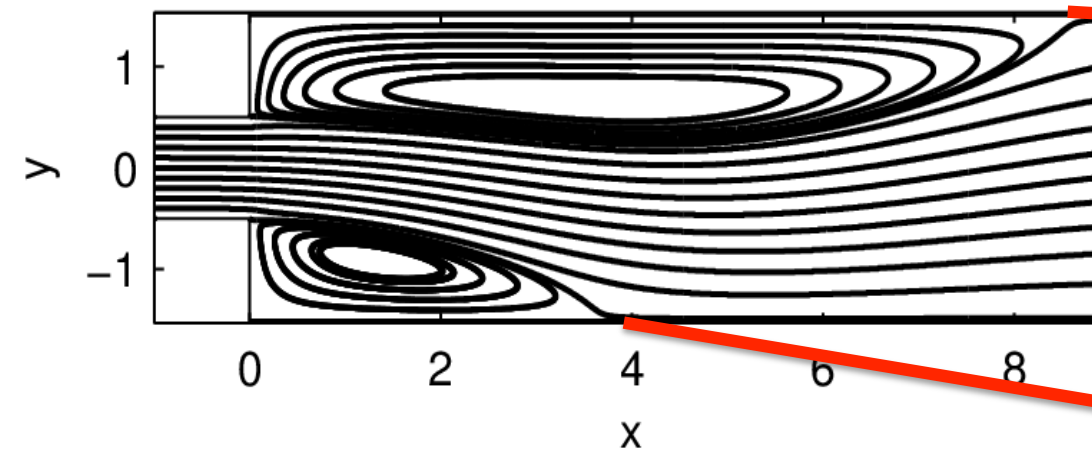
Symmetric plane channel with a sudden expansion



UNIVERSITÀ DI PISA

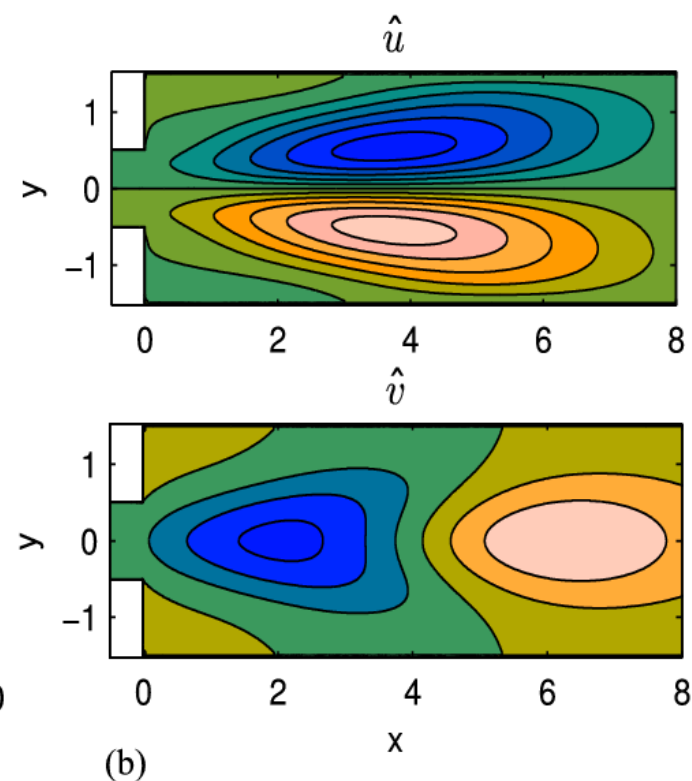
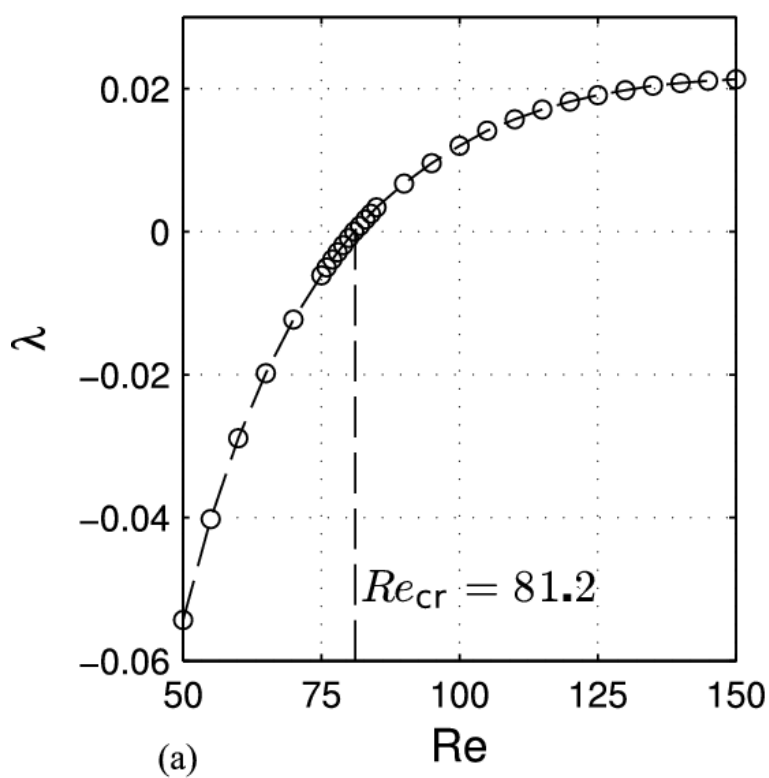


Either symmetric or asymmetric solution depending on the flow Reynolds number as compared to some critical value



I: Stability analysis

Real valued eigenmode is found ($\omega = 0$)





II: passive control strategy

- 1 A small **control cylinder** of diameter d^* , introduced in the channel at the position (x_0, y_0)



II: passive control strategy

- 1 A small **control cylinder** of diameter d^* , introduced in the channel at the position (x_0, y_0)
- 2 The cylinder is modeled by the force it exerts on the flow



II: passive control strategy

- 1 A small **control cylinder** of diameter d^* , introduced in the channel at the position (x_0, y_0)
- 2 The cylinder is modeled by the force it exerts on the flow

- 3 Linearized drag force:

$$F \approx -\alpha \left[\|U_b\| (U_b + \hat{u}) + \left(\frac{U_b}{\|U_b\|} \cdot \hat{u} \right) U_b \right] \delta(x - x_0, y - y_0)$$

II: passive control strategy

① A small **control cylinder** of diameter d^* , introduced in the channel at the position (x_0, y_0)

② The cylinder is modeled by the force it exerts on the flow

③ Linearized drag force:

$$F \approx -\alpha \left[\|U_b\| (U_b + \hat{u}) + \left(\frac{U_b}{\|U_b\|} \cdot \hat{u} \right) U_b \right] \delta(x - x_0, y - y_0)$$

④ $\alpha = \alpha(d^*)$ The force amplitude is a function of the cylinder diameter.

II: passive control strategy

① A small **control cylinder** of diameter d^* , introduced in the channel at the position (x_0, y_0)

② The cylinder is modeled by the force it exerts on the flow

③ Linearized drag force:

$$F \approx -\alpha \left[\|U_b\| (U_b + \hat{u}) + \left(\frac{U_b}{\|U_b\|} \cdot \hat{u} \right) U_b \right] \delta(x - x_0, y - y_0)$$

④ $\alpha = \alpha(d^*)$ The force amplitude is a function of the cylinder diameter.

Eigenvalue variation caused by the cylinder

The drag is a function of both base flow and perturbation.

$$\delta\sigma = \delta\sigma(U_b, \hat{u})$$

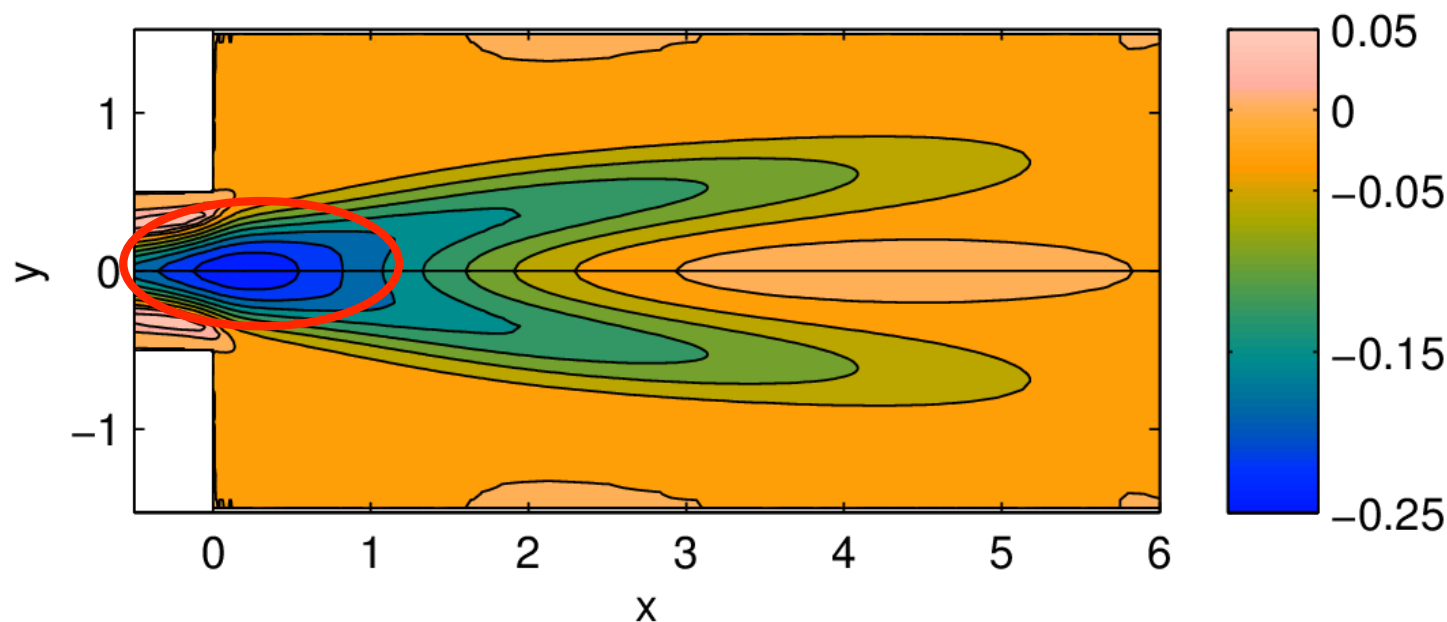
We can estimate the effect of both the two different contributions to the force on the instability using the previous analysis.

II: passive control strategy

We can define a sensitivity function S , which gives the eigenvalue variation for each position of the cylinder (x_0, y_0) :

$$\delta\sigma = \alpha S(x_0, y_0)$$

α is a function of the cylinder diameter d^*



The minimum value of S is at $x_0 = 0.15$ $y = 0 \rightarrow$ **optimal position**

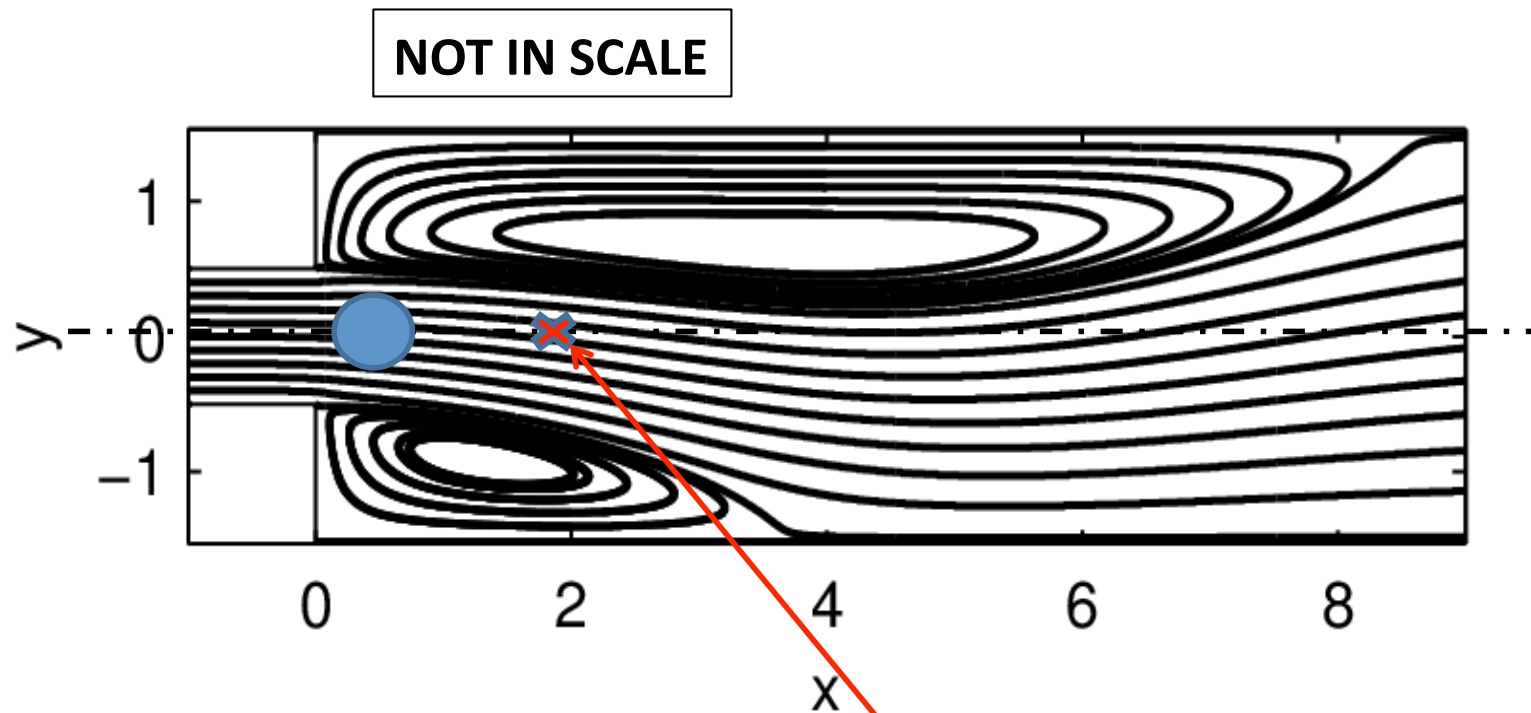
III: Investigation of the control strategy by DNS



UNIVERSITÀ DI PISA

Cylinder introduced impulsively, starting from the asymmetric state

$$d^* = 0.02 \quad x_0 = 0.15 \quad y_0 = 0$$



Vertical velocity measured in a point on the centerline

III: Investigation of the control strategy by DNS

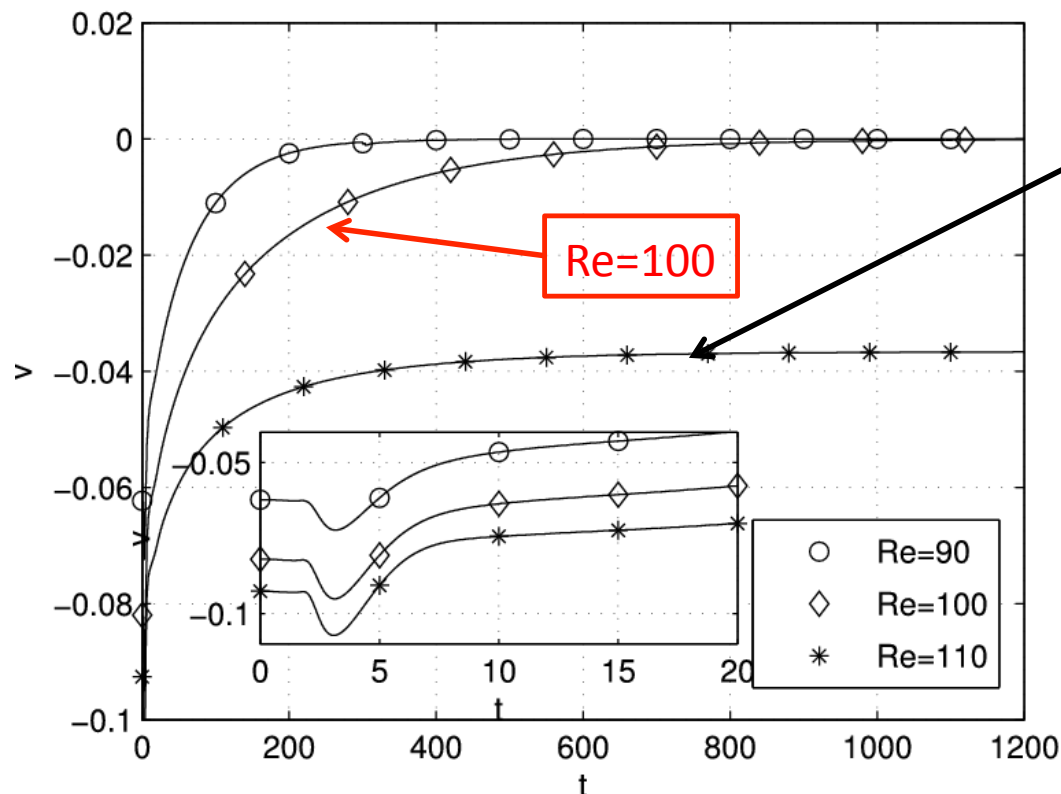


UNIVERSITÀ DI PISA

Cylinder introduced impulsively, starting from the asymmetric state

$$d^* = 0.02 \quad x_0 = 0.15 \quad y_0 = 0$$

Time trace of the vertical velocity
in a point along the centerline

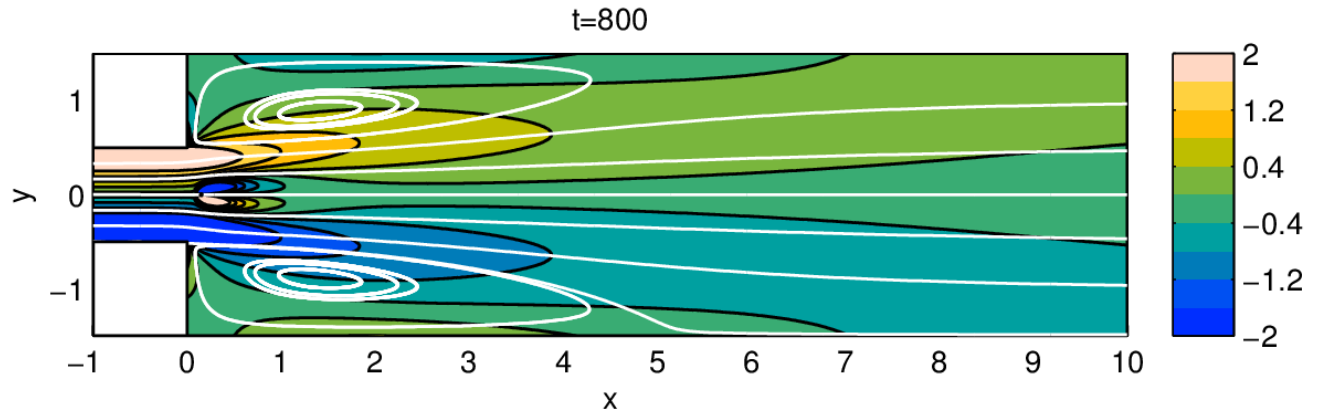
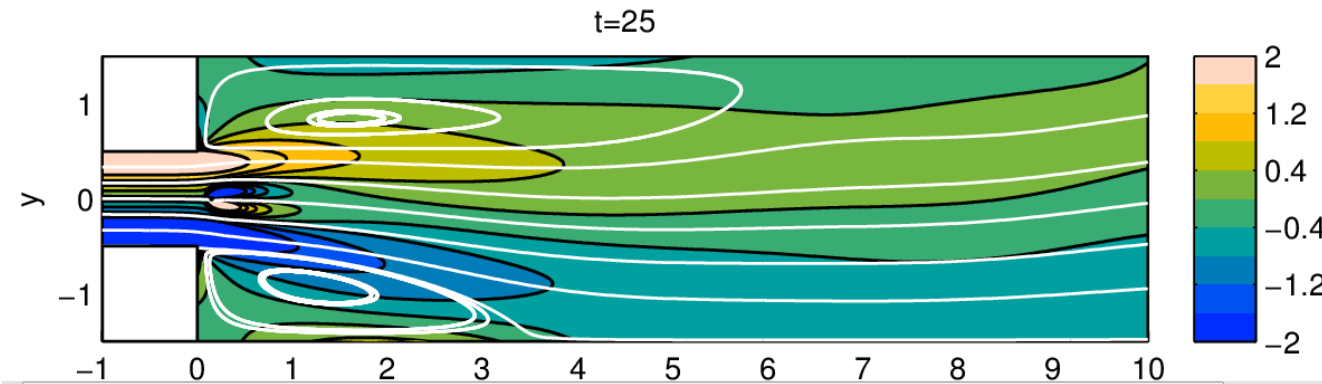
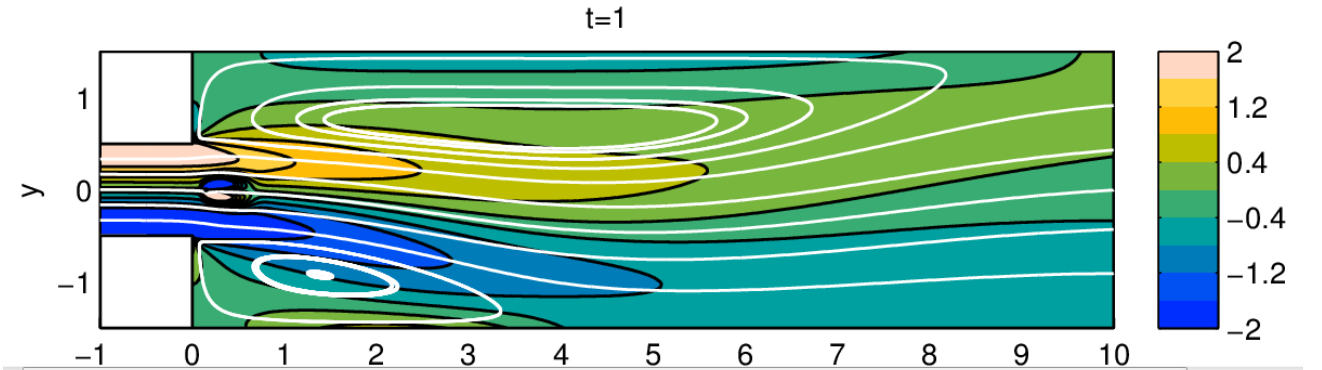


III: Investigation of the control strategy by DNS



UNIVERSITÀ DI PISA

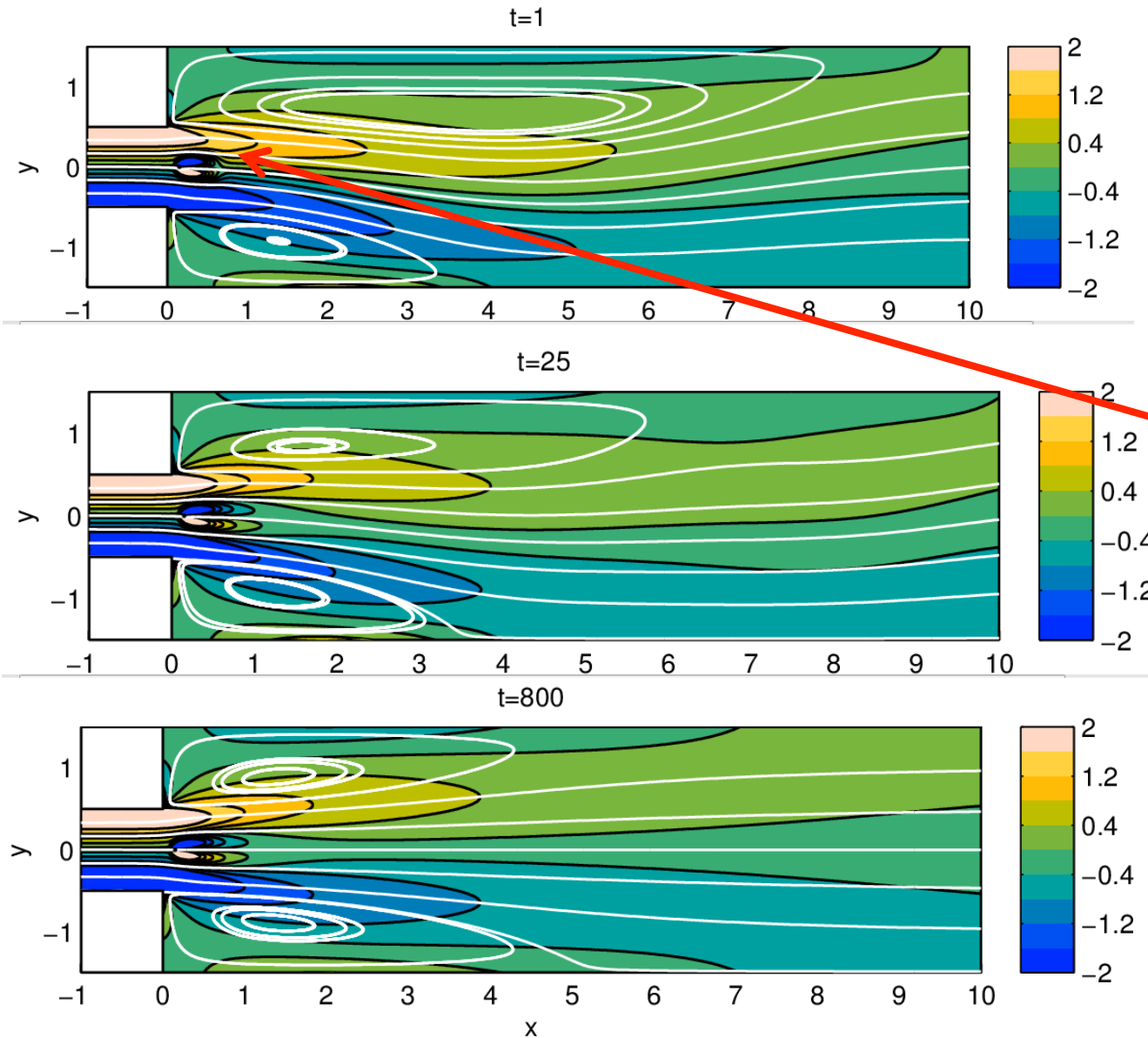
$Re=100 \quad d^* = 0.02$



III: Investigation of the control strategy by DNS



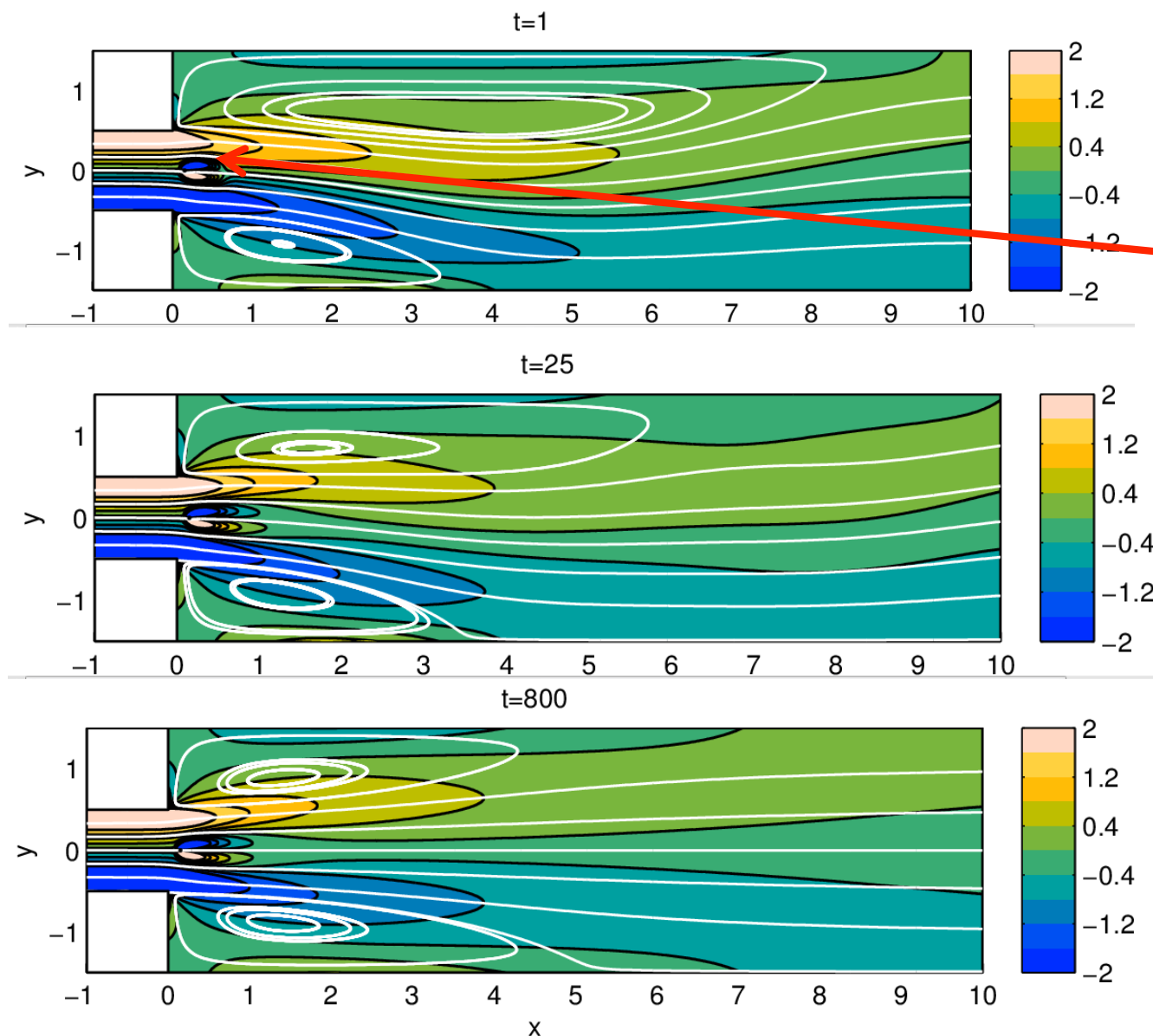
UNIVERSITÀ DI PISA



$Re=100 \quad d^* = 0.02$

Weak interaction between the vorticity of the cylinder wake and the wall vorticity

III: Investigation of the control strategy by DNS

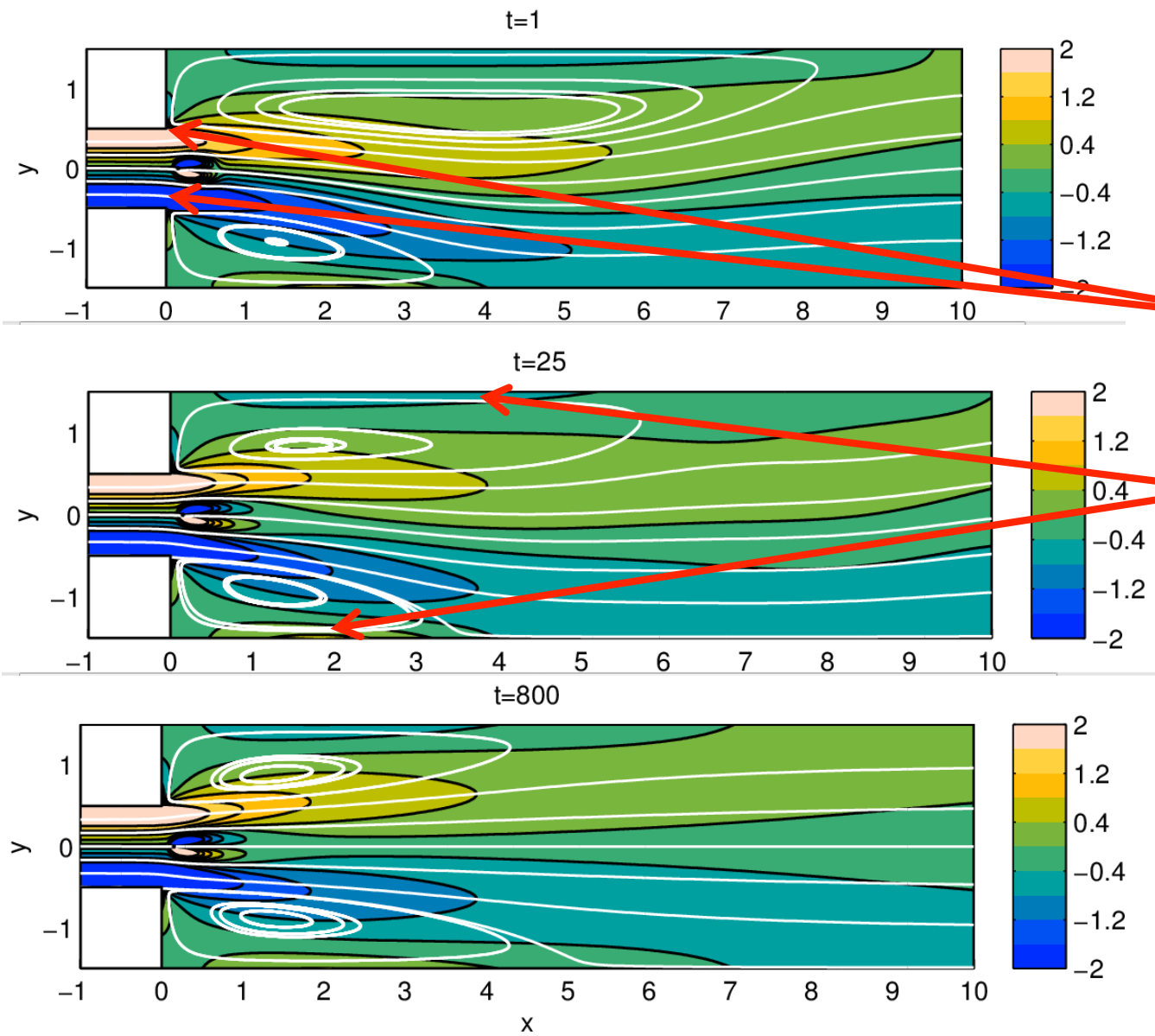


$$\text{Re}=100 \quad d^* = 0.02$$

- **Deviation** of the streamlines entering the channel from the smaller one.
- **Asymmetric** deviation: the streamline on the centerline is deviated towards the part where the separation is smaller

III: Investigation of the control strategy by DNS

$Re=100 \quad d^* = 0.02$

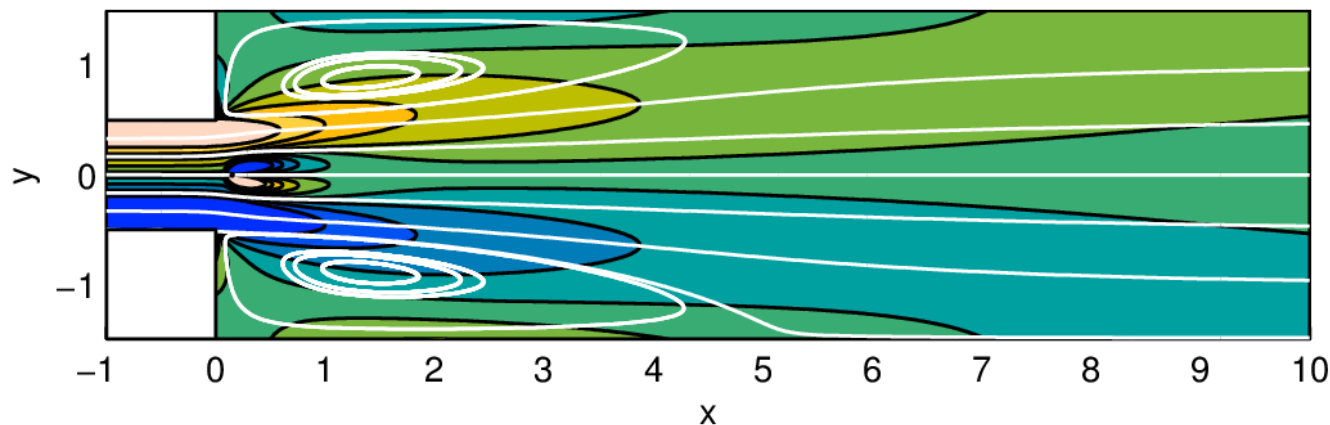


Two effects:

1. Convection of vorticity from the smaller channels
2. Alteration of the streamlines and production of vorticity at the channel walls.

III: Investigation of the control strategy by DNS UNIVERSITÀ DI PISA

We try to isolate one of the two effect to understand their role in the control



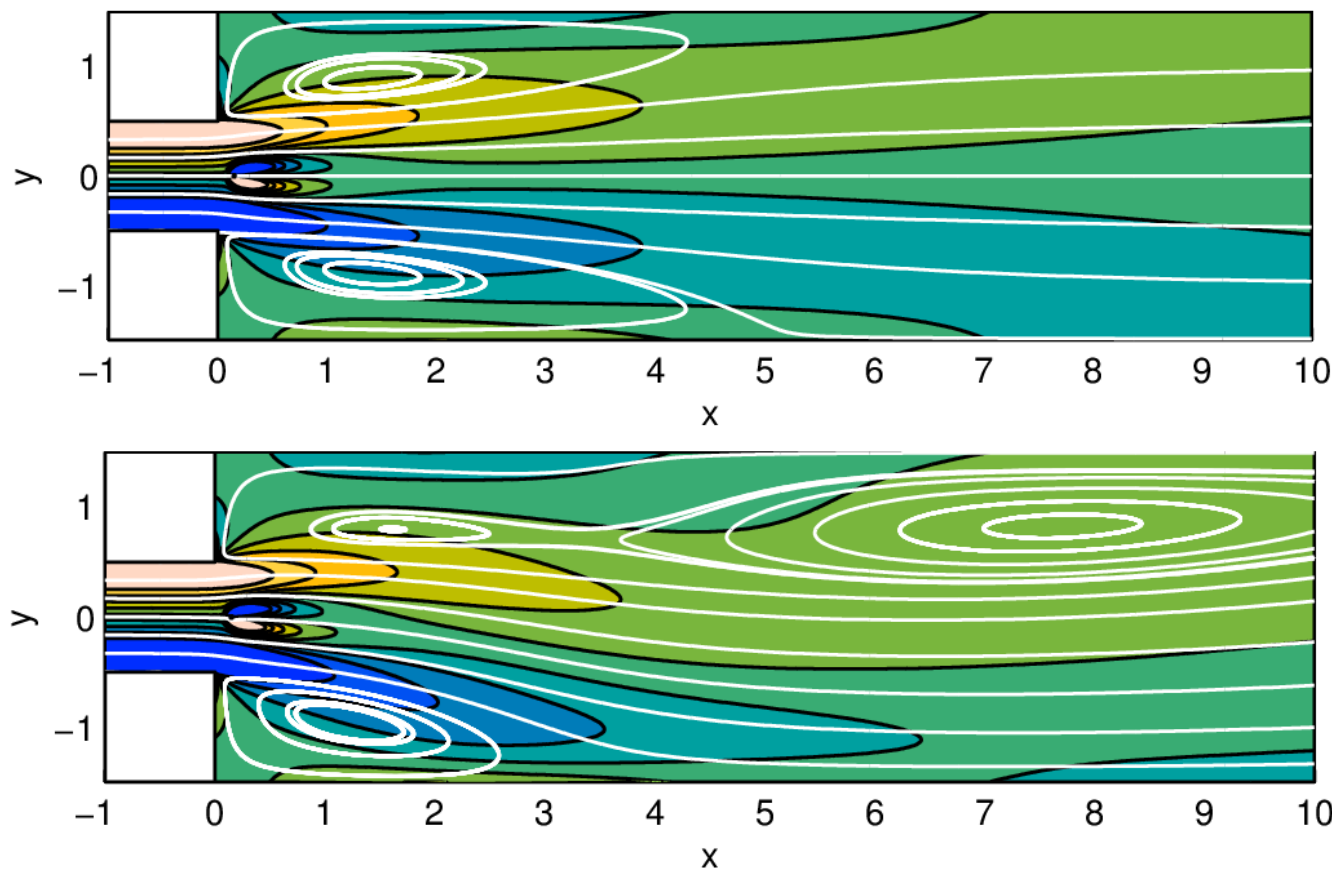
The initial state is the controlled symmetric solution

Ad hoc simulation where the production of new vorticity from the walls in the larger channel is annihilated :

- Navier Stokes equations in terms of disturbance
- Slip condition for the perturbation

III: Investigation of the control strategy by DNS

We try to isolate one of the two effect to understand their role in the control



Ad hoc simulation where the production of new vorticity from the walls in the larger channel is annihilated :

- Navier Stokes equations in terms of disturbance
- Slip condition for the perturbation

Modifications in terms of convection of vorticity from the smaller channel is not sufficient to control the instability



III: Non linear effects of the controlling force amplitude on the eigenvalue estimation

Eigenvalue drift evaluated with sensitivity analysis is exact only for **infinitesimal** perturbations.

$\bar{\lambda} = \lambda_0 + \alpha S(x_0, y_0)$ where $\bar{\lambda}$ is the growth rate predicted by the sensitivity analysis and λ_0 is the growth rate for the uncontrolled flow.



III: Non linear effects of the controlling force amplitude on the eigenvalue estimation

Eigenvalue drift evaluated with sensitivity analysis is exact only for **infinitesimal** perturbations.

$\bar{\lambda} = \lambda_0 + \alpha S(x_0, y_0)$ where $\bar{\lambda}$ is the growth rate predicted by the sensitivity analysis and λ_0 is the growth rate for the uncontrolled flow.

We can retrieve some non-linear effects due to a finite amplitude of the forcing with the following procedure:

- 1 Application of the linearized drag force at a fixed position $(x_0 = 0.15, y_0 = 0)$

III: Non linear effects of the controlling force amplitude on the eigenvalue estimation

Eigenvalue drift evaluated with sensitivity analysis is exact only for **infinitesimal** perturbations.

$\bar{\lambda} = \lambda_0 + \alpha S(x_0, y_0)$ where $\bar{\lambda}$ is the growth rate predicted by the sensitivity analysis and λ_0 is the growth rate for the uncontrolled flow.

We can retrieve some non-linear effects due to a finite amplitude of the forcing with the following procedure:

- 1 Application of the linearized drag force at a fixed position ($x_0 = 0.15, y_0 = 0$)
- 2 Computation of the forced baseflow for different amplitudes (α):

$$U'_b \cdot \nabla U'_b + \nabla P'_b - \frac{1}{Re} \nabla^2 U'_b = \delta F$$
$$\nabla \cdot U'_b = 0$$

III: Non linear effects of the controlling force amplitude on the eigenvalue estimation

Eigenvalue drift evaluated with sensitivity analysis is exact only for **infinitesimal** perturbations.

$\bar{\lambda} = \lambda_0 + \alpha S(x_0, y_0)$ where $\bar{\lambda}$ is the growth rate predicted by the sensitivity analysis and λ_0 is the growth rate for the uncontrolled flow.

We can retrieve some non-linear effects due to a finite amplitude of the forcing with the following procedure:

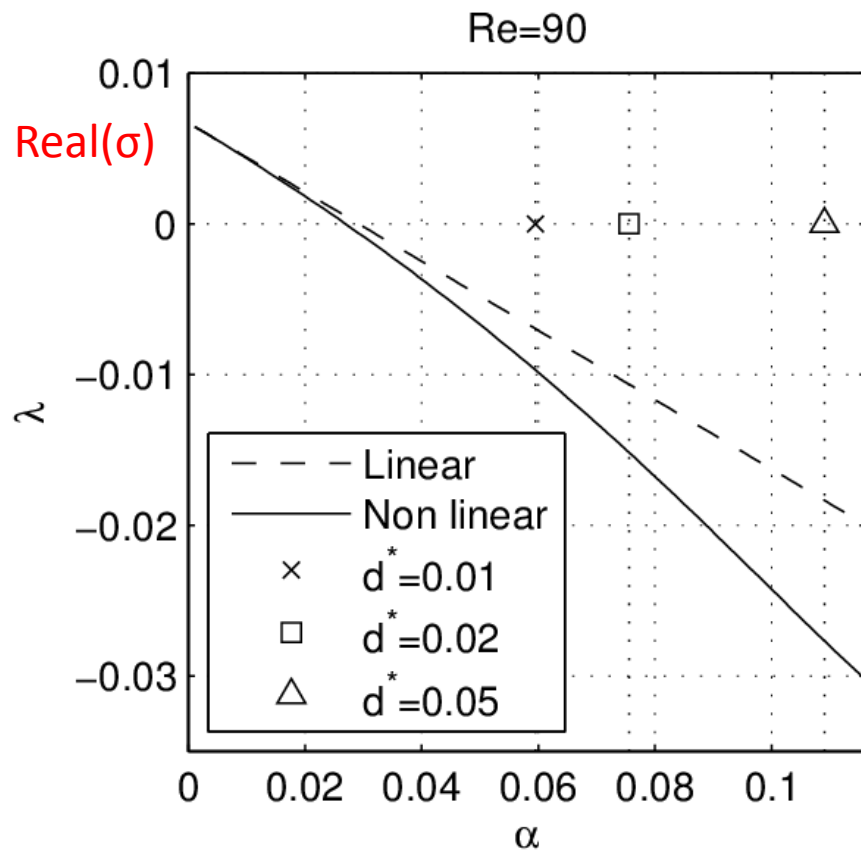
- 1 Application of the linearized drag force at a fixed position ($x_0 = 0.15, y_0 = 0$)
- 2 Computation of the forced baseflow for different amplitudes (α):

$$U'_b \cdot \nabla U'_b + \nabla P'_b - \frac{1}{Re} \nabla^2 U'_b = \delta F$$
$$\nabla \cdot U'_b = 0$$

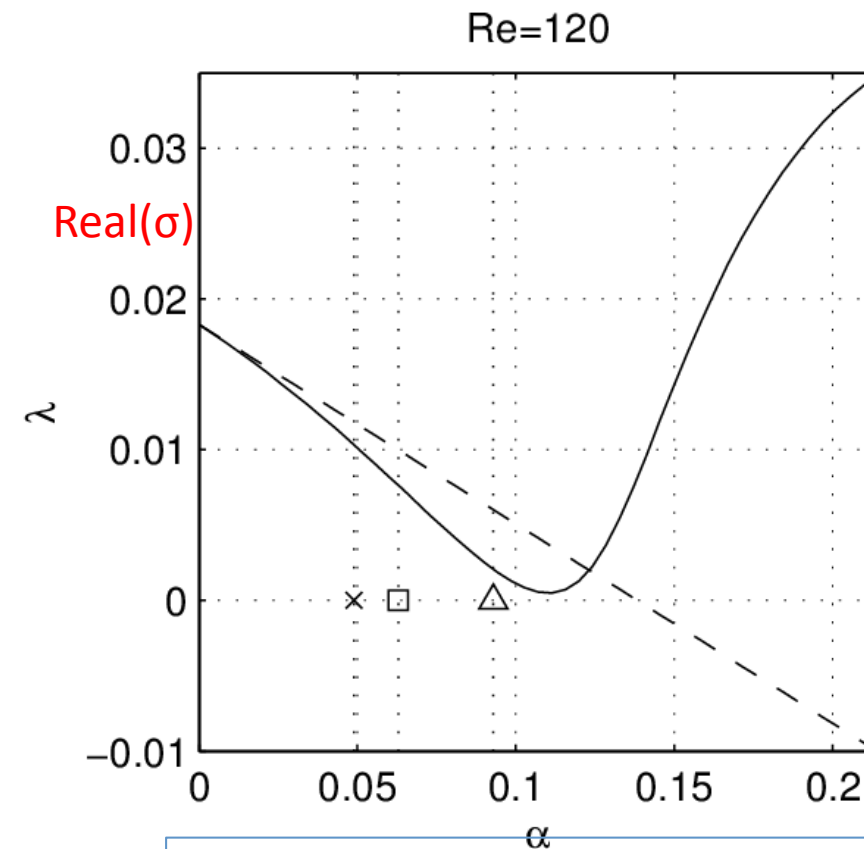
- 3 Linear stability analysis on the forced baseflow U'_b : $\rightarrow \lambda'$



III: Non linear effects of the controlling force amplitude on the eigenvalue estimation



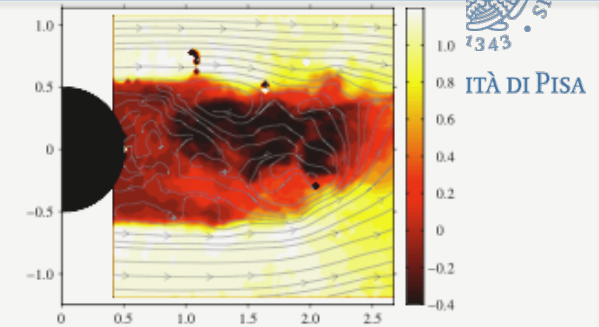
At moderate values of the force amplitudes the non linear effects has a stabilizing effects



At higher Reynolds number it is not possible to stabilize the flow vtrying α and fixing the cylinder position

Sensitivity analysis at high Reynolds number:
Application to PIV data past a porous cylinder

S. Camarri, B. E. G. Fallenius, and J. H. M. Fransson, JFM 715, 2013.

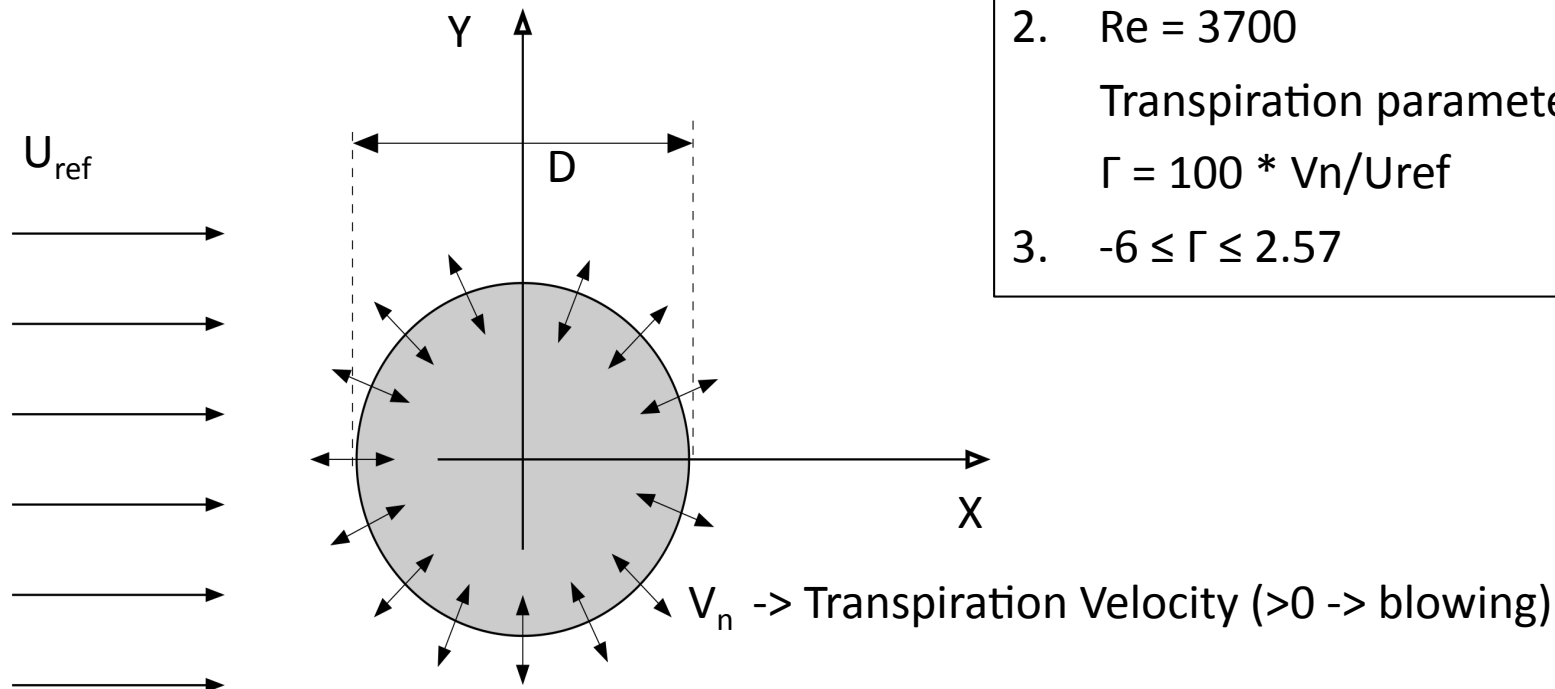


Applications to flow analysis and control

Stability and sensitivity analysis of
experimental flow fields measured past a
porous cylinder

Funding by C.M. Lerici Foundation is gratefully acknowledged

Configuration: flow around a porous cylinder (uniform transpiration)



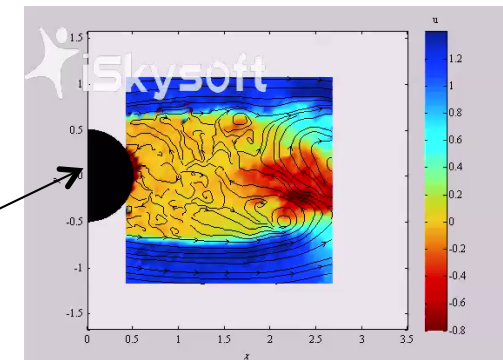
Flow parameters:

1. Reference quantities: U_{ref} , D
 2. $Re = 3700$
- Transpiration parameter:
- $$\Gamma = 100 * V_n / U_{ref}$$
3. $-6 \leq \Gamma \leq 2.57$

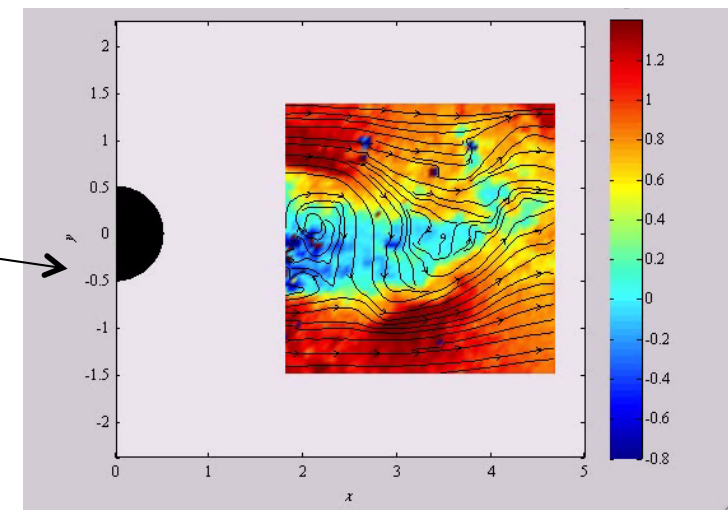
Experimental PIV database

- About 1000 instantaneous PIV snapshots for each Γ
- Approximately 2 snapshots per shedding cycle
- Spatial resolution: 62 X 62
- Measured quantities: U , V , planar Reynolds stresses

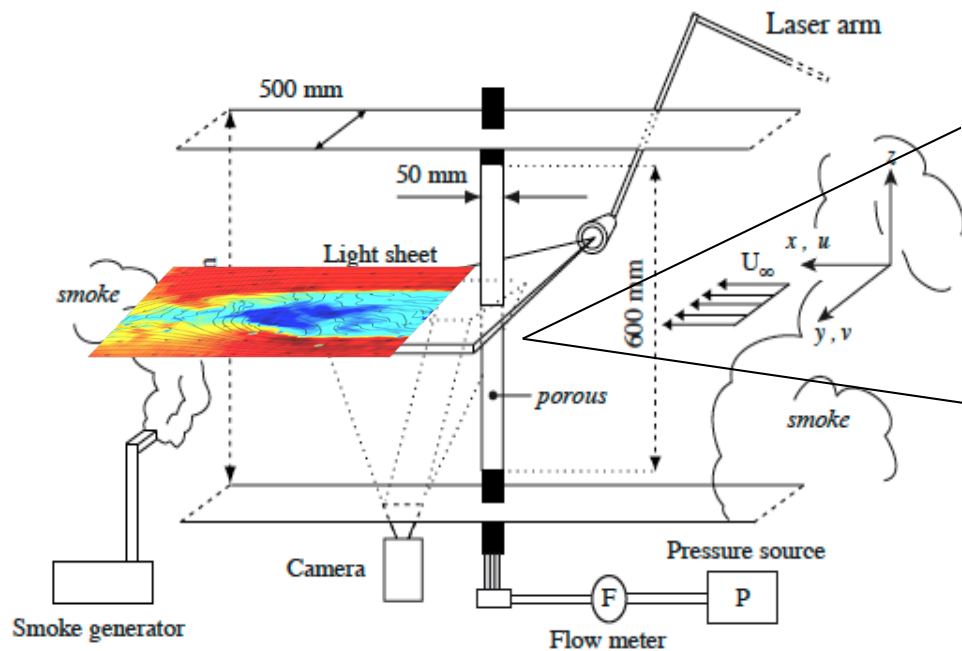
Suction cases: small window



Blowing cases: small window + large window



Streamwise velocity and streamlines





Stability analysis of mean flow fields

- For bluff-body flows correct prediction of the Strouhal number of vortex shedding, associated to a nearly marginally stable mode
- Shown by DNS up to $Re=600$ (*Leontini et al., JFM 2010*)
- Inspiring physical interpretation in terms of baseflow modifications in a ROM framework (*Noack et al., JFM 2003*)
- Models to include Reynolds stresses (e.g. *Reynolds & Hussain, JFM 1972; Kitsios et al., JFM 2010*) here neglected.

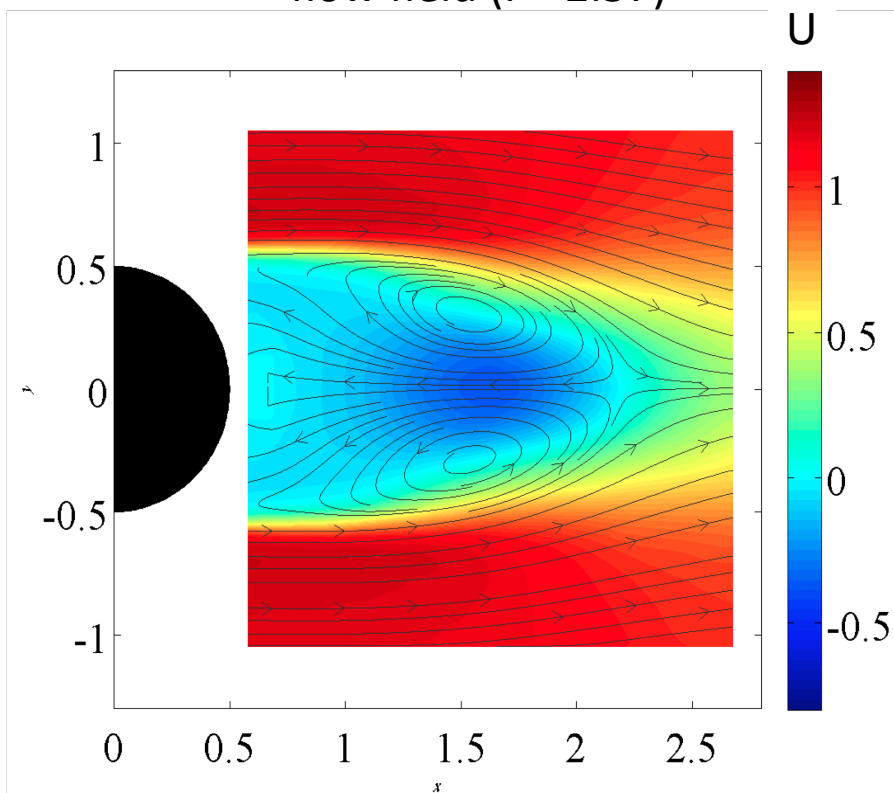


Objectives

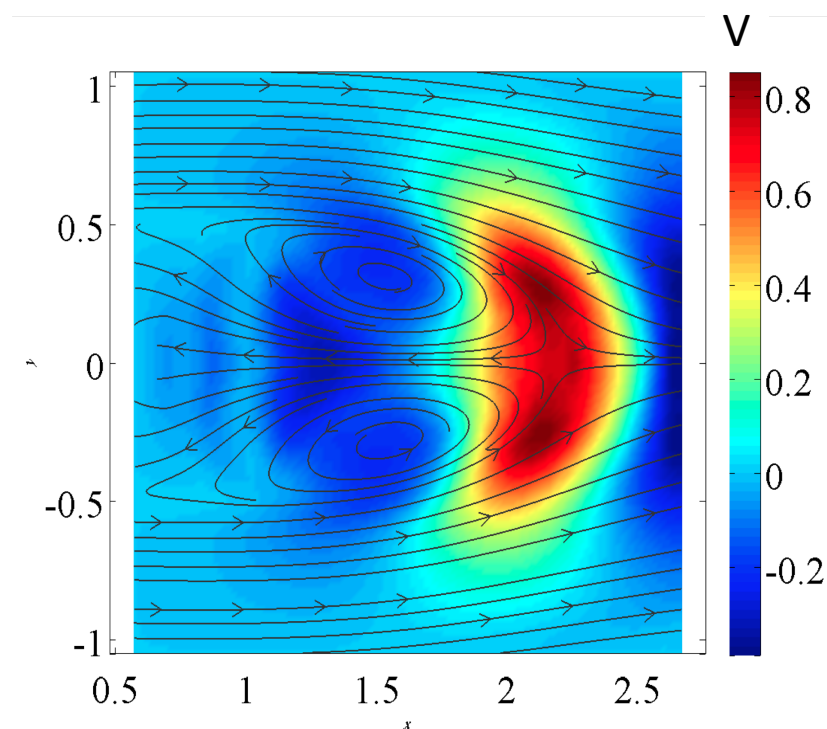
1. Verify whether or not global stability analysis, when applied to the experimental mean flow fields at $Re=3700$, still predicts the vortex shedding (VS) frequency with a sufficient accuracy to highlight the effect of Γ
 - Difficulties: noisy data, low spatial resolution, small measuring window
2. Use the results of the stability analysis to extract information about the large scale vortical structures from available database
3. Provide a strategy to apply sensitivity analysis for flow control using mean flow fields (similar work based on RANS simulations in *Meliga et al. PoF 2012*).

Stability analysis - procedure

1) Computation of the time-averaged flow field ($\Gamma=-2.57$)



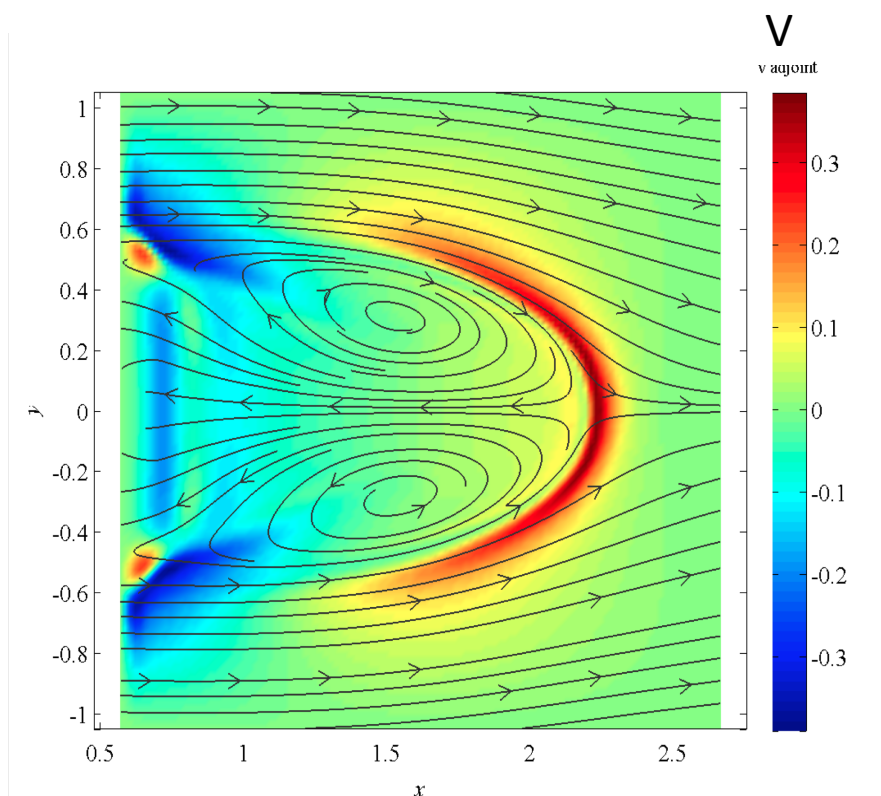
2) Stability analysis: marginally stable direct mode ($\Gamma=-2.57$)



small window: necessarily unrealistic bc's on global mode

Stability analysis - procedure

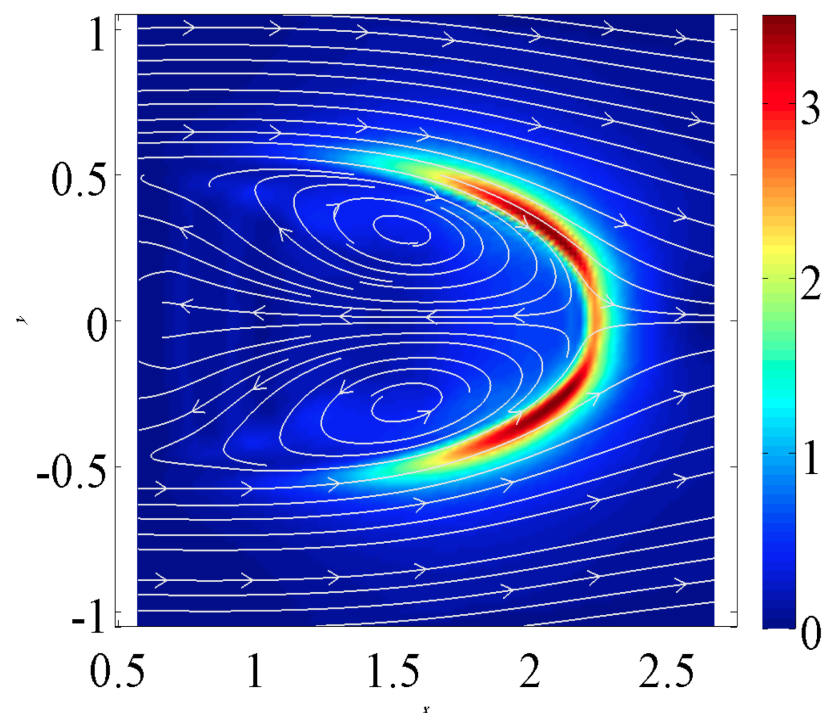
3) Computation of the associated
adjoint mode ($\Gamma = -2.57$)



Adjoint velocity field

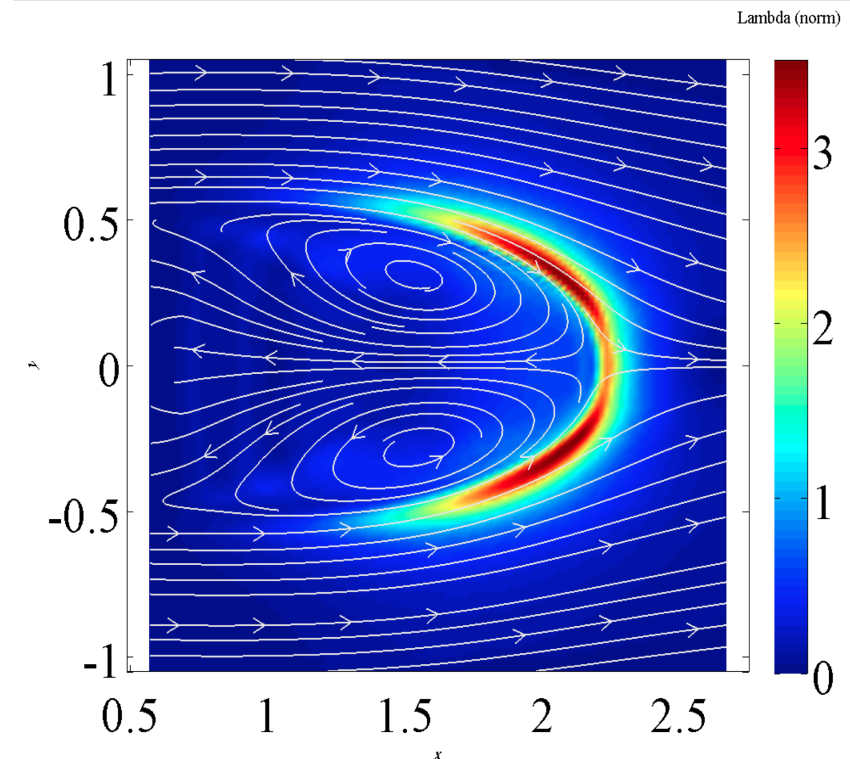
$$\Lambda(x, y) = \|\hat{\mathbf{u}}^+(x, y)\| \|\hat{\mathbf{u}}(x, y)\|$$

direct velocity field



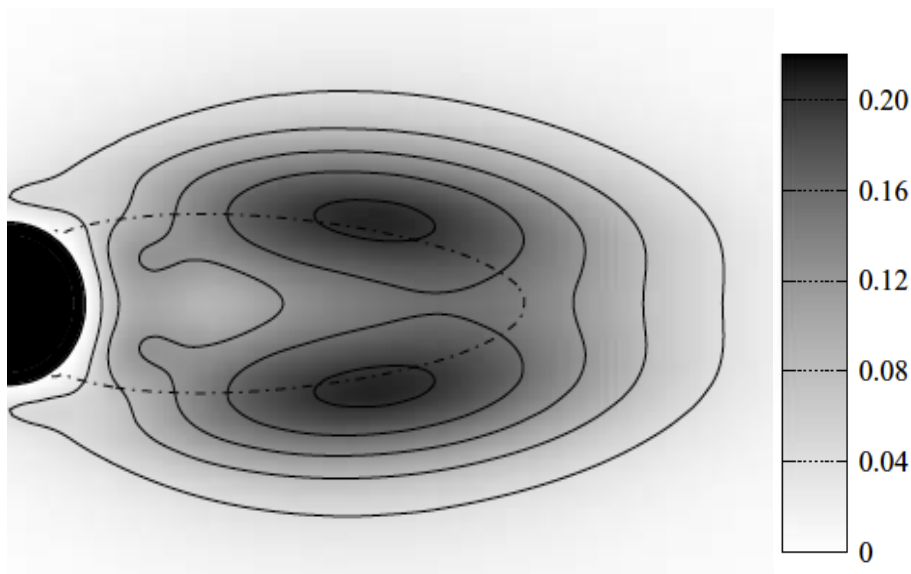
Stability analysis - procedure

- 4) Localization of the overlapping between direct and adjoint mode: core of the instability, i.e. region of the baseflow which mostly affect the estimation of the global mode (*Giannetti & Luchini, JFM*)



Stability analysis - procedure

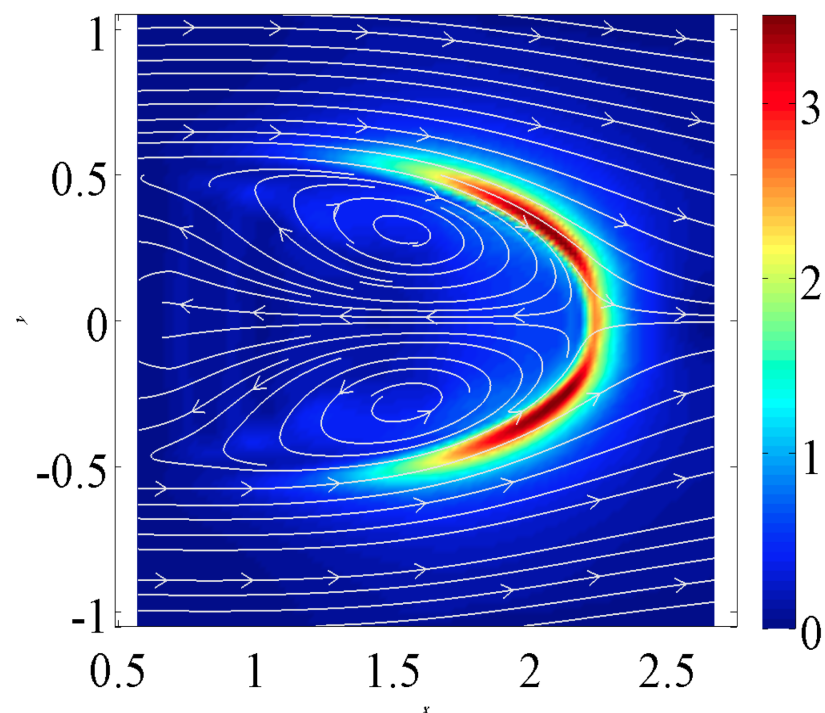
3) Numerical estimation of Λ at $Re=50$
 (Giannetti & Luchini, *JFM* 2007)



Adjoint velocity field

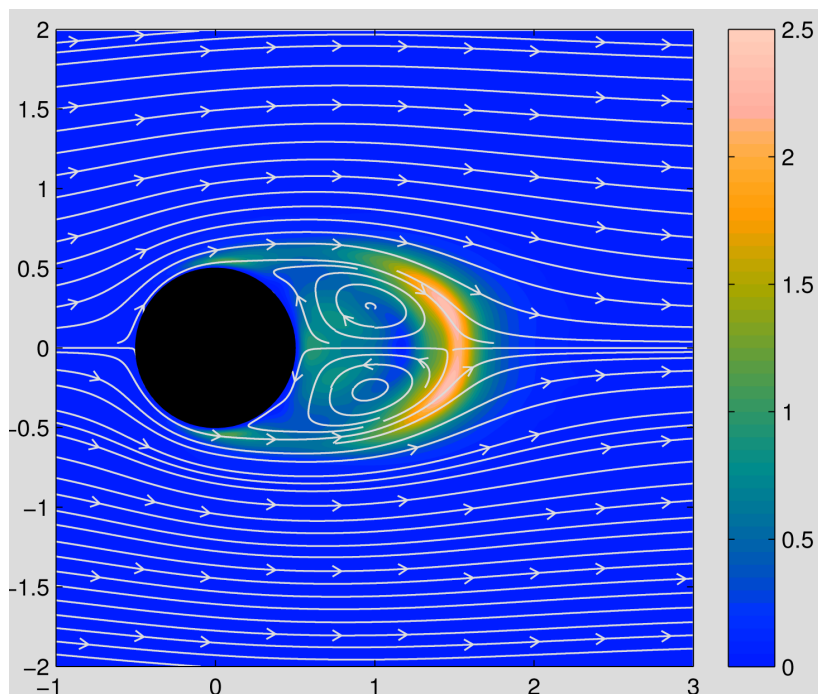
$$\Lambda(x, y) = \|\hat{\mathbf{u}}^+(x, y)\| \|\hat{\mathbf{u}}(x, y)\|$$

direct velocity field



Stability analysis - procedure

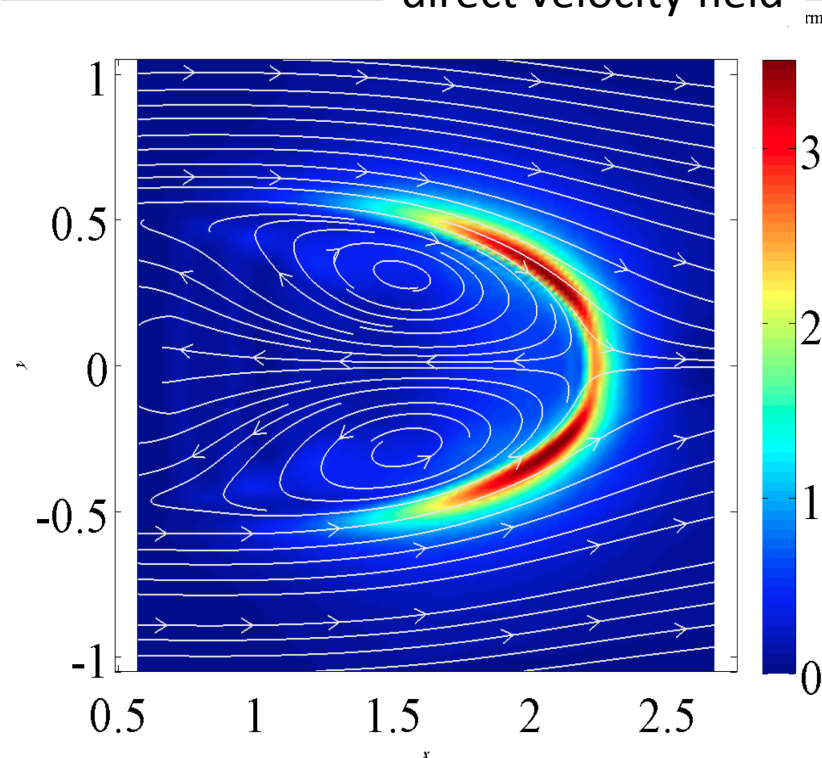
3) Numerical estimation of Λ at $Re=400$
 (mean flow field)
 (Camarri et al., JFM 2013)



Adjoint velocity field

$$\Lambda(x, y) = \|\hat{\mathbf{u}}^+(x, y)\| \|\hat{\mathbf{u}}(x, y)\|$$

direct velocity field





Stability analysis - results

Γ	Resolution	Stabilized	Strouhal N.	Experimental St	Error (%)
-6	120X120	Y	stable	stable	–
-5	120X120	Y	0.290	–	–
-3.86	120X120	Y	0.266	–	–
-3.21	120X120	Y	0.255	–	–
-2.57	120X120	Y	0.285	0.283	0.7%
-1.93	120X120	Y	0.267	0.241	9.7%
-1.37*	120X120	Y	0.308	0.216	30.0%
0	120X120	Y	0.232	0.2	13.8%
+0.68	120X120	Y	0.218	0.190	12.8%
+1.93	120X120	Y	0.193	0.188	2.6%
+2.57*	120X120	Y	0.1919	0.176	8.31%

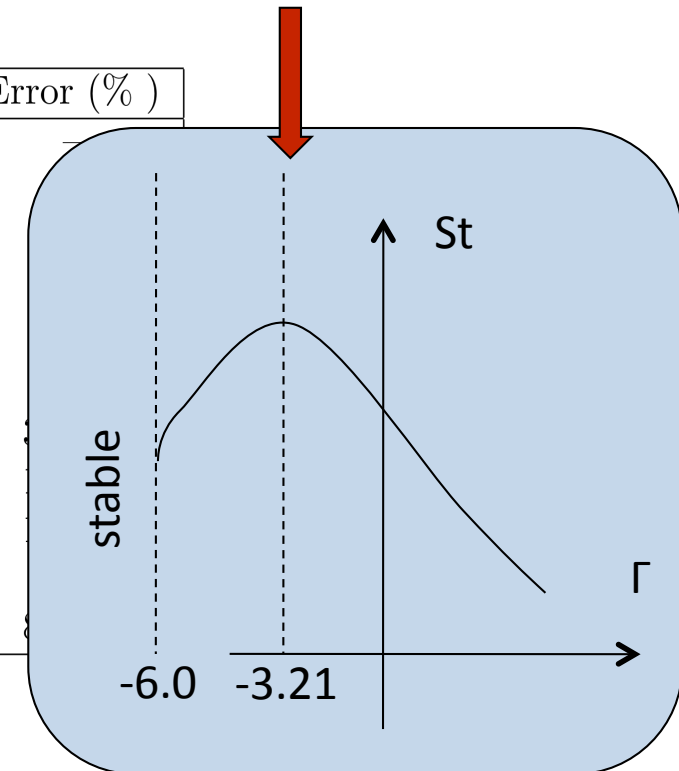
Stability analysis - results

Γ	Resolution	Stabilized	Strouhal N.	Experimental St	Error (%)
-6	120X120	Y	stable	stable	–
-5	120X120	Y	0.290	–	–
-3.86	120X120	Y	0.266	–	–
-3.21	120X120	Y	0.255	–	–
-2.57	120X120	Y	0.285	0.283	0.7%
-1.93	120X120	Y	0.267	0.241	9.7%
-1.37*	120X120	Y	0.308	0.216	30.0%
0	120X120	Y	0.232	0.2	13.8%
+0.68	120X120	Y	0.218	0.190	12.8%
+1.93	120X120	Y	0.193	0.188	2.6%
+2.57*	120X120	Y	0.1919	0.176	8.31%

- Accuracy on the value of St within 14 %

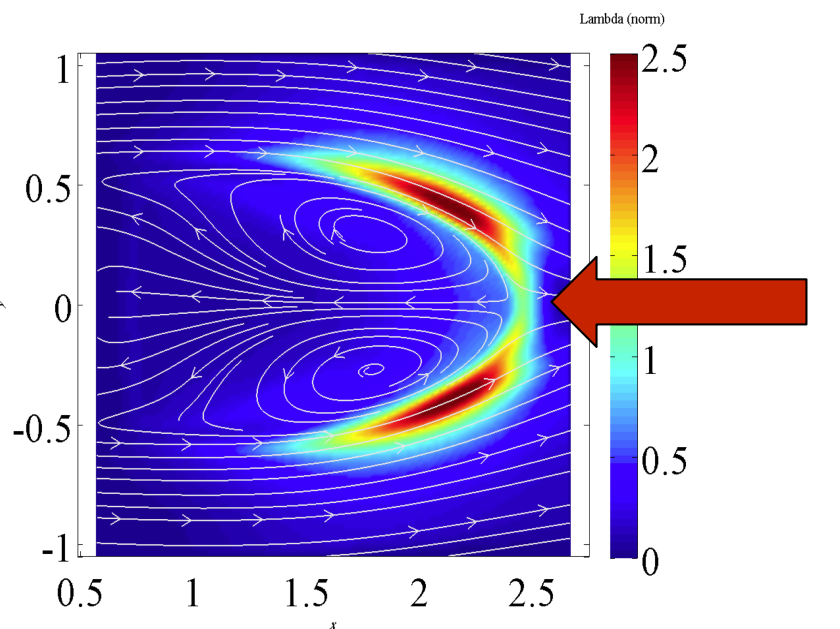
Stability analysis - results

Γ	Resolution	Stabilized	Strouhal N.	Experimental St	Error (%)
-6	120X120	Y	stable	stable	
-5	120X120	Y	0.290	–	
-3.86	120X120	Y	0.266	–	
-3.21	120X120	Y	0.255	–	
-2.57	120X120	Y	0.285	0.283	
-1.93	120X120	Y	0.267	0.241	
-1.37*	120X120	Y	0.308	0.216	
0	120X120	Y	0.232	0.2	
+0.68	120X120	Y	0.218	0.190	
+1.93	120X120	Y	0.193	0.188	
+2.57*	120X120	Y	0.1919	0.176	



- Accuracy on the value of St within 14 %
- Variations of St vs Γ in agreement with experiments

Stability



Γ	Resolution	Stabilized	Strouhal		
-6	120X120	Y	stable		
-5	120X120	Y	0.290		
-3.86	120X120	Y	0.266		
-3.21	120X120	Y	0.255		
-2.57	120X120	Y	0.285		
-1.93	120X120	Y	0.267		
-1.37*	120X120	Y	0.308	0.216	30.0%
0	120X120	Y	0.232	0.2	13.8%
+0.68	120X120	Y	0.218	0.190	12.8%
+1.93	120X120	Y	0.193	0.188	2.6%
+2.57*	120X120	Y	0.1919	0.176	8.31%

- Accuracy on the value of St within 14 %
- Variations of St vs Γ in agreement with experiments
- Errors when the instability core approaches the boundaries of the measurement window



Sensitivity analysis

perturbation of the baseflow field

- Perturbed problem:

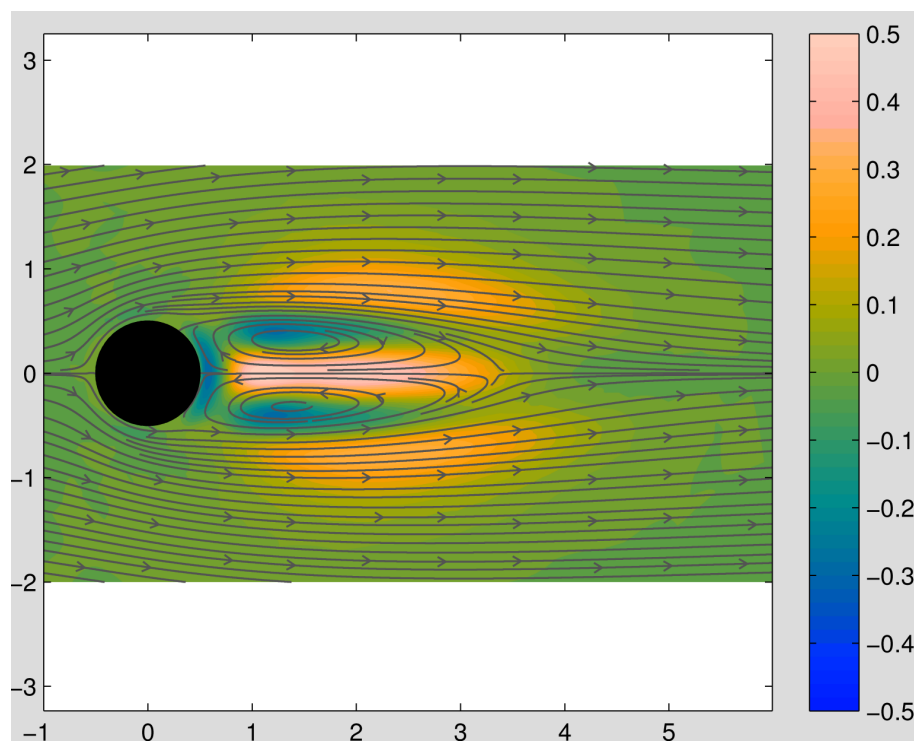
$$\tilde{\sigma} \mathbf{u} + \tilde{\mathbf{u}} \cdot \nabla \tilde{\mathbf{U}}_b + \tilde{\mathbf{U}}_b \cdot \nabla \tilde{\mathbf{u}} + \tilde{\nabla} p - \frac{1}{Re} \nabla^2 \tilde{\mathbf{u}} = \mathbf{0}$$
$$\nabla \cdot \tilde{\mathbf{u}} = 0$$

- Result of the sensitivity analysis (adjoint stab. equations involved):

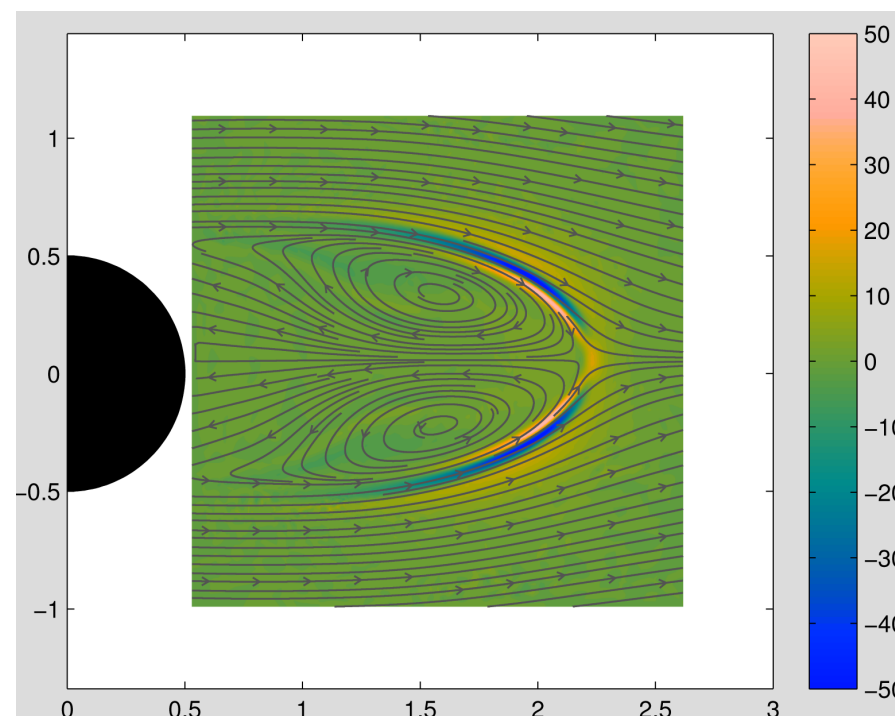
$$\delta\sigma = \frac{(M^+, \delta\mathbf{U}_b)}{(\hat{\mathbf{u}}^+, \hat{\mathbf{u}})}$$
$$M^+ = \hat{\mathbf{u}}^* \cdot \nabla \hat{\mathbf{u}}^+ - \nabla \hat{\mathbf{u}}^* \cdot \hat{\mathbf{u}}^+$$

Sensitivity of mode frequency a generic baseflow modification

Case at $Re=50$ computed on the steady unstable solution of NS eqs.

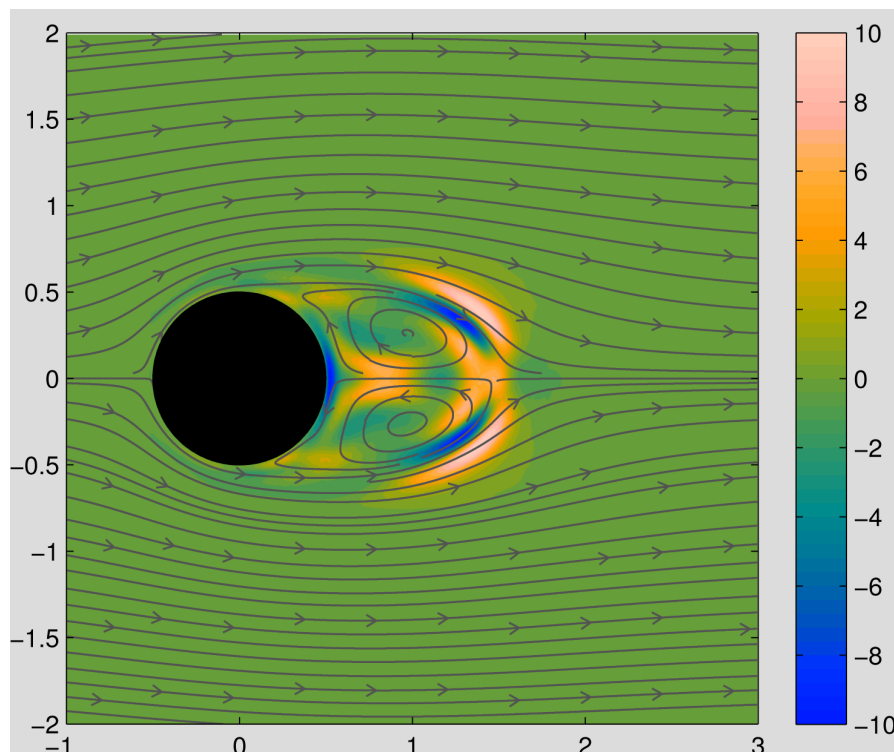


Sensitivity to a generic perturbation of the baseflow horizontal velocity

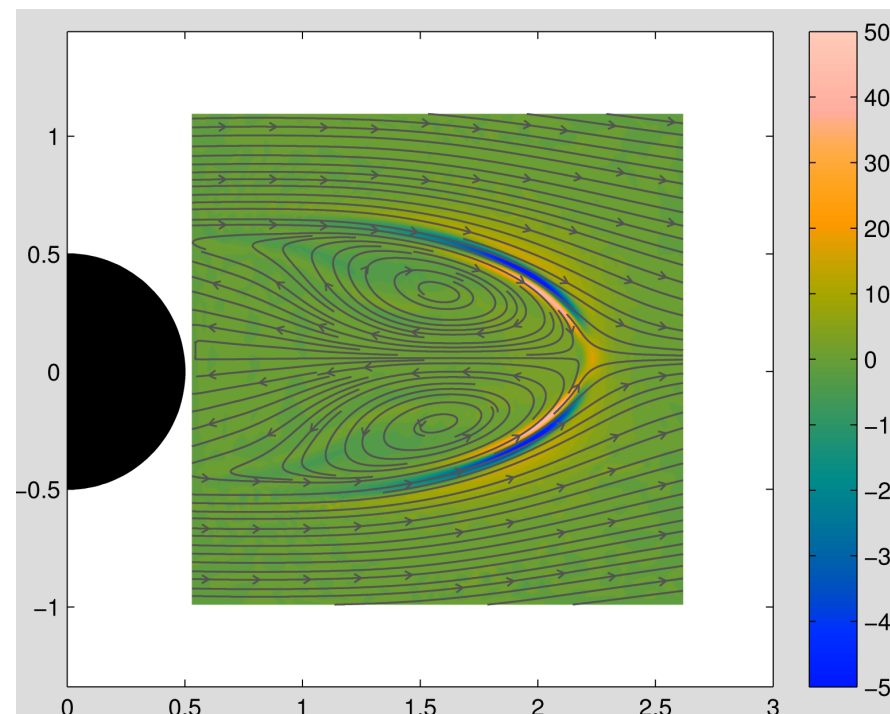


Sensitivity of mode frequency a generic baseflow modification

Case at $Re=400$ computed on the mean flow field

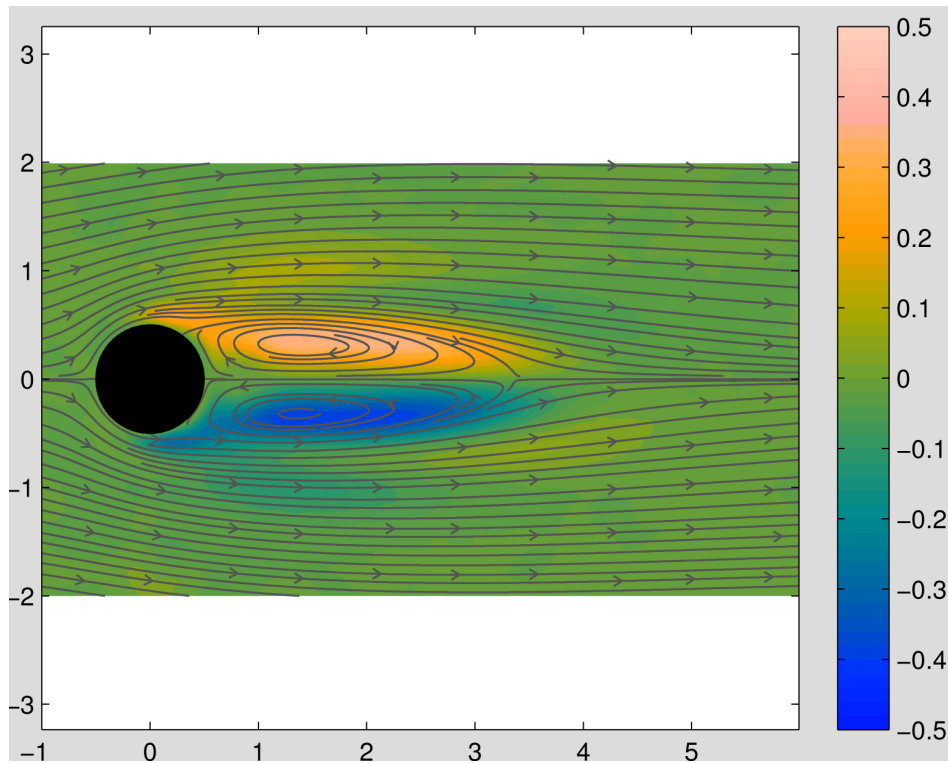


Sensitivity to a generic perturbation of the baseflow horizontal velocity

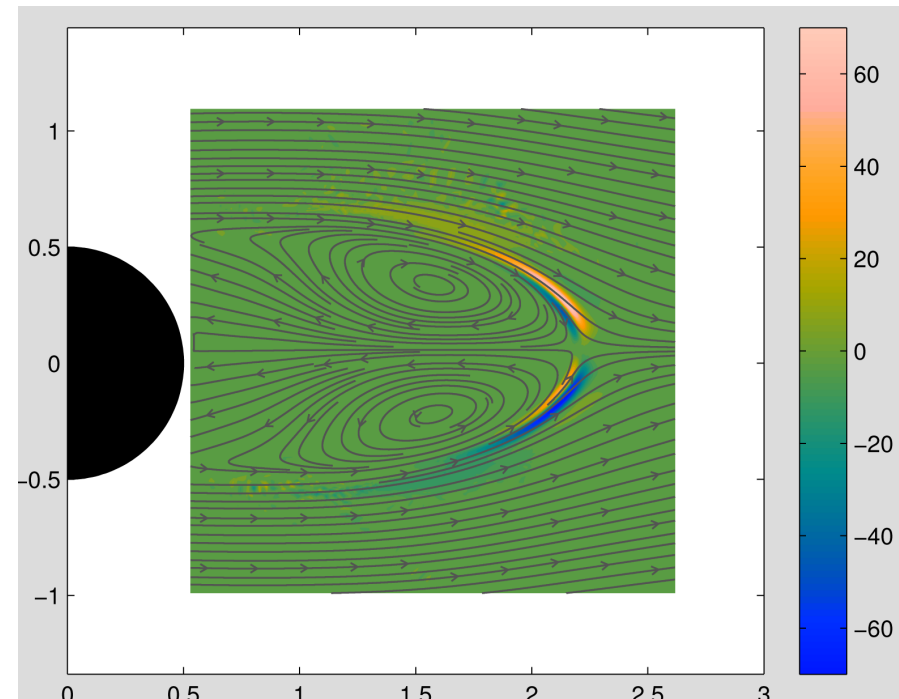


Sensitivity of mode frequency a generic baseflow modification

Case at $Re=50$ computed on the steady unstable solution of NS eqs.

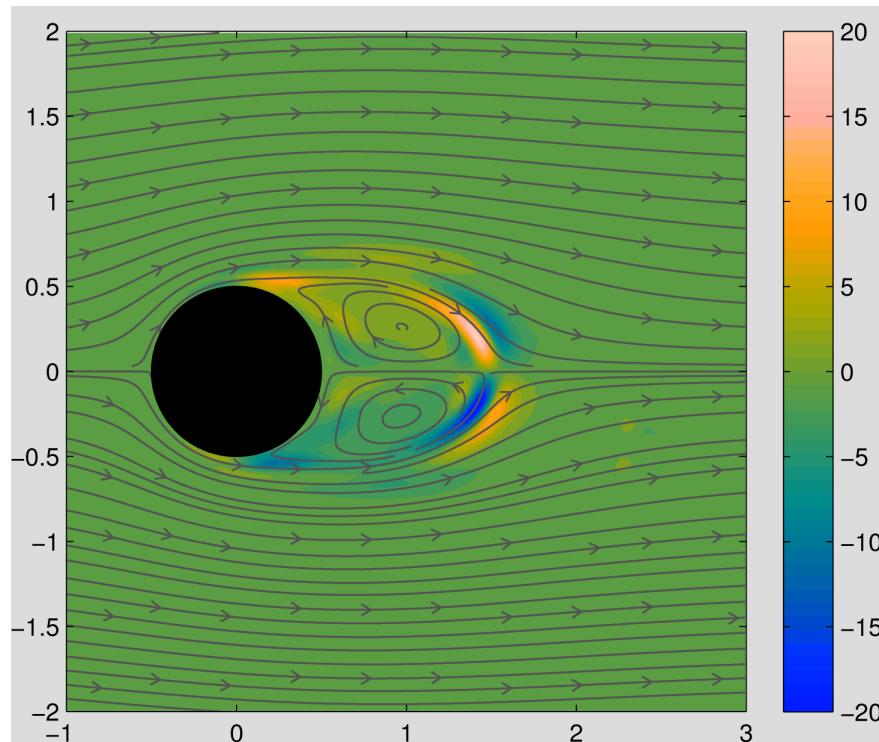


Sensitivity to a generic perturbation of the baseflow horizontal velocity

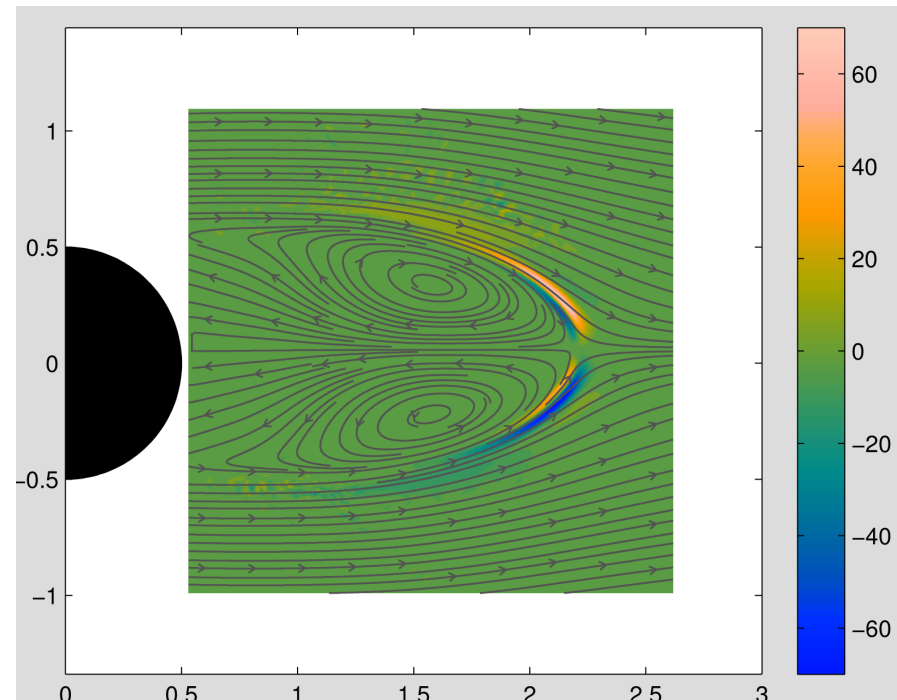


Sensitivity of mode frequency a generic baseflow modification

Case at $Re=400$ computed on the mean flow field



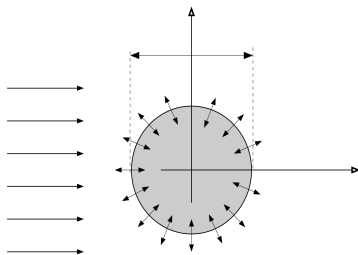
Sensitivity to a generic perturbation of the baseflow horizontal velocity



Focus on control: sensitivity to a generic baseflow modification

- Verification of the sensitivity maps: **control parameter Γ**

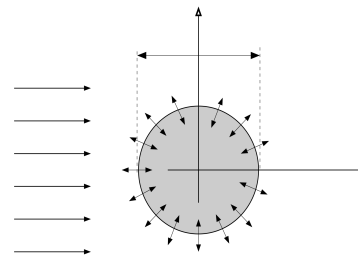
Reference baseflow: $U_{b_{ref}}$



Reference case: $\Gamma = -1.93$

reference St number:
from experiments

Controlled baseflow: U_{b_c}



Different value of Γ

$$\delta \mathbf{U}_b = \mathbf{U}_{b_c} - \mathbf{U}_{b_{ref}}$$

Estimation of controlled St
Comparison with EXPs

$$\delta \sigma = \frac{(M^+, \delta \mathbf{U}_b)}{(\hat{\mathbf{u}}^+, \hat{\mathbf{u}})}$$

$$M^+ = \hat{\mathbf{u}}^* \cdot \nabla \hat{\mathbf{u}}^+ - \nabla \hat{\mathbf{u}}^* \cdot \hat{\mathbf{u}}^+$$

Focus on control: sensitivity to a generic baseflow modification

- Example of application:
 - control parameter: transpiration Γ
 - From PIV measurements the variation of baseflow is known
 - We use the map derived for $\Gamma=-1.93$ to estimate variations of Strouhal number thanks to the result of sensitivity analysis:

Γ	Estimated Strouhal N.	Computed Strouhal N.	Difference (%)
-5.0	0.333	0.290	14.8
-3.86	0.261	0.266	-1.9
-3.21	0.252	0.255	-1.2
-2.57	0.282	0.285	-1.0
0	0.223	0.232	-3.9
0.68	0.210	0.218	-3.7
1.93	0.161	0.193	-16.6

Example of flow analysis based on stability results: phase alignment of snapshots

- Use of global modes to extraction of information on the large scale wake vortices
 - Global modes (stability analysis) are used to estimate the phase of each snapshot with respect to VS
 - Snapshots are aligned with respect to the VS phase
 - Phase average carried out on the ordered database

- Phase estimation

$$\mathbf{u}_{vs}(x, y, t) = \mathbf{U}_m + \frac{A}{2} (\exp(i\omega t) \hat{\mathbf{u}}(x, y) + \exp(-i\omega t) \hat{\mathbf{u}}^*(x, y))$$

Phase angle $\Phi_T = \omega t$

Assumed velocity decomposition

Time averaged velocity

Global mode

Phase alignment of snapshots

- Extraction of information on the large scale wake vortices
 - Global modes (stability analysis) are used to estimate the phase of each snapshot with respect to VS
 - Snapshots are aligned with respect to the VS phase
 - Phase average carried out on the ordered database

- Phase estimation

$$\mathbf{u}_{vs}(x, y, t) = \mathbf{U}_m + \frac{A}{2} (\exp(i\omega t) \hat{\mathbf{u}}(x, y) + \exp(-i\omega t) \hat{\mathbf{u}}^*(x, y))$$

First strategy (only global mode nec.)

$$\mathbf{r} = \hat{\mathbf{u}} - \frac{\langle \hat{\mathbf{u}}, \hat{\mathbf{u}}^* \rangle}{\langle \hat{\mathbf{u}}^*, \hat{\mathbf{u}}^* \rangle} \hat{\mathbf{u}}^*$$

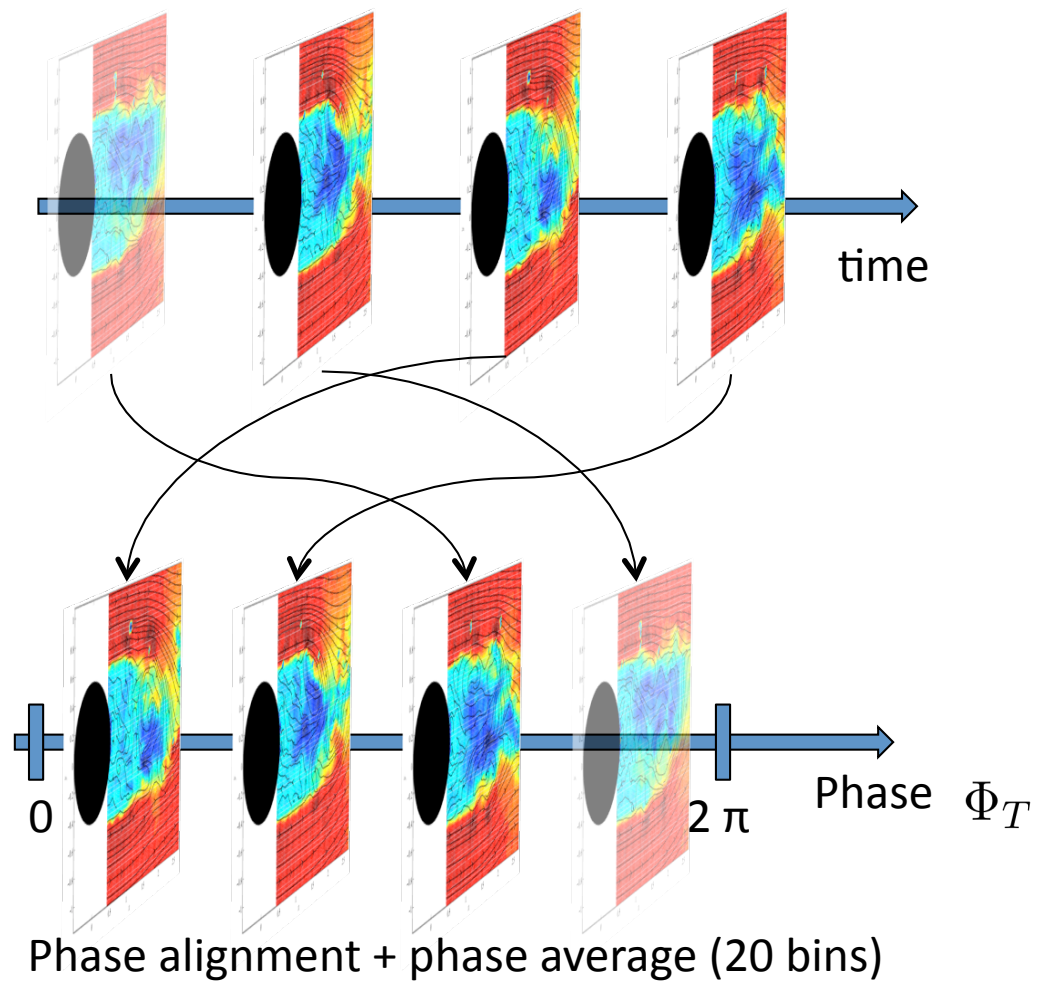
$$\Phi_T = \text{Phase}(\langle \mathbf{r}, \mathbf{u}(x, y, t) - \mathbf{U}_m \rangle)$$

Second strategy (adjoint based)

$$\frac{A}{2} \exp(i\Phi_T) = \langle \hat{\mathbf{u}}^+, \mathbf{u}(x, y, t) - \mathbf{U}_m \rangle$$

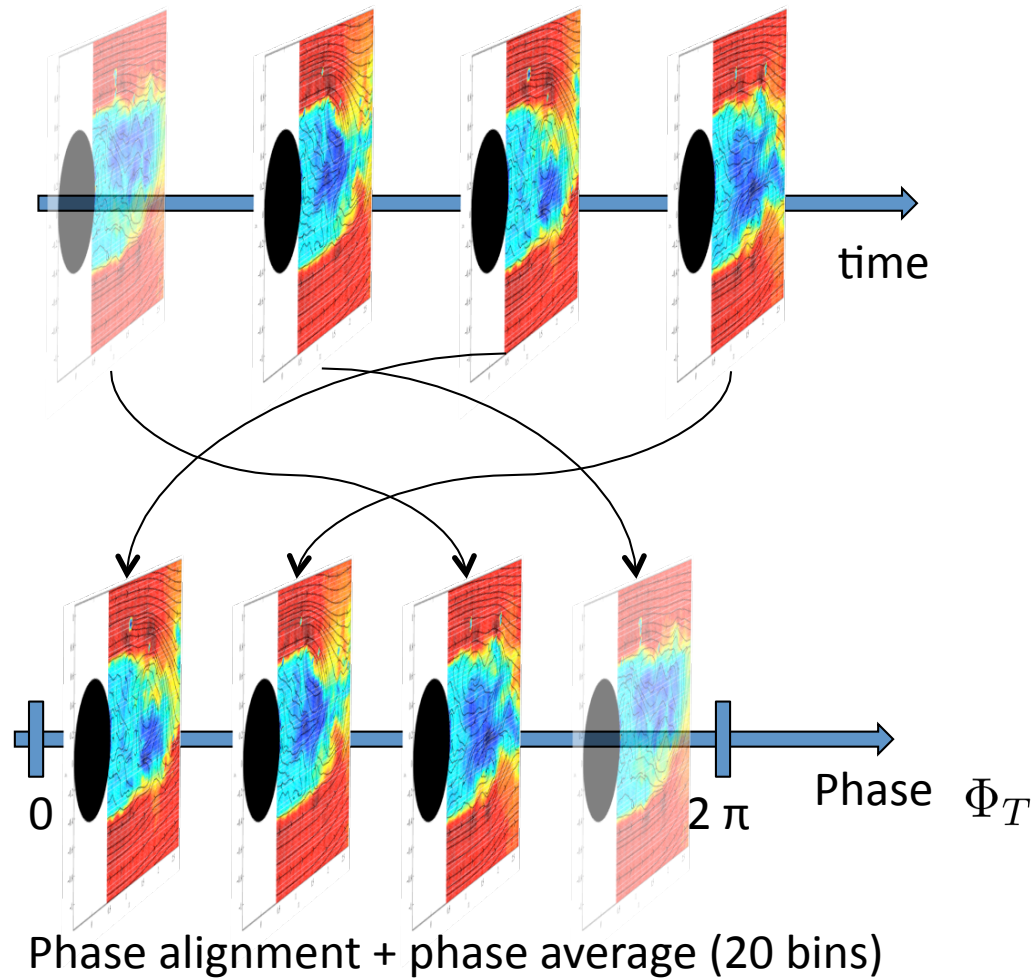
Phase alignment of snapshots

Typical example ($\Gamma = -2.57$)

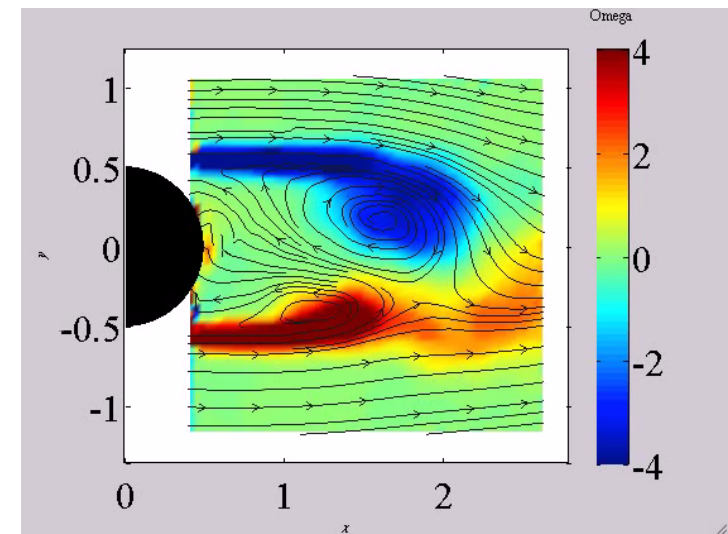
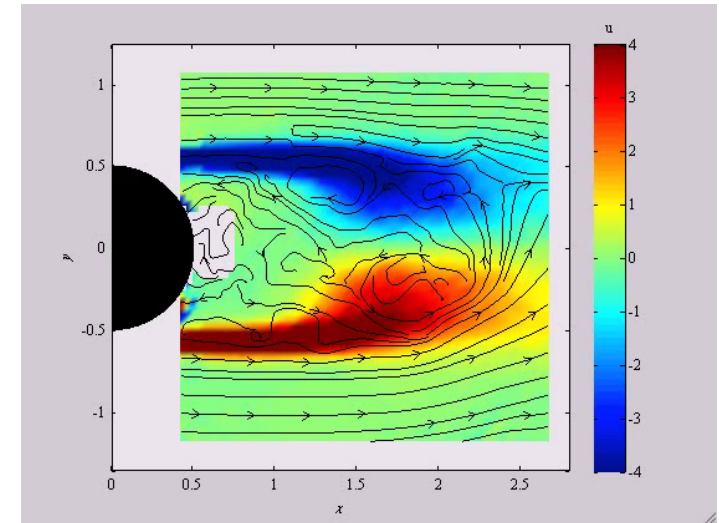


Phase alignment of snapshots

Typical example ($\Gamma = -2.57$)

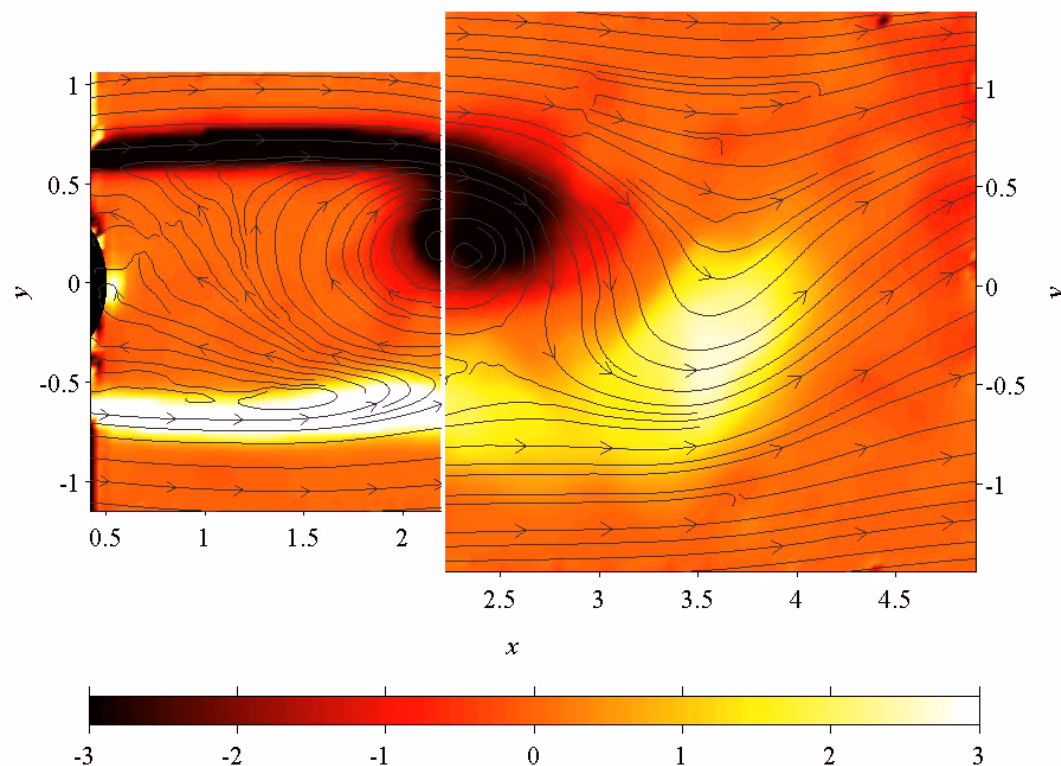


Vorticity (colormap) and streamlines



Phase alignment of snapshots

Blowing case ($\Gamma=0$)



Phase averaged vorticity field

- **Far and close windows: two different experimental runs**
- Sincronization is automatic because a single global mode is used to identify the phase

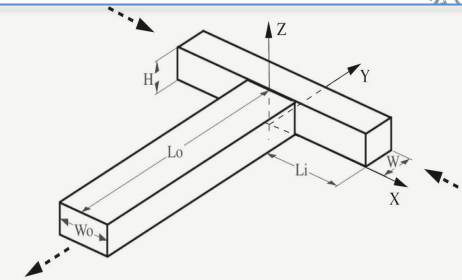


On-going developments

- Development passive wake controls using only experimental mean flow fields and final implementation in experiments for a thick plate (KTH Mechanics)
- Use of adjoint methods for data reconstruction problems in support to experiments on (KTH Mechanics):
 - Separated wakes
 - Controlled boundary layers
- Applications to fully 3D mixers for microfluidics applications:
 - Flow analysis
 - Control applications oriented to mixing enhancement
- Inclusion of Reynolds stresses as closure for local stability analysis of experimental flow fields past wind turbines (EPFL Lausanne)
- Application to free falling bluff bodies (Univ. Bordeaux)

Sensitivity analysis and control maps for fully 3D configs:
Application to a fully 3D T-Mixer

A. Fani, S. Camarri, and M. V. Salvetti, accepted, PoF 2013

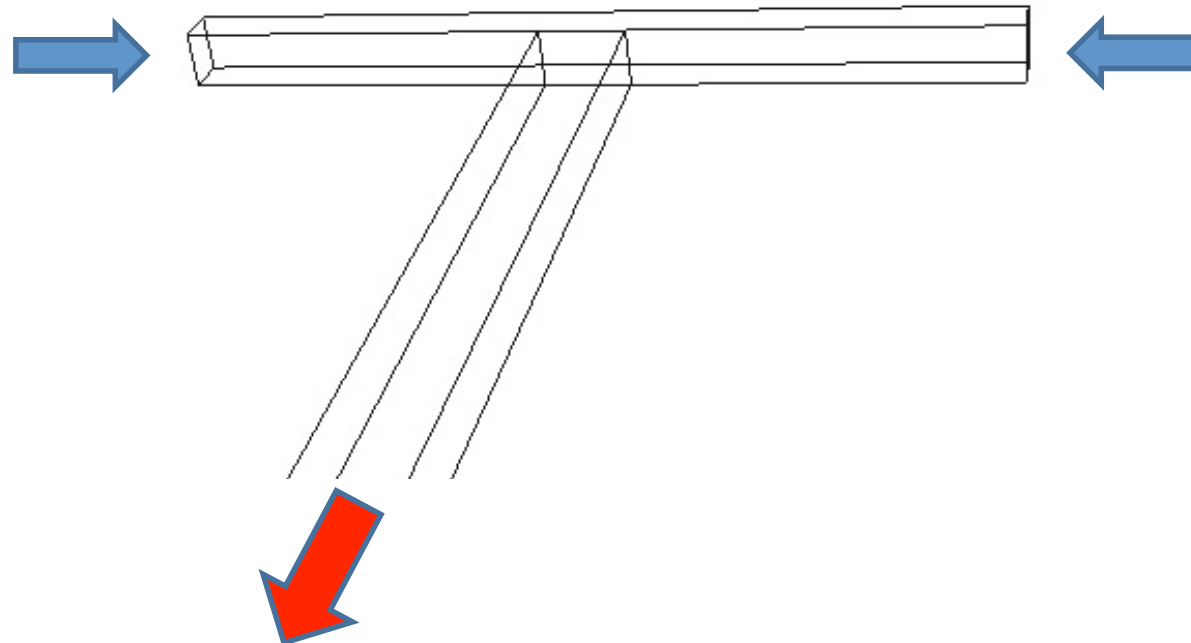


Applications to flow analysis and control

Sensitivity analysis of the engulfment
instability in a fully 3D micro T-Mixer

Micro T-mixer

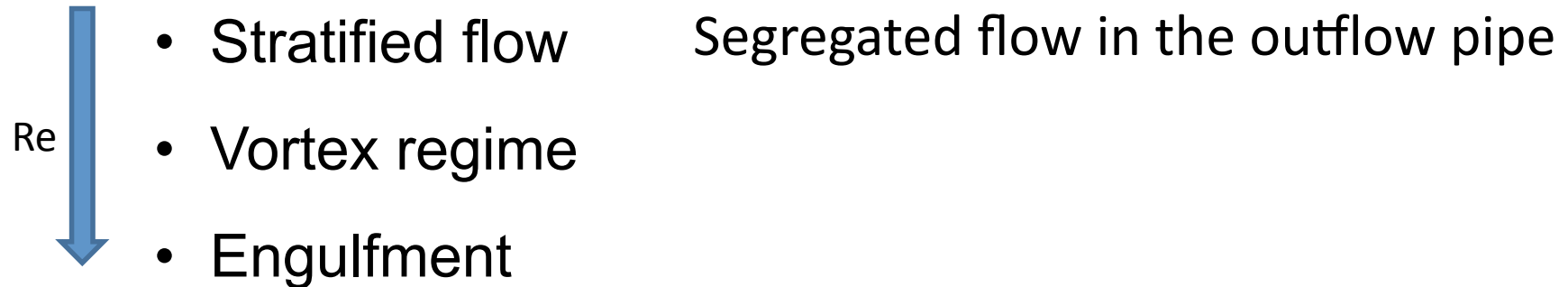
T-mixer are very common devices in microfluidics, also used as junction elements in complex micro-systems → laminar regime (low Reynolds numbers)





Motivations

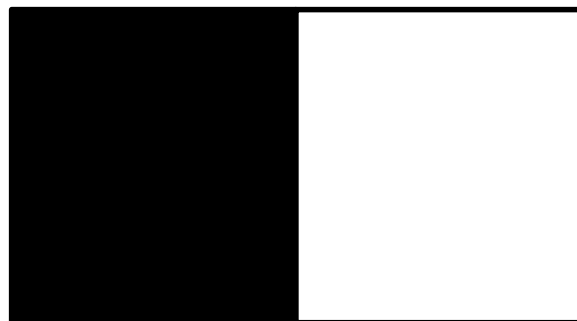
Flow regimes as a function of Reynolds number



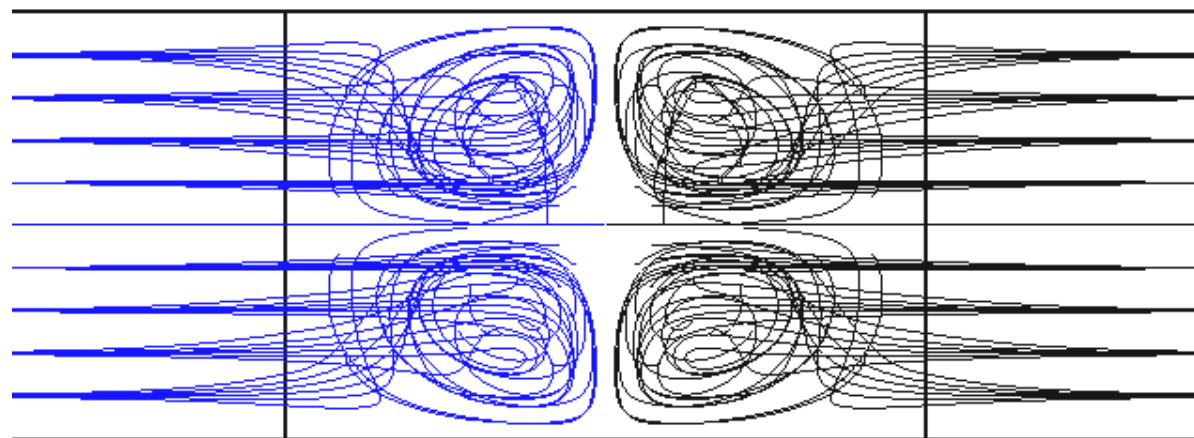
Motivations

Flow regimes as a function of Reynolds number

- Re ↓
- Stratified flow
 - Vortex regime
 - Engulfment



Secondary flow in the outcoming pipe: double pair of counter rotating vortices

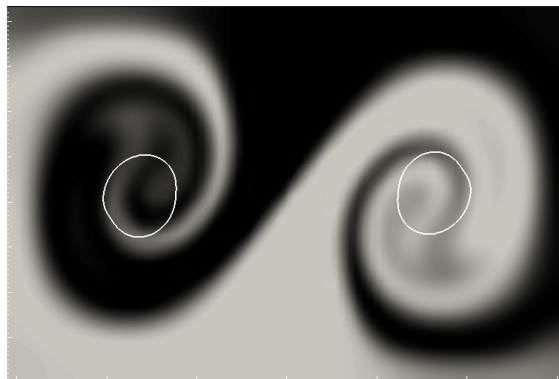


Motivations

Flow regimes as a function of Reynolds number

Re ↓

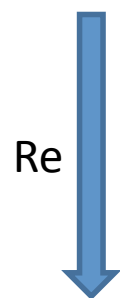
- Stratified flow
- Vortex regime
- Engulfment



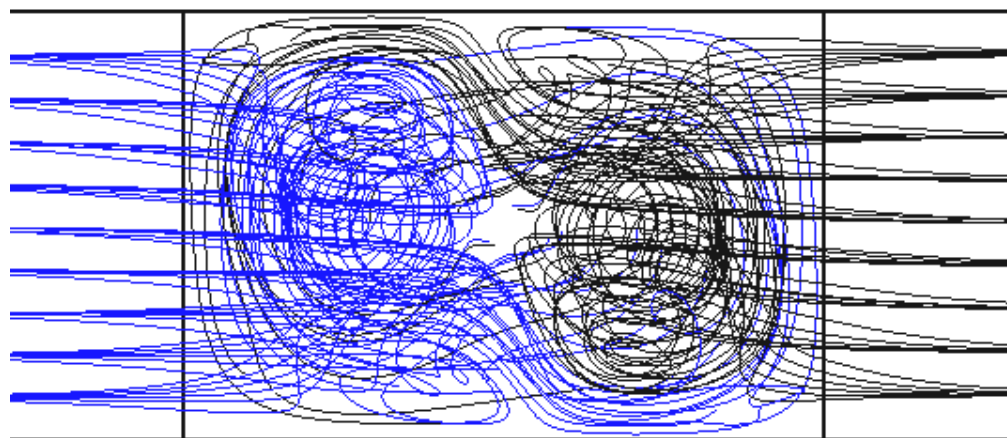
Stationary and organized pattern of vortical structures, which improve mixing in the outflow pipe.

Motivations

Flow regimes as a function of Reynolds number



- Stratified flow
- Vortex regime
- **Engulfment**



High sensitivity of the engulfment to inflow boundary conditions (Galletti et al.(2012)).

If the flow at the confluence is not fully developed engulfment occurs at larger Reynolds numbers.



Motivations

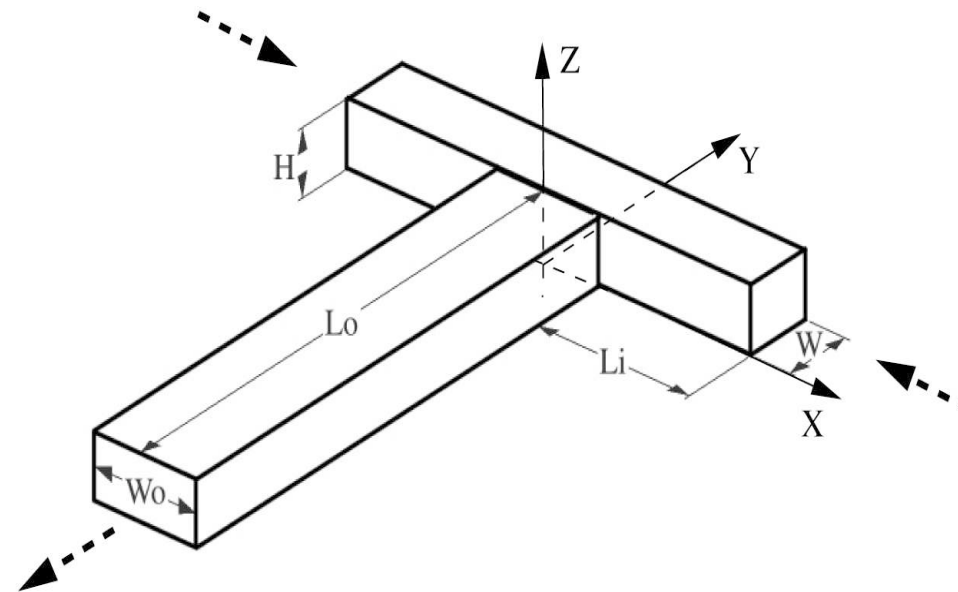
- High sensitivity to inflow conditions, as well as to other parameters, have been shown in the literature through numerical simulations and experiments
- No previous stability analysis of this configuration
- In general, stability analysis of fully 3D flows are rare

Objectives

- Aim of the present work: to carry out a systematic investigation by means of linear instability and sensitivity analyses to explain high sensitivity to inflow conditions
- Development of tools for 3D configurations
- Investigation of the flow also by DNS

Flow configuration

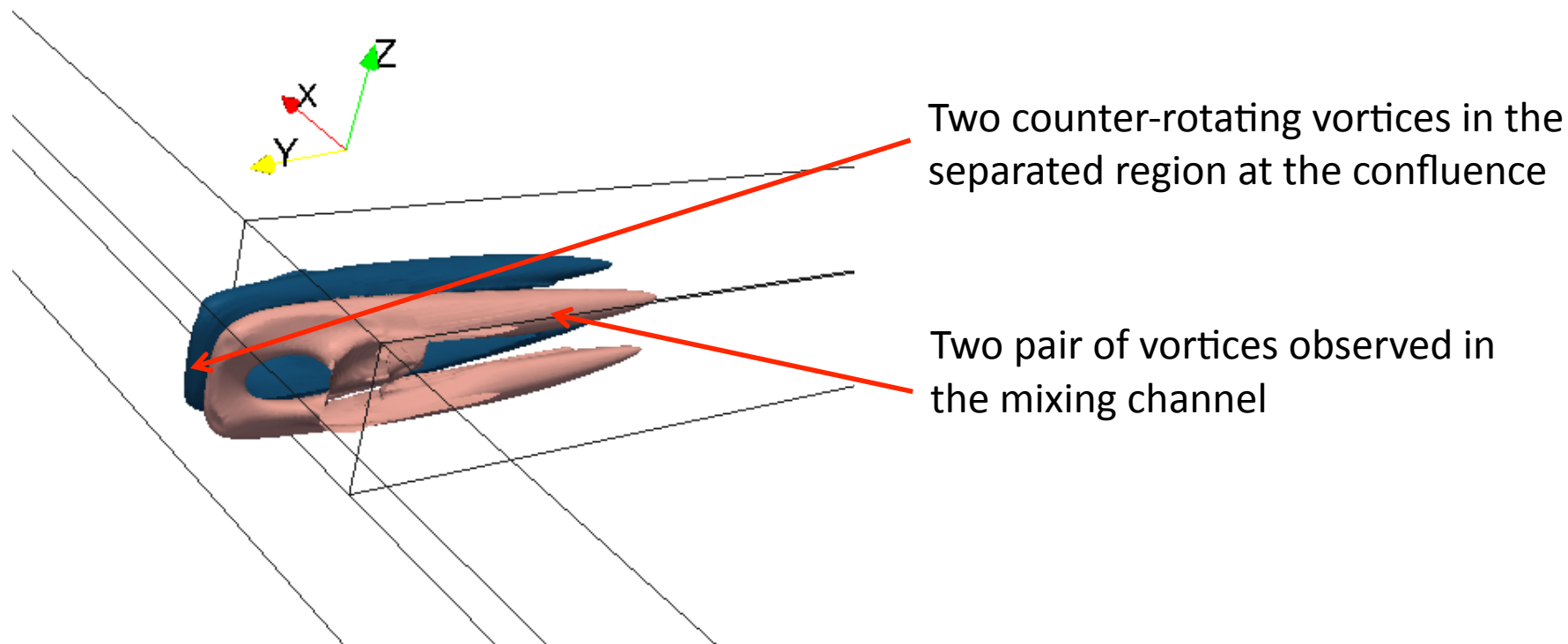
Incompressible flow in a three dimensional T-mixer



- $W_o/H = 1.5$ and $W_o/W_i = 2$ (same geometry as in Galletti et al. (2012))
- Reference length: $D_h = \frac{2W_oH}{W_o+H}$ (hydraulic diameter)
- Reference velocity: U_m bulk velocity of the inlet flow (fully developed inflow condition)

DNS investigation

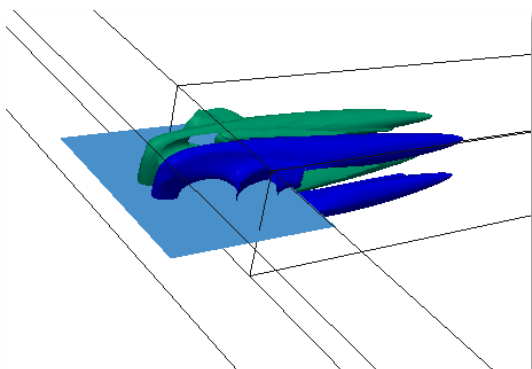
Re=140: vortex regime



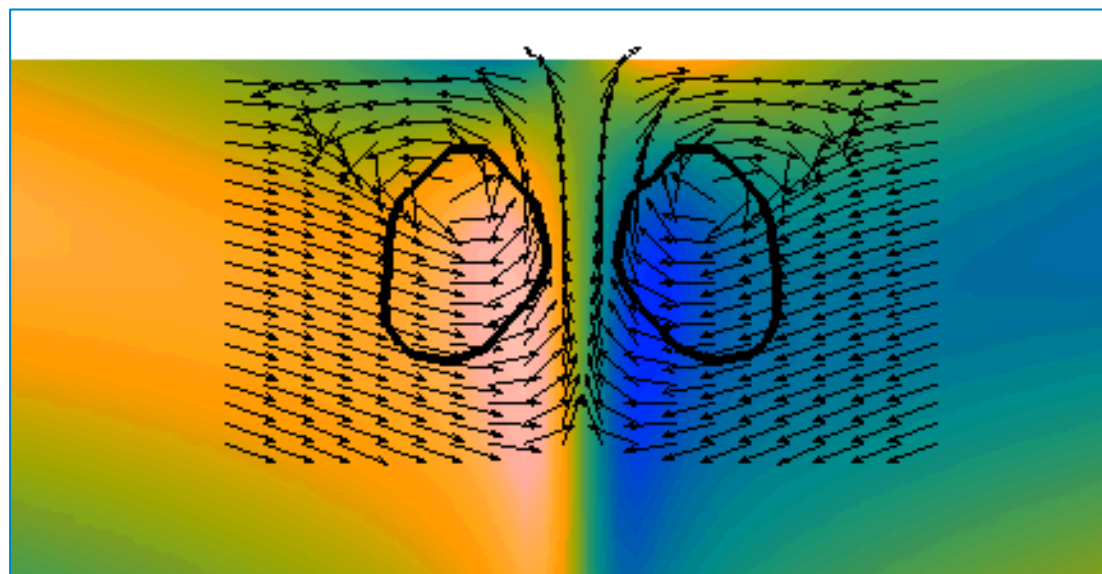
Vortex identified by λ_2 criteria

DNS investigation

Re=140: vortex regime

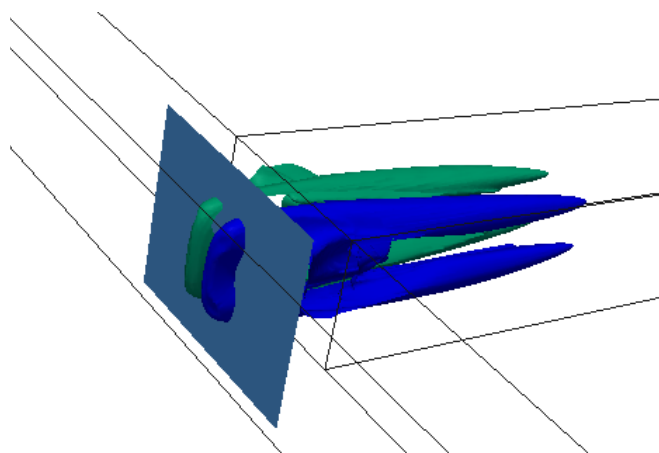


Normal vorticity component

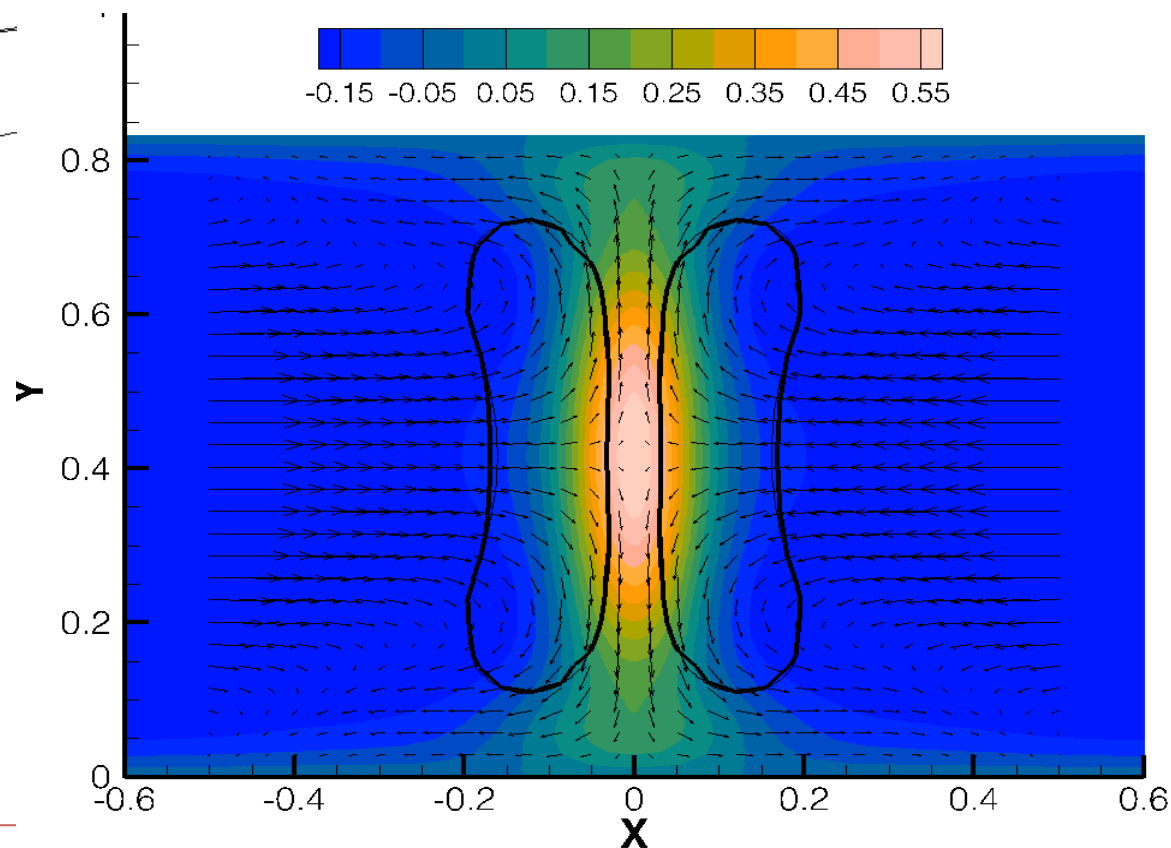


DNS investigation

Re=140: vortex regime

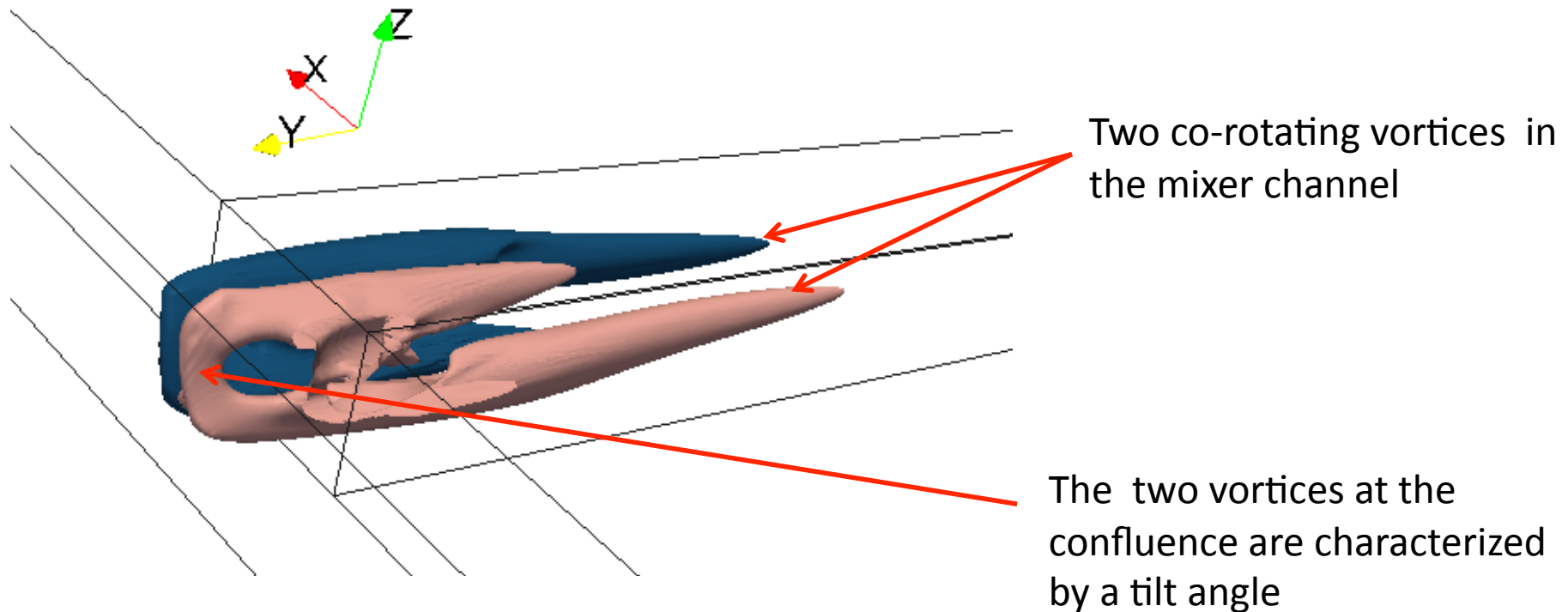


Arrow: in-plane velocities
Contour: normal to plane velocity



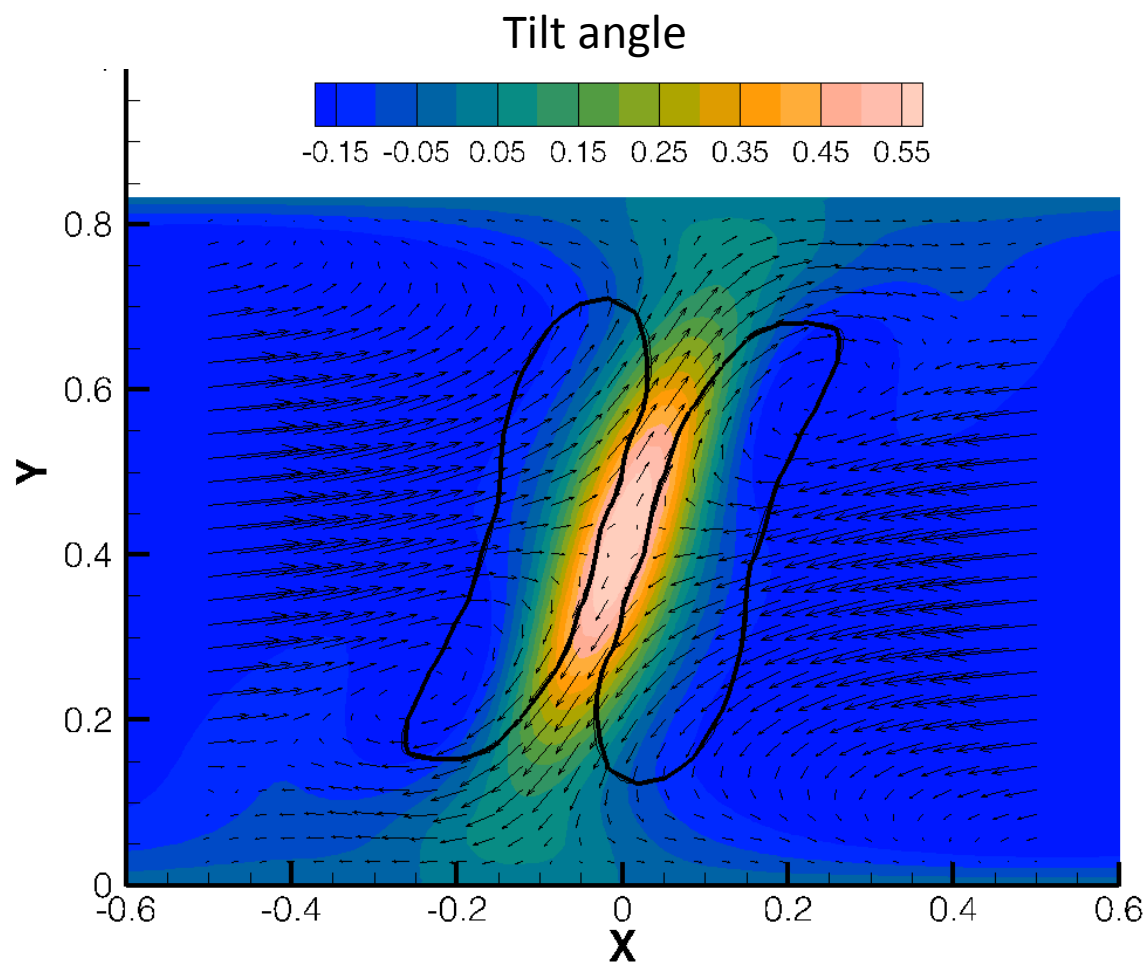
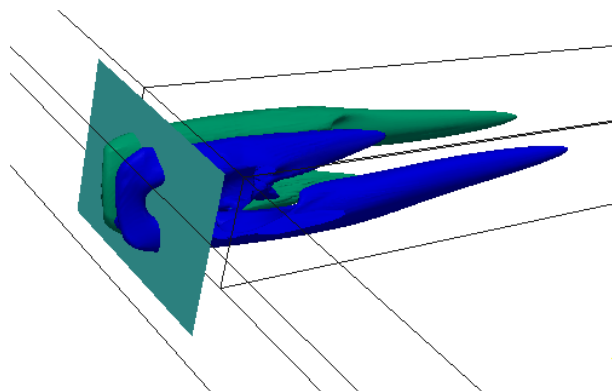
DNS investigation

Re=160: engulfment

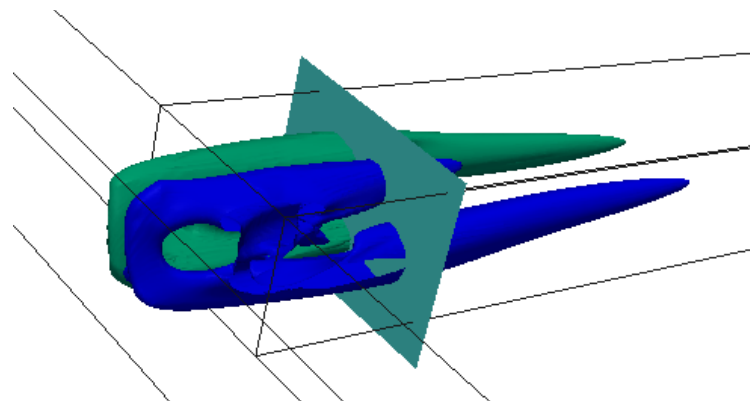


DNS investigation

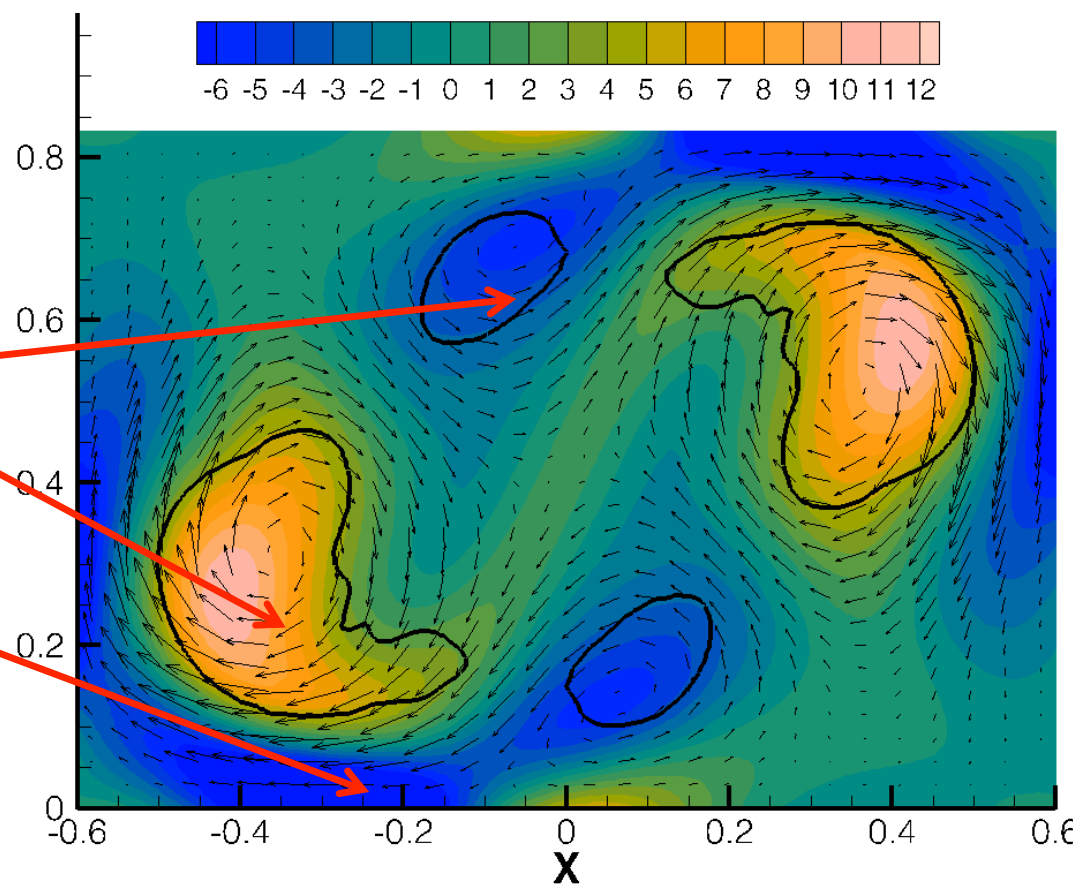
Re=160: engulfment



DNS investigation

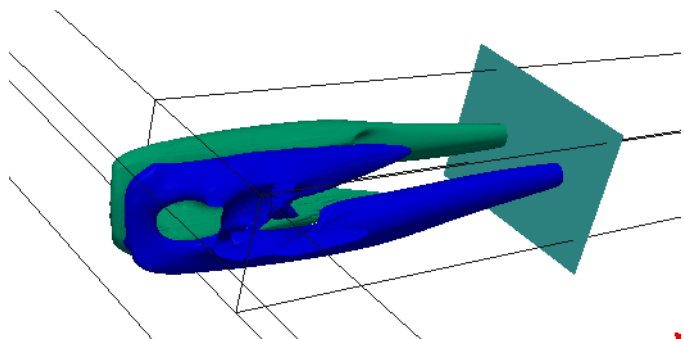


Black line: vortex countour

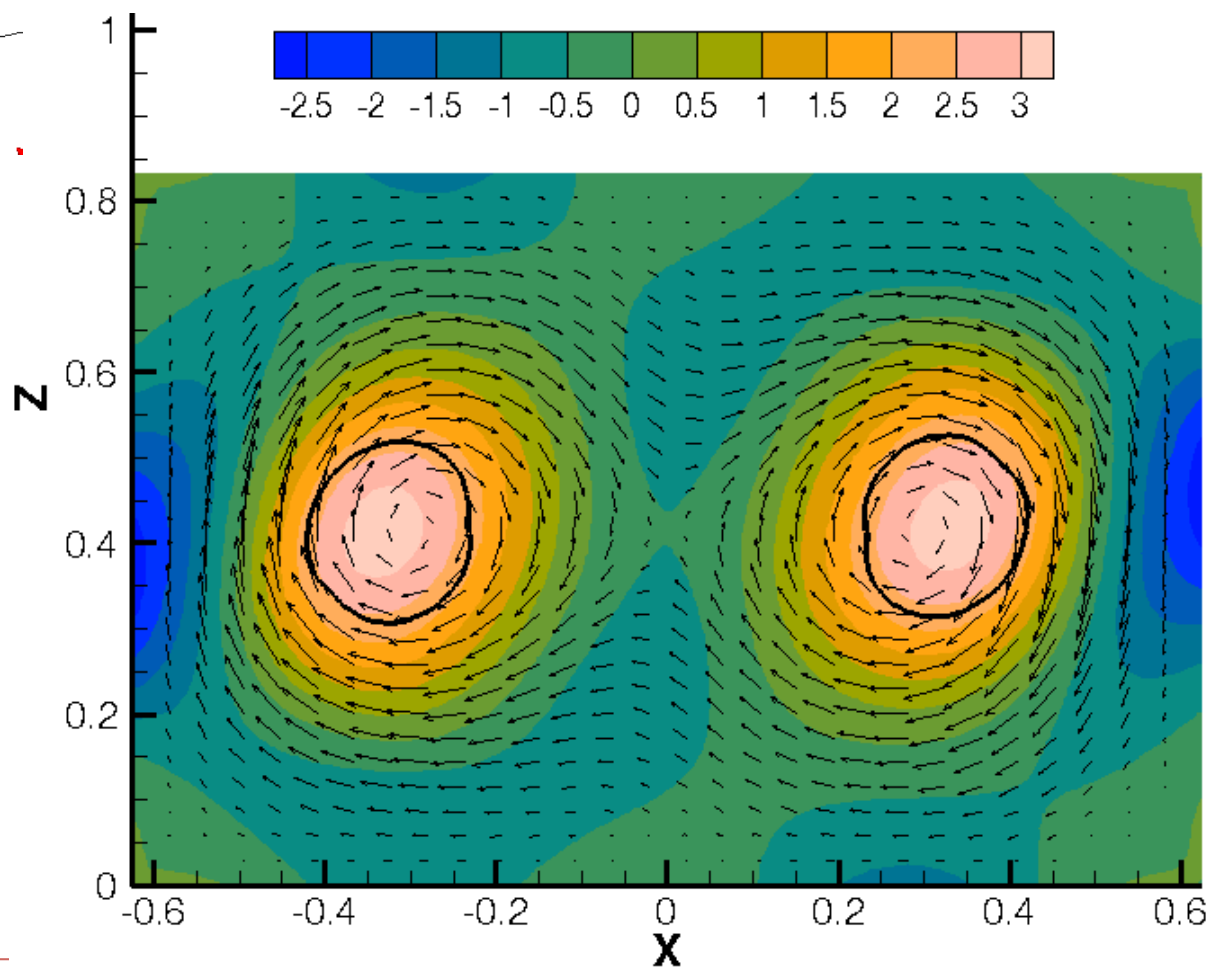


- Different intensity and position of the vortices
- Different interaction with the wall vorticity

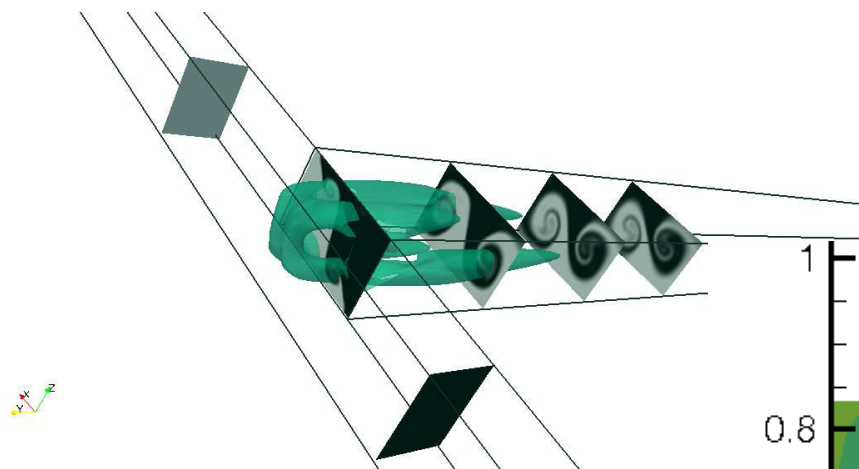
DNS investigation



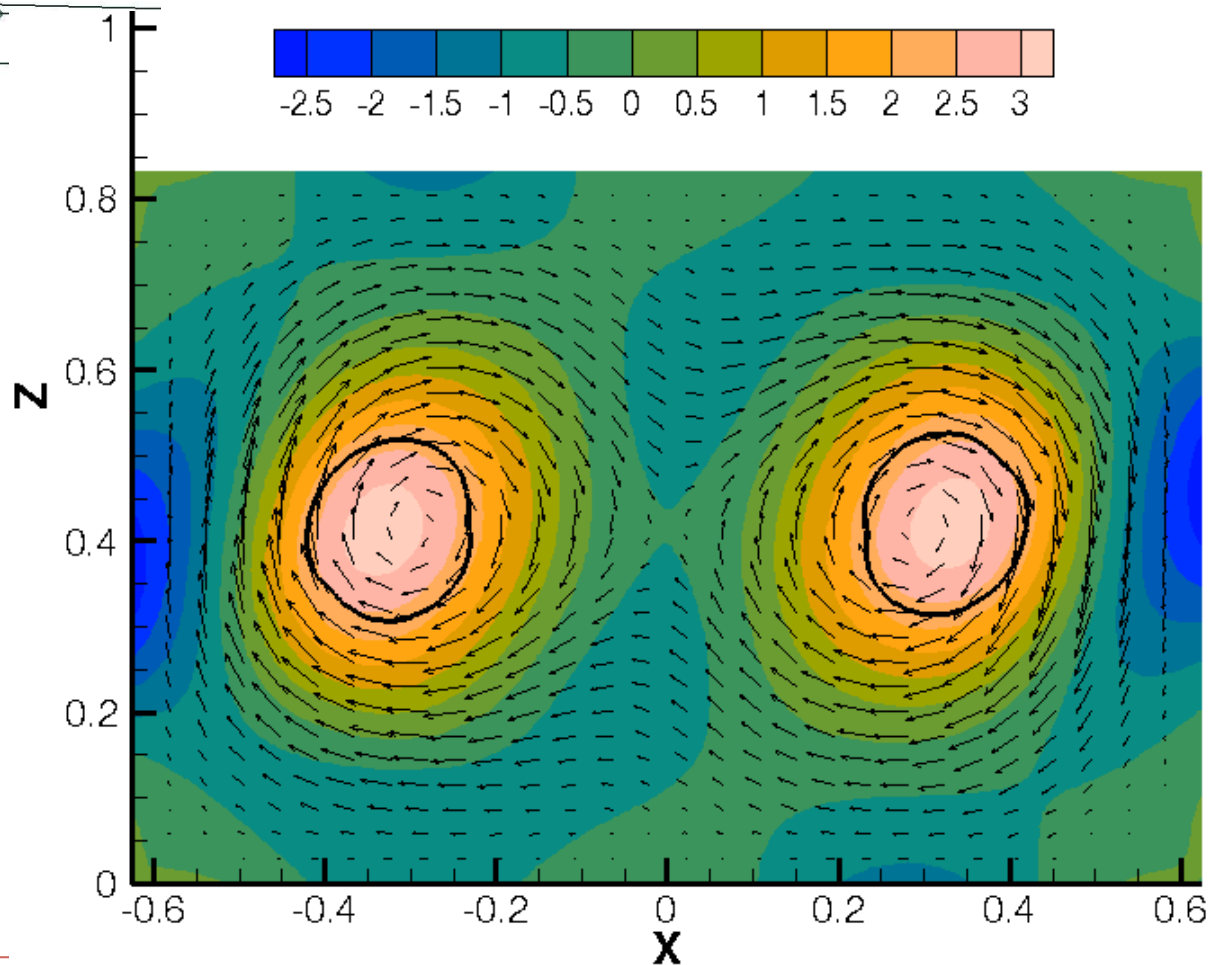
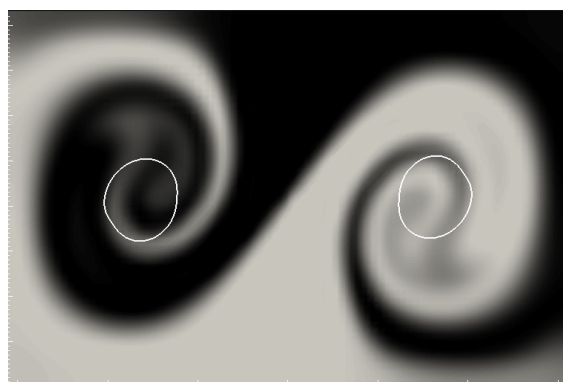
Only two pair of vortices last after the first part of the mixer



DNS investigation

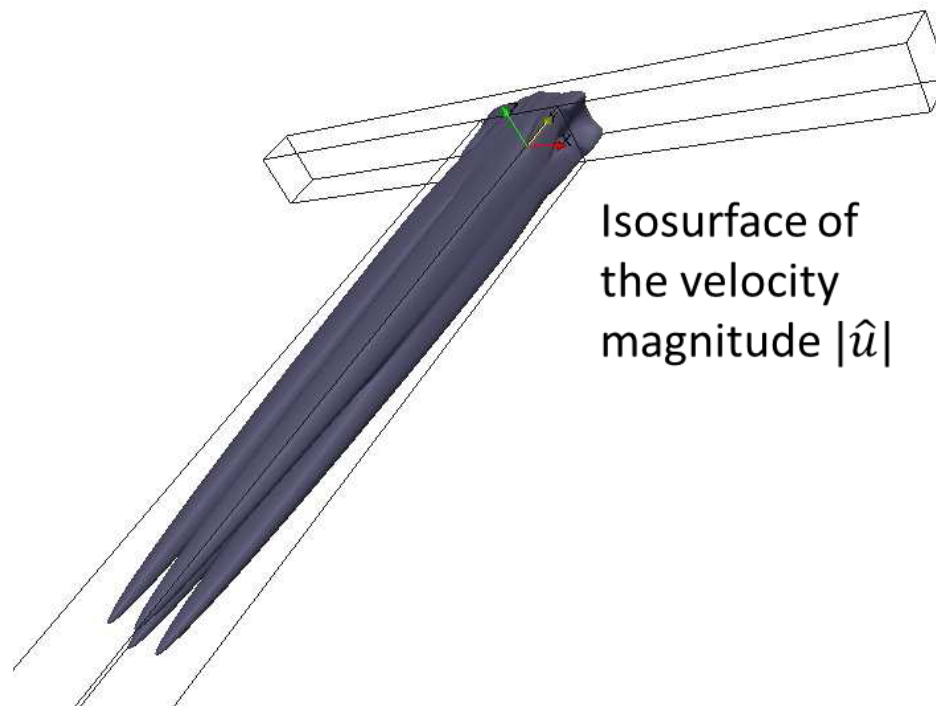


Only two pair of vortices last after the first part of the mixer



3D stability analysis

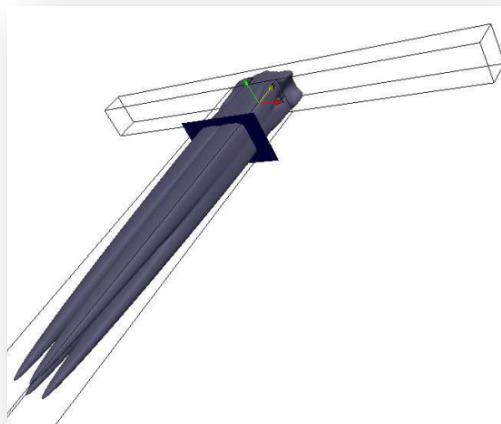
Re=140: just below the critical Reynolds number
evaluated with DNS



Stationary global mode
localized in the outflowing pipe

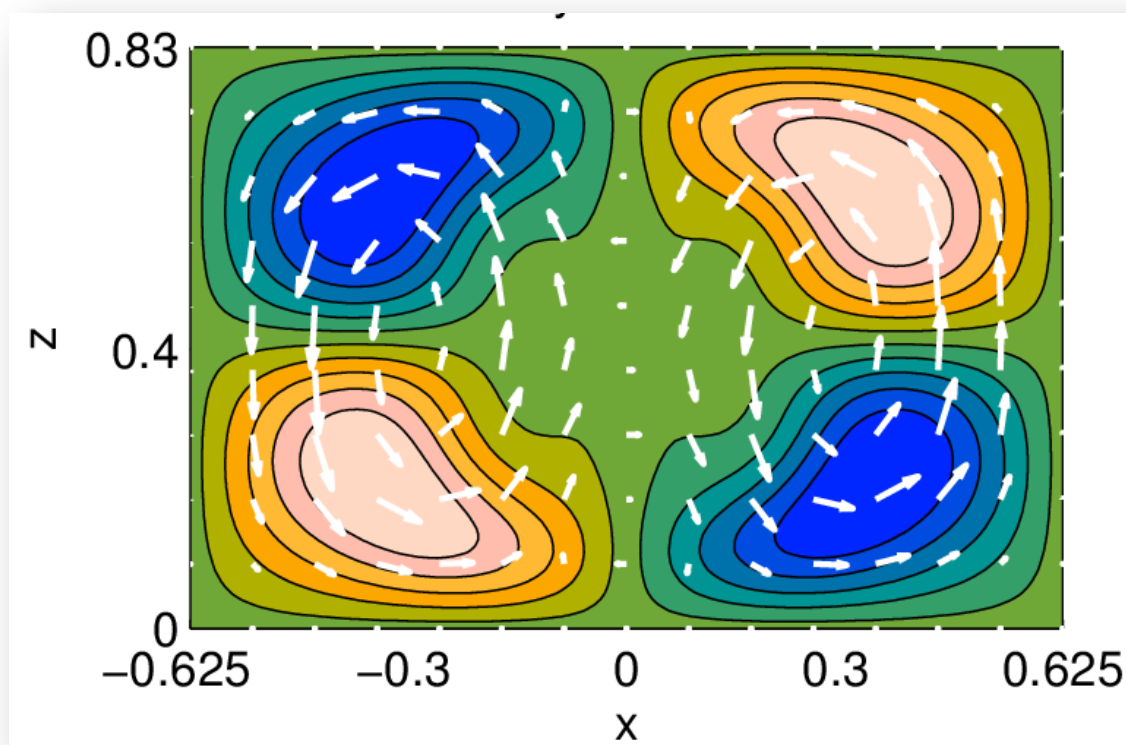
Predicted growth rate
 $\sigma = -1.5E-2$

3D stability analysis

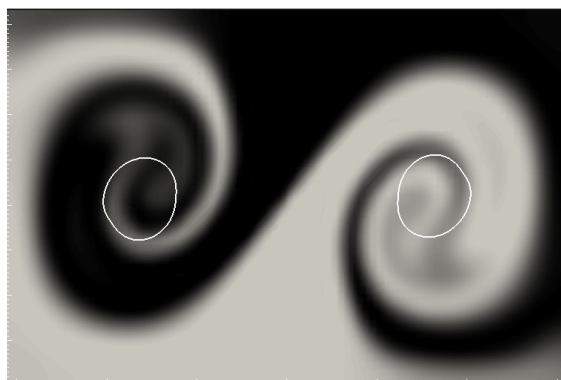


- Well defined vortical structures
- Point symmetry with respect to the center of the cross section

Contours: normal to plane velocity
Arrows: in-plane velocities

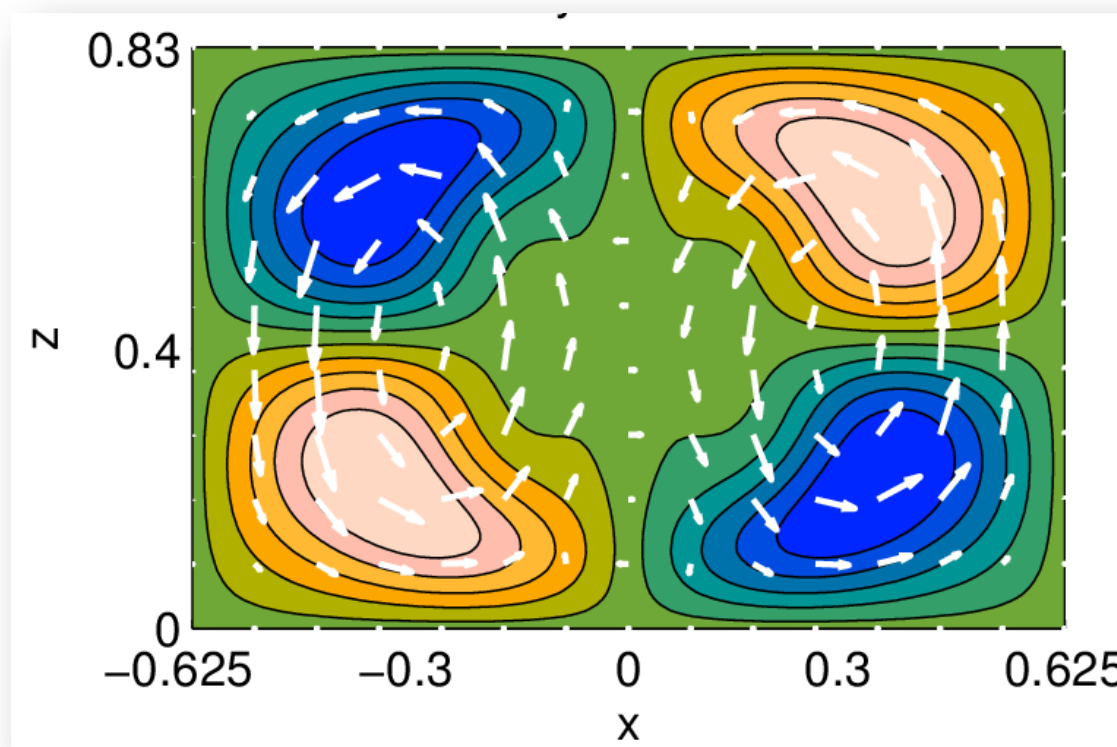


3D stability analysis

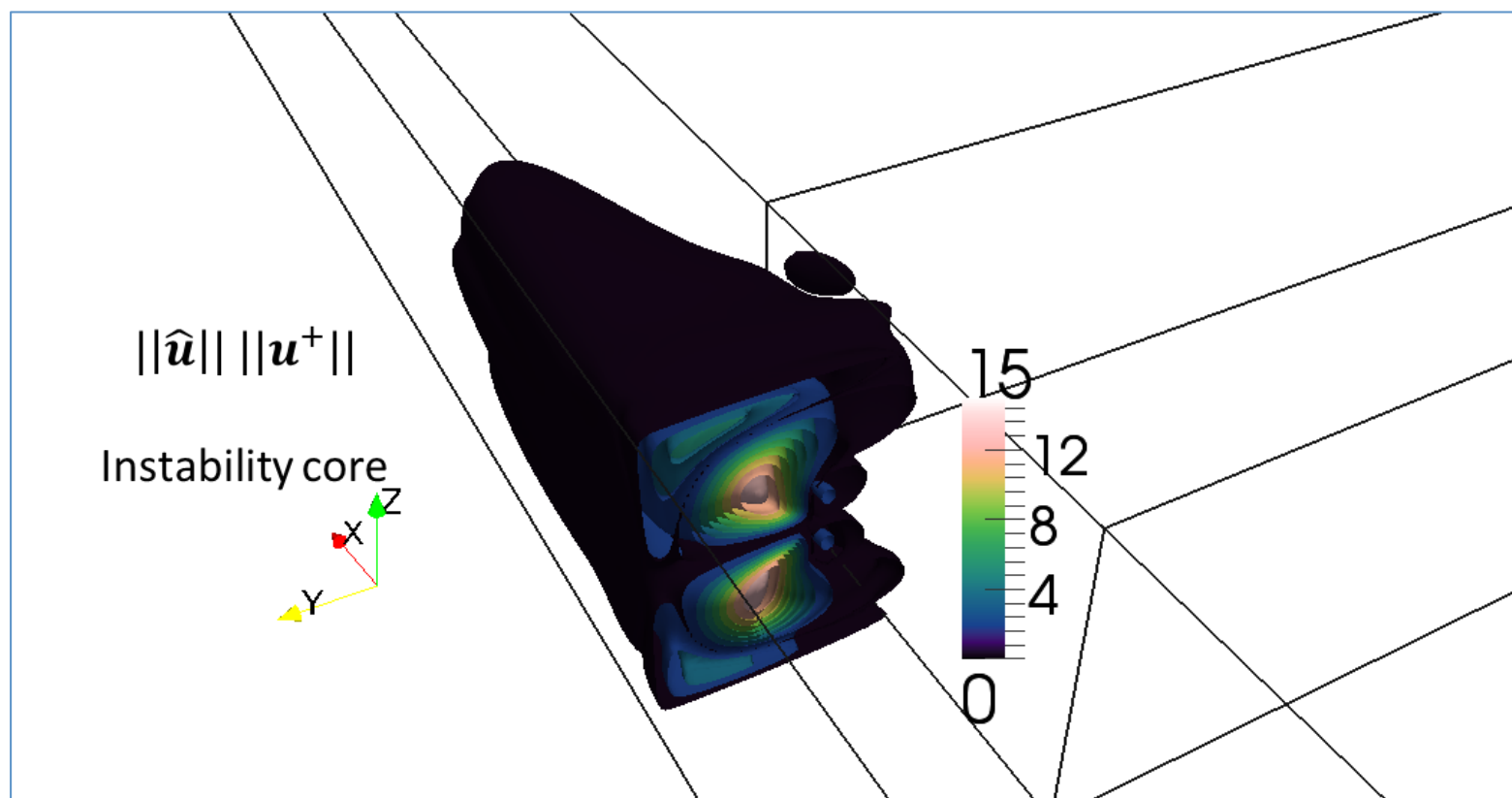


The global mode is well correlated with the S-shaped engulfment pattern

Contours: normal to plane velocity
Arrows: in-plane velocities



Instability core



The region where global and adjoint fields overlap is the intersection of inlet and outflowing pipes.



Sensitivity to perturbation of the inlet velocity conditions

Following the approach of Marquet et al. (2008), we obtain:

$$\delta\sigma = \frac{\langle P_b^+ \mathbf{n} + Re^{-1} \mathbf{n}^T \nabla U_b^+, \delta U_i \rangle_{\Gamma_i}}{\langle \mathbf{u}^+, \hat{\mathbf{u}} \rangle}$$

\mathbf{n} : normal unit vector to the boundary pointing outside the flow domain

$\langle *, * \rangle_{\Gamma_i}$ complex scalar product computed on the inlet surface

We observed that the flow is almost receptive only to a perturbation of the component of velocity normal to the inflow boundary:

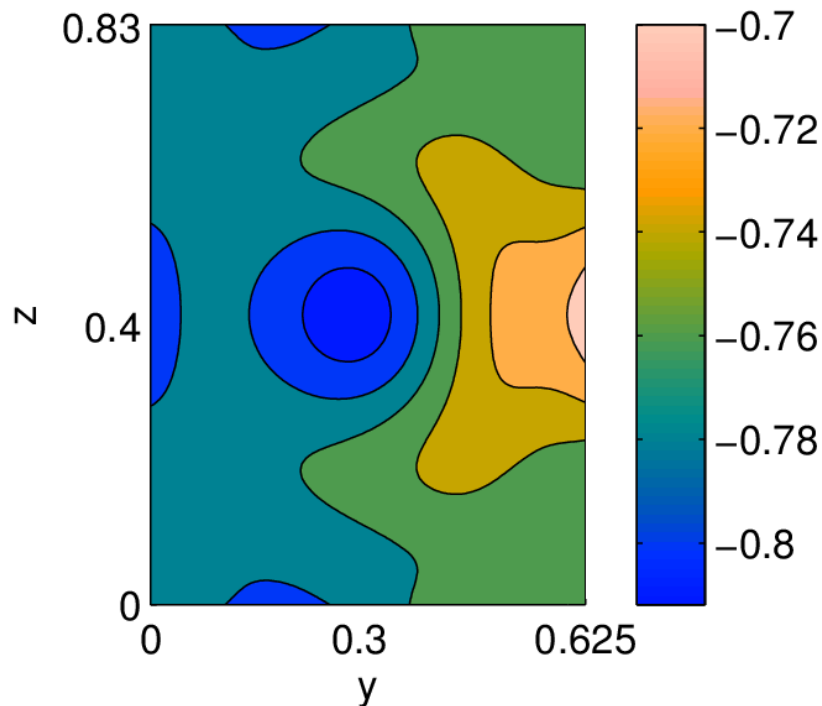
$$\delta\sigma = \frac{\langle P_b^+ \mathbf{n}, \delta U_i \rangle_{\Gamma_i}}{\langle \mathbf{u}^+, \hat{\mathbf{u}} \rangle}$$

Sensitivity to perturbation of the inlet velocity conditions

If we consider a perturbation of the form $\delta \mathbf{U}_i = U_i \delta(y, z) \mathbf{n}$ we can write:

$$\delta \sigma = U_i S(y, z)$$

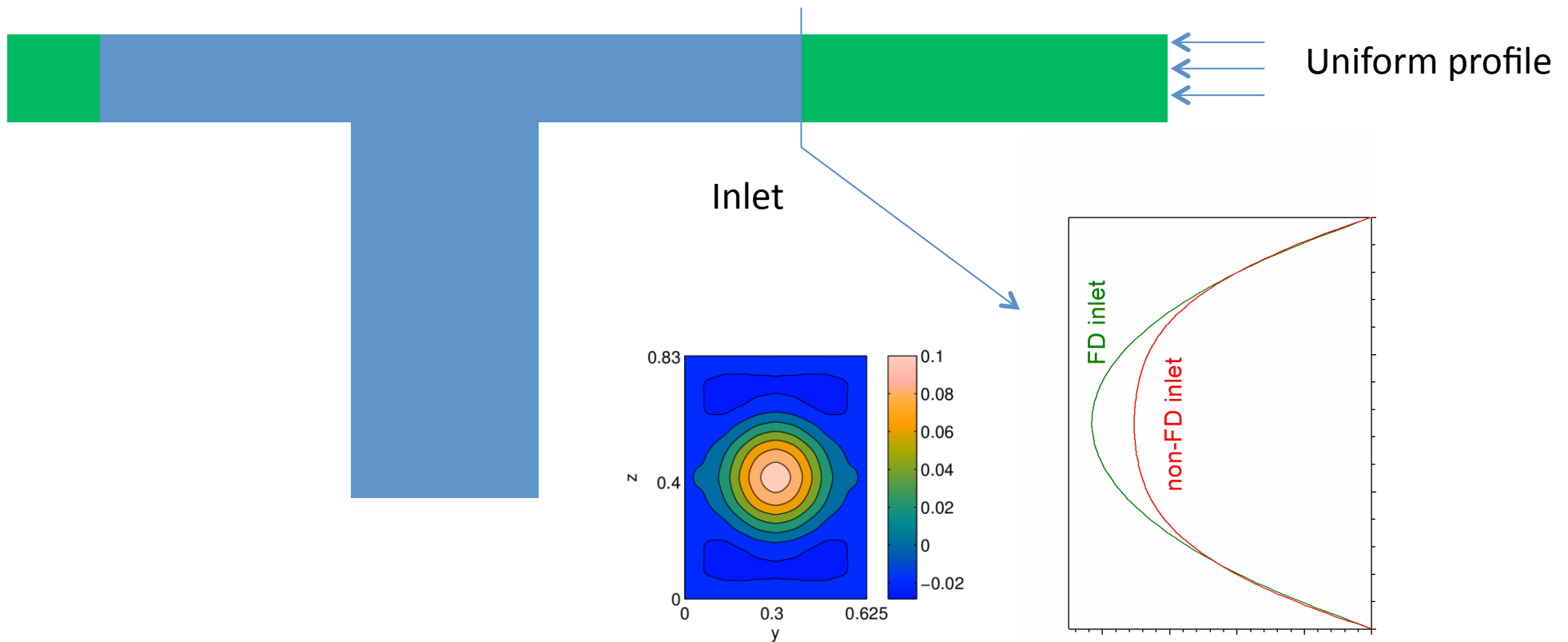
S : sensitivity map of the eigenvalue with respect to a localized modification of the wall normal component of the inflow velocity, computed on the inlet surface.



- A decrease of the inflow velocity at a generic location of the inflow section always implies a negative $\delta \sigma$
- Influence of the location of the velocity perturbation on the stabilizing/destabilizing effect

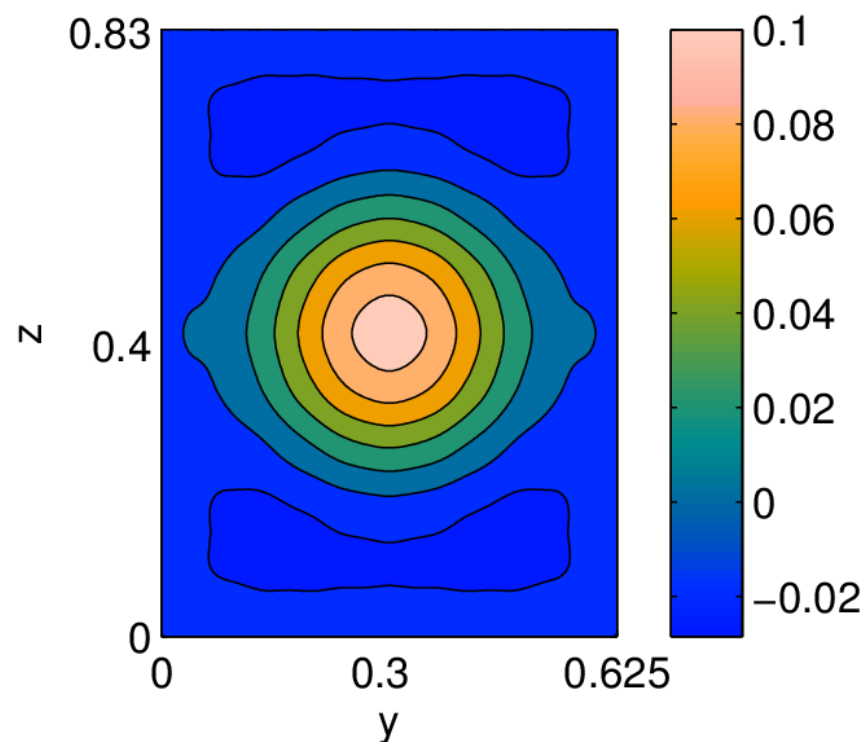
Application of the sensitivity map

Velocity perturbation (U_i) associated with a not fully developed inflow condition



Application of the sensitivity map

Velocity perturbation (U_i) associated with a not fully developed inflow condition



$$\delta\sigma < 0$$

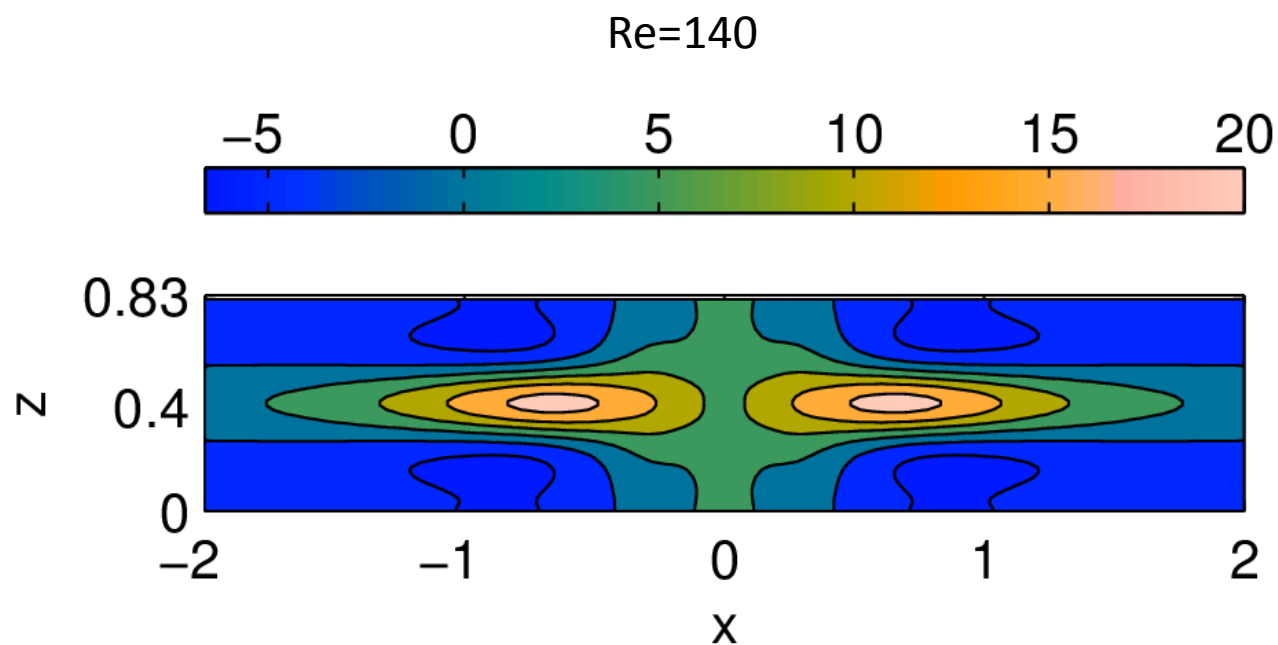
The global mode is more stable, i.e. engulfment occurs at a larger Reynolds number.

The results agrees with the conclusions drawn in Galletti et al. (2012)

A stability analysis carried out on the base-flow with the non fully developed inflow conditions has confirmed the results.

Sensitivity maps for micro-jets at the T-mixer walls

The same sensitivity maps, computed on the mixer walls, can be used to evaluate the effect of micro-jets on the instability.



$$\delta\sigma = U_{jet}S$$

Suction ($U_{jet} > 0$) has a destabilizing effect where S is positive valued



On-going developments

- Development passive wake controls using only experimental mean flow fields and final implementation in experiments for a thick plate (KTH Mechanics)
- Use of adjoint methods for data reconstruction problems in support to experiments on (KTH Mechanics):
 - Separated wakes
 - Controlled boundary layers
- Applications to fully 3D mixers for microfluidics applications:
 - Flow analysis
 - Control applications oriented to mixing enhancement
- Inclusion of Reynolds stresses as closure for local stability analysis of experimental flow fields past wind turbines (EPFL Lausanne)
- Application to free falling bluff bodies (Univ. Bordeaux)